# PRODUCTION OF BIOBUTANOL THROUGH SIMULTANEOUS SACCHARIFICATION AND FERMENTATION OF ELEPHANT GRASS

**BY**

**OLAYEMI WINNER TEMILOLUWA**

**ENG1905032**

**DEPARTMENT OF CHEMICAL ENGINEERING**

**FACULTY OF ENGINEERING**

**UNIVERSITY OF BENIN**

**BENIN CITY, EDO STATE.**

**FEBRUARY 2025**

# PRODUCTION OF BIOBUTANOL THROUGH SIMULTANEOUS SACCHARIFICATION AND FERMENTATION OF ELEPHANT GRASS

**BY**

**OLAYEMI WINNER TEMILOLUWA**

**ENG1905032**

**A PROJECT SUBMITTED TO THE DEPARTMENT OF CHEMICAL ENGINEERING**

**IN PARTIAL FUFILMENT OF THE REQUIREMENTS FOR THE AWARD OF BACHELOR OF ENGINEERING (B.ENG) DEGREE OF THE UNIVERSITY OF BENIN**

# CERTIFICATION

This is to certify that this research project was carried out by OLAYEMI WINNER TEMILOLUWA with matriculation number ENG1905032 in the Department of Chemical Engineering, University of Benin, Benin City, Edo State Nigeria.

---------- ----------

Engr. I.P. Egharevba **Date**

**Project Supervisor**

---------- ----------

Engr. Prof. S.E. Uwadiae **Date**

**Project Coordinator**

---------- ----------

Engr. Prof. (Mrs) E.T. Akhihiero **Date**

**Head of Department**

---------- ----------

**External Examiner** **Date**

# DEDICATION

I dedicate this research project to God Almighty for His guidance, my parents and siblings - Sharon and Miracle - for their unwavering support, and my mentor, Mr. Oweh, for his invaluable guidance and encouragement.

# ACKNOWLEDGEMENT

I sincerely appreciate my supervisor, Engr. I.P. Egharevba, my Head of Department, and the staff of my department for their invaluable guidance and support throughout this research. My deepest gratitude goes to my parents and siblings, whose unwavering encouragement has been my strength, and to my aunt, Mrs. Shola, and uncle, Mr. Gbenga, for their constant assistance and kindness.

A special thank you to Pastor Biodun, whose words of motivation continually pushed me to strive for excellence as a chemical engineering student. I am especially grateful to Mr. Gbolahan, whose unwavering support, guidance, and belief in me have been a source of strength throughout this journey. To my group members, I appreciate the teamwork and shared effort that made this project possible. Lastly, my heartfelt thanks go to Uncle Biodun, whose constant support and check-ins have meant so much to me.

# ABSTRACT

The increasing demand for renewable energy sources has driven research into advanced biofuels like biobutanol, which offers several advantages over ethanol. This study focuses on optimizing Simultaneous Saccharification and Fermentation (SSF) for biobutanol production from elephant grass (***Pennisetum purpureum***), a promising lignocellulosic feedstock due to its high biomass yield and cellulose content. The research aimed to evaluate SSF efficiency by optimizing key parameters, including enzyme concentrations, pH, temperature, and inoculum size, to maximize biobutanol yield.

Elephant grass was pretreated using dilute sulfuric acid, which reduced cellulose crystallinity and improved enzyme accessibility, as confirmed by X-ray diffraction (XRD) and Fourier Transform Infrared Spectroscopy (FTIR). Enzymatic hydrolysis was optimized using cellulase, beta-glucosidase, laccase, and xylanase, achieving a maximum efficiency of 46.41% at enzyme concentrations of 32.13 mg/g beta-glucosidase, 10.00 mg/g laccase, and 10.00 mg/g xylanase. The SSF process was further optimized using Response Surface Methodology (RSM), which identified optimal conditions of pH 5.5, inoculum size of 12.75% v/v, and temperature of 37.5°C, resulting in a biobutanol yield of 8.75% v/v.

The findings demonstrate that elephant grass is a viable feedstock for biobutanol production, and the optimized SSF process provides a sustainable and efficient method for converting lignocellulosic biomass into advanced biofuels. This study offers insights into the potential of SSF for large-scale biobutanol production, supporting renewable energy development and reducing fossil fuel reliance.

# TABLE OF CONTENTS

# LIST OF FIGURES

# LIST OF TABLES

# NOMENCLATURE

1. ABE: Acetone-Butanol-Ethanol
2. AFEX: Ammonia Fiber Explosion
3. BSA: Bovine Serum Albumin
4. CMM: Cooked Meat Medium
5. DNS: 3,5-Dinitrosalicylic Acid
6. DOE: Design of Experiments
7. FTIR: Fourier Transform Infrared Spectroscopy
8. GHG: Greenhouse Gas
9. HMF: 5-Hydroxymethylfurfural
10. HPLC – High-Performance Liquid Chromatography
11. $KH_2PO_4$ – Potassium Dihydrogen Phosphate
12. $K_2HPO_4$ – Dipotassium Hydrogen Phosphate
13. LCB: Lignocellulosic Biomass
14. RSM: Response Surface Methodology
15. SEM: Scanning Electron Microscopy
16. SHF: Separate Hydrolysis and Fermentation
17. SSF: Simultaneous Saccharification and Fermentation
18. XRD: X-ray Diffraction

# CHAPTER ONE

## INTRODUCTION

### 1.1 BACKGROUND OF STUDY

The world is switching from fossil fuels to renewable biofuels. This transition is due to the unrenewable nature of fossil fuels and the significant emissions of greenhouse gases released during combustion. Fossil fuel combustion, including coal, oil, and natural gas, is the principal cause of global warming, rising sea levels, and frequent extreme weather events that threaten the environment (Masson-Delmotte et al., 2021). As the world's population increases and economic development continues, demand for energy is predicted to skyrocket in future years. However, the finite nature of fossil fuel supplies and their uneven worldwide distribution have generated worries about energy security and sustainability (Shafiee & Topal, 2009).

In response to these challenges, governments, industries, and research institutions all over the world are actively researching renewable, sustainable, and environmentally friendly energy sources. Biofuels are a promising approach for reducing GHG emissions, fossil fuel imports, and dependence on uncertain foreign suppliers (Naik et al., 2010). Biofuels are made from organic resources like agricultural crops, forestry residues, and municipal solid waste, which can be converted into liquid or gaseous fuels using a variety of chemical and biological processes.

Bioethanol and biodiesel are the most widely produced and utilised biofuels globally. Bioethanol is produced by fermenting sugars from crops like sugarcane, corn, and wheat, while biodiesel is made from vegetable oils, animal fats, or recycled cooking oils (Demirbas, 2009). This first generation of biofuels has been criticised for their influence on food prices, land use change, and poor ability to cut GHG emissions compared to fossil fuels (Searchinger et al., 2008).

To solve these issues, researchers are looking at the production of advanced biofuels, often known as second-generation or cellulosic biofuels. These biofuels are derived from lignocellulosic biomass, which includes agricultural waste, energy crops, and forestry waste (Saravanan et al., 2022). Biobutanol is a popular advanced biofuel and is produced using the acetone-butanol-ethanol (ABE) fermentation process, which employs Clostridium species to convert sugars into acetone, butanol, and ethanol in a 3:6:1 ratio.

Compared to bioethanol, biobutanol has several advantages such as:

1. High energy content: Biobutanol's energy density (29.2 MJ/L vs. 25 MJ/L for ethanol) is comparable to that of gasoline, making it a viable replacement for gasoline in vehicles (Pugazhendhi et al., 2019).

2. Lower hygroscopicity: Biobutanol is less prone to absorb water, which can cause corrosion in engines and fuel systems. This makes it easier to handle and store (Obergruber et al., 2021).

3. Infrastructure compatibility: Biobutanol can be delivered through existing pipelines and used in unmodified petrol engines, unlike bioethanol, which requires engine modifications (Pugazhendhi et al., 2019).

Despite these advantages, the industrial application of ABE fermentation faces various challenges, the most significant of which is the recovery of butanol from the fermentation broth. Low butanol concentrations in fermentation broth (less than 2% w/v) might cause product inhibition, reducing yield and efficiency (Ranjan & Moholkar, 2012). Traditional recovery technologies, such as distillation, are energy-intensive and unsustainable, leading to the need for more efficient techniques.

One developing strategy for increasing butanol recovery is gas stripping, which is an in-situ recovery process that constantly removes butanol from the fermentation broth. This process includes passing an inert gas (such as nitrogen) through the broth to remove volatile compounds like butanol, which are subsequently condensed and separated. Gas stripping reduces product inhibition, allowing for higher productivity and saves energy compared to distillation (Qureshi et al., 2001). Optimising gas stripping parameters such as gas flow rate, temperature, and pressure is critical for maximising butanol recovery and increasing process efficiency.

Another important consideration in biobutanol production is the feedstock used. The use of alternative feedstocks, notably lignocellulosic biomass, represents a viable way to improve the economics and sustainability of biobutanol production. Agricultural residue and energy crops are attractive feedstocks due to their abundance, low cost, and negligible influence on food

production (Liu et al., 2022). Elephant grass (Pennisetum purpureum) is one of the most promising candidates for biobutanol production.

Elephant grass is a perennial grass native to Africa that has been extensively farmed in tropical and subtropical areas for forage, bioenergy, and soil conservation. It is known for its rapid growth rate, high biomass yield, low water and nutrient requirements, ability to thrive in marginal areas, and tolerance to diverse climates, making it an abundant and renewable resource. It can yield up to 40 tonnes of dry matter per hectare each year, which is much more than many other biomass crops. The high cellulose and hemicellulose content makes it a sustainable and cost-effective feedstock for biobutanol production (Johannes et al., 2024).

Given the potential of elephant grass as a feedstock for biobutanol production, this study aims to investigate the performance of simultaneous saccharification and fermentation (SSF) for biobutanol production.

The SSF approach combines the enzymatic hydrolysis of lignocellulosic biomass and the fermentation of the resulting sugars to biobutanol in a single step. This method reduces the number of unit operations and has the potential to improve overall process economics by simplifying the production process and reducing costs (Cardona & Sánchez, 2007).

By evaluating key parameters and outcomes of the SSF process, such as substrate conversion rates, butanol yields, and overall process efficiency, this research seeks to optimize the production of biobutanol from elephant grass. The findings from this study will provide valuable

insights to help enhance the competitiveness of biobutanol as a sustainable alternative to fossil-based transportation fuels (Haigh et al., 2018).

The successful implementation of an efficient and cost-effective biobutanol production process from elephant grass could contribute to broader efforts to reduce greenhouse gas emissions and promote the widespread adoption of advanced biofuels.

## 1.2 PROBLEM STATEMENT

The commercial viability of biobutanol production remains a significant challenge, with factors such as low product titers and high separation costs hindering its widespread adoption as an advanced biofuel. To address these issues, this study focuses on the simultaneous saccharification and fermentation (SSF) strategy for biobutanol production using elephant grass as feedstock.

The SSF approach offers advantages in terms of process efficiency and economics by combining the hydrolysis and fermentation steps into a single process. By evaluating key parameters such as substrate conversion rates, butanol yields, and overall process efficiency, this research seeks to optimize the production of biobutanol from this non-food lignocellulosic feedstock.

## 1.3 AIM

The aim of this study is to investigate the production of biobutanol from elephant grass via the simultaneous saccharification and fermentation (SSF) strategy.

The objectives of this study are:

1. Conduct a comprehensive literature review to identify gaps and potential areas for innovation in biobutanol recovery.
2. Prepare the elephant grass feedstock and apply pretreatment methods to release fermentable sugars.
3. Perform simultaneous saccharification and fermentation (SSF) experiments to produce biobutanol.
4. Implement and optimize fermentation parameters, including pH, temperature, and innoculum size, for maximum butanol recovery during SSF.
5. Analyze the results of SSF in terms of butanol yield and recovery efficiency.

## 1.4 SCOPE OF STUDY

The scope of this study is to evaluate the production of biobutanol from elephant grass using the simultaneous saccharification and fermentation (SSF) strategy. The research will begin by thoroughly preparing and characterizing the elephant grass biomass to ensure its suitability and viability as a feedstock for biobutanol generation. This will be followed by an assessment of pretreatment techniques to efficiently release fermentable sugars from the lignocellulosic structure. Crucially, the study will conduct a detailed analysis of the SSF process. Data will be collected and analyzed to assess the biobutanol yields, productivities, and overall process efficiencies achieved through this fermentation approach.

It is important to note that this research is limited to a laboratory setting and will not involve scale-up considerations or techno-economic feasibility assessments.

## 1.5 RELEVANCE OF STUDY

The significance of this study stems from its potential to significantly contribute to the development of sustainable and cost-effective biobutanol production methods. This study focuses on the production of biobutanol from elephant grass using SSF to determine the efficiency and effectiveness of this method for producing biobutanol from this non-food lignocellulosic feedstock.

This study's findings will provide crucial insights for optimising biobutanol production from elephant grass, which can help with the shift to greener and more economical energy alternatives. The analysis of the SSF process will aid in understanding the underlying mechanisms and constraints of this approach, allowing for the development of more efficient and scalable biobutanol production systems.

# CHAPTER 2

# LITERATURE REVIEW

## 2.1 BIOBUTANOL

Butanol is a four-carbon alcohol with the chemical formula $C_4H_9OH$, and it exists in four isomeric forms: n-butanol, isobutanol, sec-butanol, and tert-butanol. Among these isomers, n-butanol and isobutanol are particularly interesting as biofuels due to their favorable properties, including higher energy density and lower hygroscopicity. When produced from renewable biomass sources through biological processes, butanol is referred to as biobutanol (Pugazhendhi et al., 2019). Biobutanol stands out for its beneficial attributes as a biofuel. It has a high energy content that is comparable to gasoline, allowing it to be blended with gasoline at higher concentrations than ethanol without the need for modifications to existing infrastructure or engines. Additionally, biobutanol has lower volatility and a higher boiling point compared to ethanol, which reduces the risk of vapor lock in fuel systems, making it a safer and more practical fuel option. Its lower hygroscopicity, or tendency to absorb water, also helps prevent corrosion in fuel storage and distribution systems (Obergruber et al., 2021; Pugazhendhi et al., 2019).

The production of biobutanol primarily occurs through the acetone-butanol-ethanol (ABE) fermentation process, which relies on anaerobic bacteria from the *Clostridium* genus. This fermentation method effectively converts sugars derived from various feedstocks into a mixture of acetone, butanol, and ethanol. One of the key advantages of producing biobutanol from

lignocellulosic biomass is its sustainability profile; it allows for the utilization of agricultural residues and non-food crops, thereby minimizing competition with food production. (Veza et al., 2021)

### 2.1.1 HISTORY OF BIOBUTANOL

The industrial production of butanol began with the acetone-butanol-ethanol (ABE) fermentation process, which uses *Clostridium acetobutylicum*. This microorganism was first isolated by Chaim Weizmann, a student of Louis Pasteur. Initially, *C. acetobutylicum* was used to produce acetone during World War I, but it later gained recognition for its ability to also produce butanol. By 1927, butanol had become the primary product of the ABE process. During World War II, biobutanol found applications in the production of synthetic rubber, further solidifying its importance in industrial processes. From the 1920s to the 1960s, butanol was primarily produced by fermenting carbohydrate-rich materials like corn and molasses. However, when petroleum prices dropped in the mid-20th century, the production of biobutanol from crops declined. Instead, butanol began to be manufactured from fossil fuels through chemical processes. Despite this shift, the growing interest in renewable energy has renewed attention on biobutanol as an alternative to gasoline (Liu et al., 2022; Pugazhendhi et al., 2019).

### 2.1.2 OVERVIEW OF BIOBUTANOL PRODUCTION

Biobutanol production involves several key stages: feedstock preparation and pretreatment, hydrolysis, fermentation, and product recovery. The ABE fermentation process is predominantly used, where *Clostridium* species convert fermentable sugars into acetone, butanol, and ethanol.

The typical ratio of these products is approximately 3:6:1, with butanol being the primary focus (Pugazhendhi et al., 2019).

The choice of feedstock significantly impacts the efficiency and economics of biobutanol production. Lignocellulosic biomass, such as agricultural residues and energy crops, is increasingly being used due to its abundance and low cost. These plant-based materials are rich in complex carbohydrates that can be broken down into simple sugars, which are then fermented by specialized bacteria to produce biobutanol (Liu et al., 2022).

Recent advancements in fermentation technologies, such as simultaneous saccharification and fermentation (SSF) and separate hydrolysis and fermentation (SHF), have shown promise in improving the overall efficiency of biobutanol production. These methods aim to reduce the number of processing steps and enhance sugar conversion rates, ultimately leading to higher butanol yields (Pratto et al., 2020).

## 2.2 BIOMASS

Biomass, which comes from living organisms, has emerged as a solution to the global energy crisis. Among the various types of biomass, plant-based biomass is the most abundant and accessible resource on Earth. Its potential to contribute to biofuel production is impressive, with estimates suggesting it could meet up to 14% of the world's energy needs (Mahalingam et al., 2022). The unique structure of plant biomass, particularly the plant cell wall, makes it an ideal feedstock. The cell wall is primarily made up of cellulose, hemicellulose, and lignin, while the cytoplasm contains a variety of organic compounds, including proteins, starch, vitamins, and

minerals (Meramo-Hurtado et al., 2020). These substances are produced through complex processes of plant metabolism and photosynthesis, which harness energy from sunlight to create intricate organic molecules. One of the key advantages of plant biomass is its ability to be broken down into simpler building blocks, or monomers, through various methods. This can be achieved through biological processes like fermentation and enzymatic hydrolysis, natural degradation by microorganisms, physical techniques, and chemical processes such as acid hydrolysis (Meramo-Hurtado et al., 2020). Once these monomers are produced, they can be fermented by a wide range of microbes, leading to the creation of various bioproducts, with biofuels being a primary focus.

The biomass used for biofuel production are classified into three generations. This classification is based on the type of substrate used and the resulting biofuel products. The first generation primarily uses seeds, grains, and simple sugars, with bioethanol being the main product produced through the fermentation of starches and sugars. The second generation focuses on lignocellulosic biomass (LCB), which includes materials like agricultural residues and wood. This generation produces a variety of biofuels, including bioethanol and biobutanol through enzymatic hydrolysis, as well as methanol and biodiesel via thermochemical processes. The third generation shifts the focus to algae biomass, which can yield bioethanol, biodiesel, and biohydrogen from both green and blue algae. Each generation represents a step towards more sustainable and efficient biofuel production, utilizing increasingly complex substrates to reduce competition with food resources and enhance energy yield (Dalena et al., 2019).

### 2.2.1 Lignocellulosic Biomass

Lignocellulosic biomass (LCB) is recognized as a sustainable and abundant energy resource found around the world. This type of biomass is non-edible and primarily sourced from forests and agricultural activities. Unfortunately, much of it is often treated as waste. In many developing countries, rural communities rely on traditional energy sources like crop residues and firewood. However, these conventional methods are not only costly and inefficient but also time-consuming and harmful to the environment. It is projected that LCB could supply around 38% of the global direct fuel needs and contribute to 17% of the world's electricity by 2050 (Ong et al., 2021).

LCB can be categorized into three types: virgin biomass (like trees and grasses), waste biomass (such as agricultural residues), and energy crops, which are specifically grown for high biomass yield. The shift from fossil fuels to biomass for energy production has gained momentum due to environmental concerns and the depletion of fossil resources (Yousuf et al., 2019). Plant biomass is primarily made up of three main structural components: cellulose, hemicellulose, and lignin. These components are unevenly distributed within the plant cell wall, working together to create a strong framework for the plant (Ong et al., 2021).

Cellulose molecules are organized into both crystalline and amorphous regions, forming microfibrils that are held together by hydrogen and Van Der Waals bonds, with hemicellulose and lignin providing additional structural support. Carbohydrates, which are the main components of cellulose and hemicellulose, make up about 70% of the dry weight of LCB. These carbohydrates serve as feedstock for various bio-based products and chemical intermediates,

regardless of whether the conversion method is biological or thermochemical. Lignin, which accounts for roughly 25% of the biomass weight, is a significant source of aromatic compounds and is also a valuable solid biofuel. Generally, LCB has great potential to contribute to the energy sector by enabling the production of various energy forms, including solid fuels like briquettes, liquid fuels such as bioethanol and biodiesel, and gaseous fuels like biogas and hydrogen (Yousuf et al., 2019).

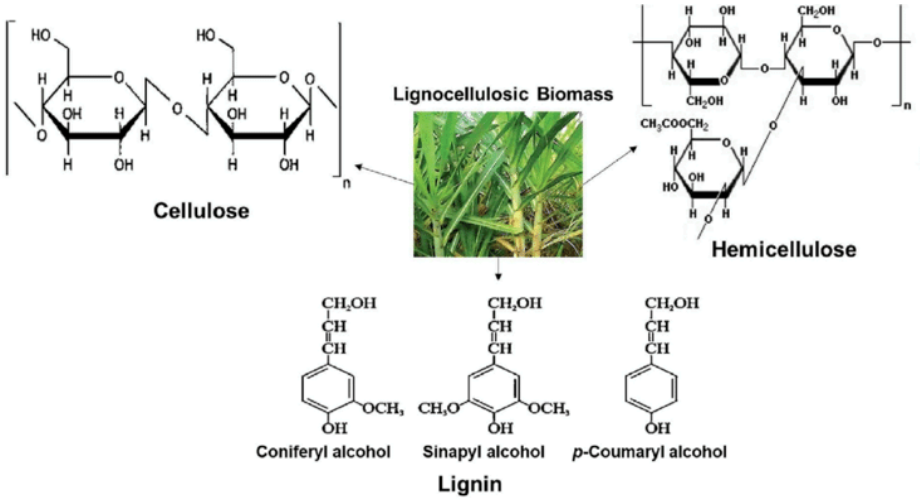


***Fig 2.1: Chemical structure of lignin, cellulose and hemicellulose (adapted from (Khaire et al., 2021))***

### 2.2.1.1 Cellulose

Cellulose is a key component of LCB and is a polysaccharide polymer made up of D-glucose units linked together by β-(1-4) glycosidic bonds, creating a straight-chain structure. As the most abundant organic polymer on the planet, cellulose is found in plants, algae, and oomycetes, with its content varying across materials like wood, cotton, and hemp (Yousuf et al., 2019). The structural integrity of cellulose comes from strong hydrogen bonding between its molecules, which leads to the formation of cellulose microfibrils that can be either crystalline or amorphous (Ummalyma et al., 2019).

The process of cellulose biosynthesis involves individual molecules aggregating into fibrils through hydrogen bonds, eventually forming microfibrils and cellulose fibers (Okolie et al., 2021). Cellulose is resistant to enzymatic breakdown due to factors like its crystallinity, interactions with hemicellulose, and the presence of lignin. This resistance often necessitates pretreatment methods to enhance its digestibility (Ummalyma et al., 2019; Zoghlami & Paës, 2019).

#### 2.2.1.2 Hemicellulose

Hemicellulose is a crucial component of lignocellulosic biomass and is a complex, branched heteropolymer composed of various sugar units. These include pentoses like xylose and arabinose, hexoses such as glucose, mannose, and galactose, as well as sugar acids including glucuronic acid and galacturonic acid (Okolie et al., 2021; Zoghlami & Paës, 2019). Hemicellulose plays a vital role in strengthening the plant cell wall by cross-linking with cellulose and lignin. (Zoghlami & Paës, 2019). Xylans are the most abundant polysaccharides in hemicelluloses, with their composition varying based on the source material, such as birch wood, corn fiber, and wheat. The content of hemicellulose itself differs depending on the source of lignocellulosic biomass, with softwoods, hardwoods, and herbaceous plants having varying percentages of this component.

One key advantage of hemicellulose is its lower degree of polymerization and amorphous structure compared to cellulose, making it more easily degradable in acidic or hot aqueous mediums (Okolie et al., 2021). Additionally, the structural diversity and reactive hydroxyl groups of hemicellulose offer opportunities for regioselective chemical and enzymatic modifications. (Zoghlami & Paës, 2019)

#### 2.2.1.3 Lignin

Lignin is the second most abundant polymer in lignocellulosic biomass, and it plays a crucial role in making biomass resistant to enzymatic hydrolysis due to its complex structure and composition. Made up of phenylpropane monomers, lignin provides rigidity to plant cell walls and acts as a physical barrier, limiting enzyme access to cellulose. Removing lignin can enhance enzymatic digestibility by disrupting the lignin-carbohydrate matrix and reducing non-productive enzyme binding sites.

The ratio of syringyl to guaiacyl units in lignin, known as the S/G ratio, influences its recalcitrance, although research has shown conflicting results regarding its correlation with hydrolysis yields across different biomass sources (Okolie et al., 2021; Zoghlami & Paës, 2019). Lignin's presence can hinder the conversion of biomass to bioenergy, making pretreatment steps necessary to improve cellulose accessibility (Ummalyma et al., 2019).

***Table 2.1 Some lignocellulose materials and their cellulose, hemicellulose and lignin contents (adapted from (Yousuf et. al, 2019))***

| Raw material | Cellulose (%) | Hemicellulose (%) | Lignin (%) |
|---|---|---|---|
| Energy crops | 21 – 54 | 5 – 30 | 5 – 10 |
| Grasses | 25 – 40 | 25 – 50 | 10 – 30 |
| Softwoods | 45 – 50 | 25 – 35 | 25 – 35 |
| Hardwoods | 45 – 55 | 24 – 40 | 18 – 25 |

## 2.3 ELEPHANT GRASS

Elephant grass (*Pennisetum purpureum*) is a robust and versatile perennial grass found in tropical regions. It is highly valued for its impressive biomass yield, which can range from 25 to 35 oven-dry tons per hectare annually (Mohammed et al., 2019). It is exceptionally adaptable to harsh conditions, growing rapidly to heights of up to 6 meters and allowing for multiple harvest cycles within a single year (Pereira et al., 2021).

With a high cellulose content of around 38.75%, hemicellulose content of 19.76%, and lignin content of 26.99%, elephant grass is a promising feedstock for biofuel production, particularly biobutanol (Mohammed et al., 2019). Research has demonstrated its potential for bioethanol production through processes like pretreatment, hydrolysis, and fermentation, achieving significant ethanol yields. In addition to its biofuel applications, elephant grass offers environmental benefits, such as carbon sequestration and high photosynthetic efficiency. This makes it not only a sustainable energy crop but also useful in other industries, including paper manufacturing (Johannes et al., 2024).

### 2.3.1 Elephant Grass as Feedstock

Elephant Grass is an attractive choice for biofuel production due to its numerous advantages. It offers high biomass yields with the potential for multiple harvests per year, making it an excellent feedstock for biofuel generation. With its high cellulose content, Elephant Grass is particularly well-suited for producing biobutanol via enzymatic hydrolysis and other procedures. Additionally, Elephant Grass demonstrates extreme resilience to adverse environmental conditions, such as high temperatures and limited water supply, showcasing its suitability as an energy crop. Furthermore, its capacity for carbon sequestration contributes to environmental

sustainability, making it an appealing option for sustainable energy production. Finally, Elephant Grass boasts excellent photosynthetic efficiency, which enhances its potential as a renewable biomass source for biofuel generation. (Boonmee Kongkeitkajorn et al., n.d.; Johannes et al., 2024).

## 2.4 PRETREATMENT OF LIGNOCELLULOSIC BIOMASS

The intricate structure and chemical stability of cellulose, hemicellulose, and lignin create significant barriers to efficiently breaking down LCB into fermentable sugars. That's why pretreatment is necessary—it modifies the structural and compositional characteristics of LCB, making it more accessible for the subsequent enzymatic hydrolysis and fermentation processes (Sharma et al., 2019). The need for pretreatment stems from the inherent recalcitrance of lignocellulosic biomass, primarily due to its complex composition. Lignin, a highly cross-linked aromatic polymer, acts as a protective barrier around the cellulose fibers, significantly limiting enzyme access. Its hydrophobic nature and tendency to bind with cellulases can further inhibit enzyme activity.

Cellulose, the most abundant component, exists in a crystalline form that makes it resistant to enzymatic degradation. This crystalline structure results from the tight packing of β-D-glucopyranose units, which form strong hydrogen bonds, contributing to the rigidity and resistance of cellulose microfibrils. Hemicellulose, a heterogeneous polysaccharide, also contributes to biomass recalcitrance. Although it is more amorphous and has a lower degree of polymerization than cellulose, hemicellulose forms a matrix around the cellulose, limiting enzyme access. Its complex, branched structure can further impede enzyme action. By disrupting

these structures, pretreatment processes lower the crystallinity of cellulose, solubilize hemicellulose, and either remove or modify lignin. This transformation increases the porosity of the biomass and makes enzymes more accessible, ultimately improving the digestibility and conversion efficiency of the biomass (Zoghlami & Paës, 2019).

The importance of pretreatment goes beyond just improving enzyme accessibility. Pretreatment is essential for reducing the formation of inhibitory compounds that can affect downstream fermentation processes. For instance, acid pretreatment methods, such as using sulfuric or acetic acid, can effectively solubilize hemicellulose and make cellulose more accessible. However, they can also produce inhibitors like furfural and 5-hydroxymethylfurfural (HMF) (Jędrzejczyk et al., 2019; Zhao et al., 2022). These inhibitors can negatively impact microbial metabolism, leading to issues like DNA breakdown and reduced RNA synthesis, which ultimately hampers enzymatic activity during fermentation (Mankar et al., 2021). To address these challenges, it's crucial to optimize pretreatment conditions, including acid concentration, temperature, and duration, to minimize the formation of these inhibitors and ensure the efficiency of subsequent fermentation processes. Additionally, combining biological and chemical pretreatments has been shown to enhance lignin breakdown and improve overall efficiency, reducing the need for harsh chemicals and mitigating inhibitor production (Jędrzejczyk et al., 2019; Zhao et al., 2022). By carefully optimizing these pretreatment conditions, we can minimize inhibitor formation and boost the overall efficiency of the biofuel production process.

### 2.4.1 PHYSICAL PRETREATMENT

Physical pretreatment of lignocellulosic biomass involves changing the specific surface area, particle sizes, crystallinity index, and degree of polymerization without using chemicals. This approach helps reduce waste and inhibitors for subsequent reactions. Common techniques such as mechanical, microwave, and ultrasound methods are used to enhance the efficiency of biomass processing. Recent trends are focusing on advanced methodologies and detailed studies to boost the production of desired molecules (Jędrzejczyk et al., 2019).

Physical pretreatment methods include milling, grinding, shredding, and chipping, all aimed at reducing particle size, improving the surface area for enzymatic hydrolysis, and enhancing mass transfer. These changes ultimately facilitate downstream processes, leading to higher yields of valuable products. When considering physical pretreatment, energy consumption and the efficiency of particle size reduction are key factors (Mankar et al., 2021).

#### 2.4.1.1 Mechanical Pretreatment

Mechanical pretreatment is an important physical method used to reduce the particle size of biomass, which helps improve the efficiency of enzymatic hydrolysis (Jędrzejczyk et al., 2019). Techniques such as milling, grinding, and chipping break down the biomass into smaller pieces, increasing the surface area available for reactions (Sharma et al., 2019). This process not only reduces the crystallinity of cellulose but also enhances mass transfer, making it easier for enzymes to do their job. For instance, in a study, ball milling has been shown to significantly decrease the cellulose crystal content (from 56.1% to 99.3%), resulting in higher yields of fermentable sugars after enzymatic hydrolysis (Mankar et al., 2021). However, mechanical

pretreatment can be quite energy-intensive and may come with high operating costs and risks related to equipment wear and tear. Despite these challenges, it remains a valuable approach in the pretreatment of lignocellulosic biomass.

#### 2.4.1.2 Microwave Pretreatment

Microwave pretreatment method uses microwave radiation to generate thermal energy, effectively disrupting complex biomass structures without breaking chemical bonds. It is more energy-efficient than traditional methods and significantly enhances the digestibility of biomass during enzymatic hydrolysis. Additionally, microwave pretreatment helps to delignify the biomass by removing lignin and partially breaking down hemicellulose, which increases the solubility of cellulose. However, it's important to note that prolonged exposure to microwave radiation can degrade polysaccharides and create inhibitors, so careful optimization is necessary to maximize sugar yield while minimizing byproducts (Jędrzejczyk et al., 2019). By disrupting the lignocellulose structures, microwave pretreatment makes cellulose more accessible and facilitates the extraction of oligomers and lignin. This not only improves the efficiency of enzymatic hydrolysis but also enhances the conversion efficiency of hemicellulose and increases xylose yield as shown in a study where 12.40g/L yield of xylose and maximum hemicellulose conversion efficiency of 96.4% were obtained from pretreating walnut shells at 550-600W microwave power (Zhao et al., 2022). Furthermore, the microwave radiation can cause explosions within the biomass particles, further aiding in the disruption of recalcitrant structures. This process optimizes the accessibility of both hemicellulose and cellulose, ultimately enhancing biofuel extraction (Mankar et al., 2021).

#### 2.4.1.3 Ultrasonic Pretreatment

Ultrasonic pretreatment is a technology for enhancing biomass valorization, using acoustic energy to disrupt lignocellulosic structures and improve enzymatic hydrolysis (Jędrzejczyk et al., 2019). The effectiveness of this method depends on factors like frequency, intensity, and duration, with frequencies above 20 kHz proving particularly effective at reducing cellulose crystallinity and making biomass more accessible for further processing. When combined with chemical methods like potassium permanganate or sodium hydroxide, ultrasonic pretreatment can significantly boost lignin removal. For example, applying 25 kHz ultrasound combined with potassium permanganate increased lignin removal in coffee waste by 46%, while 20 kHz ultrasound with 1 N NaOH achieved 80%–100% lignin removal in materials like cabbage and peanut husks (Zhao et al., 2022). Additionally, using ultrasound has been shown to increase methane yields and improve hydrolysis kinetics, while also reducing hemicellulose and lignin content in biomass. This makes ultrasonic pretreatment a green and efficient option for biomass conversion (Jędrzejczyk et al., 2019).

### 2.4.2 CHEMICAL PRETREATMENT

Chemical pretreatment is a critical step in breaking down lignocellulosic biomass, using specialized chemicals to disrupt the tough structure of lignocellulose and make it more biodegradable. This method involves treating the biomass with acids, bases, ionic liquids, oxidizing agents, or organic solvents to modify its properties for further processing. Chemical pretreatment has been found to increase the surface area of lignocellulose and enhance enzymatic accessibility, leading to higher sugar yields during subsequent fermentation processes. Acids like sulfuric or hydrochloric acid are effective at removing hemicellulose, while strong bases can

alter lignin structure and even break down some of the cellulose. Organic solvents help extract lignin and hemicellulose, improving the digestibility of the remaining cellulose. However, these chemicals can be corrosive and generate inhibitory compounds that negatively impact downstream processes. To address this, researchers have developed emerging environmentally friendly pretreatment methods that combine biological and chemical approaches. These hybrid techniques aim to improve efficiency and reduce the formation of compounds that interfere with fermentation, while still achieving the benefits of chemical pretreatment in disrupting lignocellulose (Jędrzejczyk et al., 2019; Mankar et al., 2021; Zhao et al., 2022).

#### 2.4.2.1 Acid Pretreatment

Acid pretreatment involves using acids like sulfuric, acetic, and phosphoric acid to solubilize hemicellulose, which enhances the accessibility of cellulose. The effectiveness of this process is influenced by factors such as acid concentration, temperature, and duration, all of which can impact sugar yields. It can be performed using either dilute or concentrated acids, each with its own advantages and disadvantages. Strong acid hydrolysis can yield high sugar levels but requires specialized equipment due to its corrosive nature. On the other hand, diluted acids provide a cost-effective alternative, offering high hydrolysis rates with minimal formation of inhibitors. For example, sulfuric acid pretreatment can effectively remove hemicellulose and expose more cellulose, but excessive acid can degrade the cellulose itself. (Jędrzejczyk et al., 2019; Mankar et al., 2021; Zhao et al., 2022)

#### 2.4.2.2 Alkaline Pretreatment

Alkaline pretreatment uses alkaline substances like sodium hydroxide (NaOH) and potassium hydroxide (KOH) to break down the lignocellulosic structure by effectively removing lignin and hydrolyzing hemicellulose. The high pH environment created during pretreatment dissolves a significant amount of lignin and hemicellulose, which reduces cellulose crystallinity and increases the internal surface area available for enzymatic action (Jędrzejczyk et al., 2019; Zhao et al., 2022).

To optimize the process, it's crucial to consider operational parameters such as alkali concentration, temperature, and treatment duration. Typically, concentrations range from 2% to 7%, with temperatures between 100°C and 200°C for short durations of 10 to 90 minutes. For instance, treating barley straw with 2% NaOH at 105°C for 10 minutes can achieve lignin removal efficiencies of 84.8% and hemicellulose removal efficiencies of 79.5% (Zhao et al., 2022). While alkaline pretreatment is versatile and can be applied to various biomass feedstocks, it does come with challenges, including high treatment costs and complex processing steps. Recent advancements have explored combining alkaline pretreatment with other methods, such as ionic liquids, to enhance enzymatic digestibility (Tu & Hallett, 2019).

#### 2.4.2.3 Organosolv Pretreatment

Organosolv pretreatment uses organic solvents like methanol, ethanol, and acetone, often combined with catalysts such as organic acids or bases, to break down the structures of lignin and hemicellulose. By solubilizing these components, organosolv pretreatment increases the surface area of cellulose, which helps enzymes work more effectively during hydrolysis (Jędrzejczyk et al., 2019; Mankar et al., 2021). The main mechanism behind this process

involves breaking the bonds between lignin, hemicellulose, and cellulose, which ultimately leads to better sugar yields. For example, a study demonstrated that using n-propylamine as a base catalyst with 60% aqueous ethanol at 140 °C for 40 minutes resulted in a sugar yield of 83.2% and an 81.7% delignification from corn stover (Mankar et al., 2021).

Operational conditions for organosolv pretreatment typically range from 150°C to 220°C. Lower temperatures may not effectively remove lignin. For instance, treating wheat straw with acetone at 180°C for 40 minutes achieved a lignin removal efficiency of 76%, while coffee waste treated with 68% ethanol at 51°C for 45 minutes only removed 24.4% of lignin (Zhao et al., 2022). Despite its effectiveness, organosolv pretreatment comes with some challenges, including high solvent costs, volatility, and flammability. These factors complicate solvent recovery and increase energy requirements. Additionally, the pretreated biomass often needs extensive washing to remove any residual solvents, which can inhibit the enzymes used in fermentation. The high temperatures and pressures involved in the process also raise safety concerns. One significant issue is the potential loss of yield due to the degradation of hemicellulose and cellulose monomers into unwanted byproducts, such as furans. To address this, researchers have looked into adding formaldehyde during pretreatment to create reversible acetal compounds that help prevent sugar degradation and reduce the formation of humin (Tu & Hallett, 2019).

#### 2.4.2.4 Ionic Liquids Pretreatment

Ionic liquid pretreatment is a chemical method used to modify the tough structure of lignocellulosic materials by applying ionic liquids, which are non-volatile and stable. This technique allows for a wide range of operating temperatures and can significantly enhance the

digestibility of biomass, leading to higher yields of desired products. It has been verified that pretreating corn straw at 150℃ for 3.5 h result in 68.3% lignin dissolved. However, it's important to recognize that ionic liquid pretreatment has its downsides, including high energy consumption and potential toxicity, which need careful management during the process (Jędrzejczyk et al., 2019; Tu & Hallett, 2019; Zhao et al., 2022).

#### 2.4.2.5 Oxidative Pretreatment

Oxidative pretreatment methods, such as using hydrogen peroxide and ozone, are effective at breaking down lignin and hemicellulose in lignocellulosic biomass, which improves enzymatic accessibility and boosts sugar yields. Research shows that the concentration of hydrogen peroxide is key to lignin degradation, with optimal levels typically between 2-4% enhancing the process. Additionally, ozone pretreatment under alkaline conditions has proven to be more effective for lignin removal, with factors like intensity, treatment time, and pH playing a significant role in the degradation of lignin (Jędrzejczyk et al., 2019; Tu & Hallett, 2019) .

#### 2.4.2.6 Deep Eutectic Solvents Pretreatment

Deep Eutectic Solvents (DESs) are innovative green solvents made up of hydrogen bond donors and acceptors. DESs share properties similar to ionic liquids, making them effective at breaking down the bonds between lignin and carbohydrates, as well as cleaving the ether bonds in lignin-hemicellulose complexes. Research has shown that DESs can achieve impressive lignin removal rates, ranging from 92.98% to 95.13% in poplar wood, and yield efficient sugar outputs,

such as 235.3 mg of sugar per gram of biomass in sugarcane bagasse. Moreover, when combined with hydrothermal methods, DESs can significantly enhance the removal of lignin and hemicellulose while preserving the integrity of cellulose (Mankar et al., 2021; Tu & Hallett, 2019; Zhao et al., 2022).

### 2.4.3 PHYSICOCHEMICAL PRETREATMENT

Physicochemical pretreatment combines physical and chemical methods to break down the tough structure of lignocellulosic biomass, making it easier to separate its basic components for further processing. This approach is different from purely physical, chemical, or biological methods, offering a unique way to enhance the digestibility of biomass and increase the yield of desired products by altering the structure of lignocellulosic materials (Jędrzejczyk et al., 2019).

Techniques such as steam explosion, alkali-heat pretreatment, and ammonia fiber expansion have proven effective at removing lignin and reducing cellulose crystallinity. These methods play a vital role in preparing lignocellulosic biomass for conversion processes by breaking down its complex structure into more accessible forms for downstream use (Zhao et al., 2022).

#### 2.4.3.1 Steam Explosion Pretreatment

Steam explosion is a commonly used physicochemical pretreatment method for lignocellulosic biomass. It involves rapidly releasing high-pressure saturated steam to create explosive decompression, typically at temperatures between 160°C and 240°C and pressures ranging from 0.7 to 4.8 MPa. The goal of this process is to solubilize hemicellulose, improve cellulose

accessibility, and minimize the formation of inhibitory compounds that can hinder enzymatic processes. This method effectively breaks down the biomass structure by partially hydrolyzing hemicellulose, making it easier for further processing. For example, using steam explosion pretreatment on reed under 200℃ and 3.4MPa for 15 minutes, its hemicellulose was reduced by 90%, therefore the cellulose content increased from 64.48% to 81.3%. While steam explosion is successful in removing lignin and increasing cellulose content, it does have some drawbacks. These include high energy consumption, the potential generation of inhibitory compounds, and the need for harsh pretreatment conditions (Jędrzejczyk et al., 2019; Zhao et al., 2022).

#### 2.4.3.2 Alkali-Heat Pretreatment

Alkali-heat pretreatment is a physicochemical method that uses alkali substances like sodium hydroxide to dissolve lignin and reduce the crystallinity of lignocellulose. This process enhances the accessibility of enzymes to cellulose, leading to improved sugar fermentation. Studies have shown that this pretreatment can effectively remove lignin and hemicellulose, with reported removal rates of up to 54.09% and 67.67%, respectively, in corn straw. This results in increased cellulose content and higher yields of reducing sugars. However, there are some challenges associated with alkali-heat pretreatment, including high treatment costs and complex processes that can limit its widespread use, even though it performs well in retaining cellulose (Zhao et al., 2022) . Additionally, the need to neutralize post-treatment mixtures and the longer processing times are notable downsides. Despite these issues, alkali-heat pretreatment remains a strong option for effectively removing lignin and xylan under mild reaction conditions (Mankar et al., 2021).

While alkali pretreatment can achieve similar lignin and hemicellulose removal efficiencies, alkali-heat pretreatment has shown promising results with high sugar yields, although it also faces challenges like cost and complexity (Zhao et al., 2022).

#### 2.4.3.3 Ammonia Fiber Explosion (AFEX) Pretreatment

Ammonia Fiber Explosion (AFEX) is a physicochemical pretreatment method that treats lignocellulosic biomass with liquid ammonia under high pressure and moderate temperatures. This process causes the biomass to swell, increases its surface area, degrades hemicellulose, and alters the structure of lignin. AFEX has several advantages, including improved efficiency in enzymatic hydrolysis, reduced lignin content, and enhanced ethanol yields compared to other pretreatment methods. For example, the hydrolysis and fermentation of the AFEX-pretreated corn stover yielded an impressive ethanol production of 20.5 kg of ethanol per kg of biomass, significantly higher than the 14 kg yield from the dilute acid-treated sample. Research has shown that AFEX can be optimized by adjusting various parameters such as temperature, residence time, pressure, water content, and ammonia concentration to maximize the yields of glucan and xylan. Additionally, adding hydrogen peroxide during the AFEX process can further improve glucan digestibility and increase sugar yields from different biomass sources (Jędrzejczyk et al., 2019; Mankar et al., 2021; Zhao et al., 2022).

### 2.4.4 BIOLOGICAL PRETREATMENT

Biological pretreatment of lignocellulosic biomass (LCB) offers several benefits, including low operational costs, environmental sustainability, and minimal production of inhibitory

by-products. This method uses bacteria or fungi to hydrolyze cellulose and break down lignin, which helps in decomposing the biomass components for later bioenergy conversion. However, biological pretreatment typically requires longer retention times and may need to be combined with chemical or physical processes to improve efficiency and make it more commercially viable. The effectiveness of biological pretreatment is influenced by various factors, including temperature, particle size, pH, and the specific strains of bacteria or fungi used. This highlights the complexity and careful consideration involved in this approach (Tu & Hallett, 2019; Zhao et al., 2022).

#### 2.4.4.1 Bacterial Pretreatment

Bacterial pretreatment is an effective biological method that uses specific bacteria to break down complex components of biomass, making it easier to convert lignocellulosic materials into simpler sugars. Efficient bacterial strains, such as those from the genera *Cellulomonas, Thermomonospora,* and *Paenibacillus*, are particularly good at degrading cellulose and hemicellulose. Additionally, rumen bacteria like *F. succinogenes, R. flavefaciens, and R. albus* play a vital role in cellulose degradation (Sharma et al., 2019).

Bacterial pretreatment takes advantage of the natural enzymatic activity of bacteria to produce cellulases and lignin-degrading enzymes, which enhance the digestibility of biomass. For instance, *Bacillus subtilis* has been shown to achieve a 23% reduction in lignin and decrease cellulose crystallinity by 4.1%, thereby improving the biomass structure for enzymatic hydrolysis. Furthermore, *Acetobacter orientalis* has demonstrated a cellulose degradation

efficiency increase of 76.24% in banana residues, highlighting the potential of bacterial pretreatment to significantly boost biomass conversion efficiency (Zhao et al., 2022).

While bacterial pretreatment may require longer retention times, combining it with chemical or physical methods can optimize the process and shorten treatment durations.

#### 2.4.4.2 Fungal Pretreatment

Fungal pretreatment is another effective biological method for breaking down lignocellulosic biomass. Key fungi involved in this process include white rot, brown rot, and soft rot fungi. These fungi produce ligninolytic enzymes such as lignin peroxidase (LiP), manganese peroxidase (MnP), and laccase, which play a crucial role in degrading lignin. White rot fungi like *Phanerochaete chrysosporium* can significantly reduce lignin content, as demonstrated by a 34.3% removal rate in corn stover. This pretreatment enhances cellulose hydrolysis, improving biofuel yields. For example, *Irpex lacteus* pretreatment achieved an 82% hydrolysis yield for corn stalks. *Trametes versicolor* has also shown up to an 80% cellulose hydrolysis and increased methane production from treated substrates (Zhao et al., 2022). Fungi such as *Trichoderma reesei* and *Trichoderma longibrachiatum* also produce cellulolytic enzymes that complement lignin degradation (Ummalyma et al., 2019). Despite progress, challenges remain in selecting fungal strains that efficiently degrade both lignin and cellulose. Further research is needed to optimize fungal pretreatment for commercial biofuel applications.

#### 2.4.4.3 Other Types of Biological Pretreatment

In addition to fungi and bacteria, several larger organisms, including insects, worms, snails, and cud-chewing animals, play important roles in the biological pretreatment of lignocellulosic biomass. These creatures use a variety of clever tricks - mechanical, enzymatic, and microbial -

to effectively break down tough plant materials. Insects are especially notable for their ability to digest wood and other plant matter. Various insect species, such as termites, beetles, and wood wasps, have specialized digestive systems packed with enzymes and gut microbes that help them feast on cellulose and lignin (Sharma et al., 2019). Termites are particularly adept at decomposing lignocellulose. Different termite species can degrade 28-47% of the cellulose, 12.5-23.1% of the hemicellulose, and 7-32% of the lignin in wheat straw within just 20 days (Dumond et al., 2021). However, using termites for pretreatment has practical challenges, like figuring out how to collect and manage their gut microbes (Zhao et al., 2022).

Earthworms are another group with impressive lignocellulose-degrading talents. Species like the red wiggler and the nightcrawler are known for their love of rotting plant matter, which they digest through a combination of enzymes and gut microbes. The liquid that drains from worm compost, called worm tea, contains a microbial community that has shown promise as an alternative to traditional acid pretreatment. This liquid can help enzymes work better and improve fermentation for biofuel production. Snails and cud-chewing mammals like cows and sheep also contribute to cellulose digestion through their gut microbes. Studying the microbial communities inside these creatures has led to the discovery of various enzymes and microbial interactions that help break down lignocellulose (Sharma et al., 2019). While these larger organisms offer interesting biological pretreatment methods, putting them to practical use has challenges. It can be difficult to obtain specific microbes and scale up the processes. But with more research to optimize these methods and fit them into larger biofuel production systems, these creatures could play a bigger role in the future of renewable energy.

## 2.5 ENZYMATIC HYDROLYSIS OF LIGNOCELLULOSIC BIOMASS

Enzymatic hydrolysis is a biological pretreatment method that uses enzymes produced by microorganisms to convert complex plant carbohydrates into simpler sugars. This process is highly effective in breaking down plant biomass into fermentable sugars. It involves applying enzymes like cellulases and hemicellulases to the plant material. Cellulases specifically target cellulose, breaking it down into glucose and other simple sugars. Meanwhile, hemicellulases work on hemicellulose, converting it into xylose and additional simple sugars (Hasan et al., 2024). The combined action of these enzymes is crucial for maximizing sugar yields from lignocellulosic biomass (Sharma et al., 2019). Additionally, accessory enzymes like laccases and peroxidases can assist in lignin degradation, further enhancing enzyme accessibility to cellulose (Chauhan, 2020a).

Pretreating lignocellulosic biomass is a critical step that enhances the efficiency of enzymatic hydrolysis. The various methods—physical, chemical, and biological—can disrupt the crystalline structure of cellulose and remove lignin and hemicellulose, thereby increasing the surface area available for enzymatic action (Jędrzejczyk et al., 2019). The effectiveness of enzymatic hydrolysis is significantly influenced by several factors, including the type and concentration of enzymes used, the pretreatment method applied, and the characteristics of the lignocellulosic biomass itself. Optimizing these factors is essential for maximizing sugar yields and improving the overall efficiency of the hydrolysis process (Huang et al., 2022).

### 2.5.1 Cellulases

Cellulases are essential enzymes that catalyze the breakdown of cellulose into glucose for biobutanol production. Compared to acid hydrolysis, enzymatic hydrolysis is preferred due to its eco-friendly nature, specificity for substrates, and ability to operate under mild conditions, which minimizes the formation of undesirable by-products. These enzymes function by cleaving the β-1,4-glycosidic bonds in cellulose and include three main types: endoglucanases, exoglucanases, and β-glucosidases. These enzymes act synergistically to ensure complete hydrolysis. (Kolpe et al., 2022; Muharja et al., 2023).

The hydrolysis process begins when cellulases bind to the cellulose surface, where they cleave the β-glycosidic bonds, releasing cellobiose and glucose. The efficiency of this process is influenced by several factors, including the degree of cellulose polymerization, the presence of complex side groups, and interactions with hemicellulose and lignin (Ilić et al., 2023). Endoglucanases create free chain ends by breaking internal bonds in the cellulose, while exoglucanases remove terminal glucose units, resulting in the release of cellobiose and glucose. Finally, β-glucosidases convert cellobiose into glucose, although this step can be limited by the accumulation of glucose, which inhibits their activity (Fernandes et al., 2022).

The overall efficiency of cellulases is affected by various factors, such as enzyme concentration, substrate characteristics, and reaction conditions, including pH and temperature. Recent advancements in enzyme immobilization techniques have improved the stability, activity, and reusability of cellulases, making them more suitable for industrial applications (Kolpe et al., 2022). Improving enzyme production and activity is vital for increasing hydrolysis efficiency. This may involve exploring different fermentation strategies, investigating various microbial

sources, and utilizing genetic engineering to develop more effective cellulase variants (Shubakov A.A. et al., 2022).

### 2.5.2 Hemicellulases

Like cellulases, hemicellulases convert hemicellulose into fermentable sugars. Hemicellulose, a major component of plant cell walls, consists of a diverse mixture of polysaccharides, including xylose, arabinose, and mannose, linked by various glycosidic bonds (Ethiraj et al., 2023). Breaking down hemicellulose is essential for maximizing sugar recovery during biobutanol production, as it complements the action of cellulases.

The hydrolysis process involves several types of hemicellulases, such as xylanases, arabinofuranosidases, and glucuronidases. Xylanases specifically target xylan, the most abundant hemicellulose component, cleaving the β-1,4-glycosidic bonds to release xylose and other sugars. Arabinofuranosidases act on arabinose side chains, while glucuronidases help in the degradation of glucuronoxylans (Marcolongo et al., 2021).

The efficiency of hemicellulases in hydrolysis is influenced by the structural complexity of the hemicellulose, the presence of lignin, and the reaction conditions like pH and temperature. Lignin can obstruct the accessibility of hemicellulases to hemicellulose, which is why pretreatment methods are often necessary to improve enzyme efficiency (Cebreiros et al., 2019). Recent studies have shown that incorporating hemicellulases into the enzymatic hydrolysis process can significantly boost sugar yields. For instance, a research on hemp biomass found that the addition of hemicellulases to the enzymatic cocktail significantly enhanced the hydrolysis process. Specifically, after 72 hours of treatment, the glucose yield reached 62.0%, while xylose yield was reported at 95.8% from the saccharification of pretreated hemp biomass

(Marcolongo et al., 2021). Moreover, auxiliary enzymes have been reported to enhance the overall efficiency of hydrolysis by breaking down hemicellulose more effectively, leading to improved sugar recovery (Ethiraj et al., 2023).

### 2.5.3 Ligninases

Ligninases are a group of enzymes that play a crucial role in the degradation of lignin. The presence of lignin in biomass presents significant challenges due to its recalcitrance, making lignin degradation a key step in the overall process of biomass conversion (Carlos dos Santos et al., 2019).

There are several types of ligninases, each with unique mechanisms of action. Peroxidases utilize hydrogen peroxide to oxidize lignin, effectively cleaving various linkages within its structure. They are particularly skilled at breaking down β-O-4 ether linkages, which are common in lignin. By generating phenoxy radicals, peroxidases help to depolymerize lignin into smaller, more manageable fragments (Nargotra et al., 2023). Laccases, on the other hand, are multi-copper oxidases that oxidize phenolic compounds in lignin, facilitating the degradation process. They produce reactive radicals that aid in breaking down lignin, especially when used with mediators that enhance their oxidative capacity. Laccases are particularly effective in delignification processes, making lignin more accessible for further enzymatic action (Cajnko et al., 2021). Additionally, β-etherases specifically target β-O-4 aryl ether linkages in lignin, cleaving them with stereoselective activity, which improves the efficiency of lignin degradation (Chauhan, 2020b). By breaking down lignin, these enzymes improve the accessibility of cellulose and hemicellulose to cellulolytic enzymes, which are essential for converting these polysaccharides into fermentable sugars (Carlos dos Santos et al., 2019). Moreover, lignin can inhibit the activity of cellulolytic enzymes by adsorbing them, which can hinder the overall efficiency of biomass

conversion. Ligninases help mitigate this inhibitory effect, enhancing the performance of cellulases and hemicellulases during the hydrolysis process (Nargotra et al., 2023).

### 2.5.4 Factors Affecting Enzymatic Hydrolysis

1. **Crystallinity of Cellulose**: The proportion of crystalline regions in cellulose compared to amorphous regions affects hydrolysis rates. Crystalline cellulose is more resistant to enzymatic action, with hydrolysis rates 3-30 times lower than in amorphous zones. Some studies have shown a negative correlation between crystallinity and initial hydrolysis rates, particularly in pre-treated biomass such as wheat straw and corn stover. However, other research indicates that crystallinity may be less critical than other physical features, such as degree of polymerization (DP), pore volume, accessible surface area, and particle size (Backes et al., 2023; Zoghlami & Paës, 2019).

2. **Degree of Polymerization (DP):** Higher DP indicates longer cellulose chains, which can hinder enzyme accessibility to the substrate, reducing hydrolysis efficiency. This factor is interconnected with crystallinity and the overall structural complexity of the biomass. A higher DP typically correlates with increased crystallinity, as the presence of more hydrogen bonds in longer cellulose chains contributes to recalcitrance, making it more challenging for enzymes to perform hydrolysis effectively (Ilić et al., 2023; Zoghlami & Paës, 2019).

3. **Accessible Surface Area and Pore Volume:** A greater surface area allows more enzymes to interact with the substrate, enhancing hydrolysis rates. Limited accessibility due to structural barriers can impede enzymatic action. The available surface area is influenced by the porosity and particle size of the biomass. Smaller particle sizes and higher porosity lead to increased surface area, allowing enzymes to penetrate and act on the biomass more effectively (Ilić et al., 2023; Zoghlami & Paës, 2019).

4. **Enzyme Concentration:** The amount of enzyme used directly impacts the rate of hydrolysis. Higher concentrations of commercial cellulase lead to increased hydrolysis efficiency, particularly for soybean hulls (SH) and corn stover and cobs (CSC). However, it was noted that increasing pectinase concentration led to a reduction in hydrolysis efficiency for CSC, suggesting that the balance of enzyme types is crucial for optimal results. Insufficient enzyme loading can lead to incomplete hydrolysis, while excessive enzyme amounts may not proportionally increase sugar yields due to substrate saturation (Backes et al., 2023; Ethiraj et al., 2023).

5. **Reaction Time:** Sufficient reaction time is necessary for complete degradation of both amorphous and crystalline cellulose fractions. The most effective hydrolysis occurred after specific durations for different substrates: 22 hours for SH and 14 hours for CSC when using commercial cellulase. Insufficient reaction time may not allow for thorough hydrolysis (Backes et al., 2023).

6. **Agitation:** Higher agitation rates positively affect hydrolysis by enhancing enzyme-substrate interaction, with optimal rates varying for different substrates. The results demonstrated that higher agitation rates positively affected the hydrolysis of both SH and CSC, with optimal hydrolysis observed at 300 rpm for SH and 350 rpm for CSC (Backes et al., 2023).

7. **Temperature:** Temperature influences enzyme activity, and maintaining optimal conditions is essential for maximizing hydrolysis efficiency. The study highlights that both agitation and temperature significantly affect the action of cellulase on CSC (Backes et al., 2023; Ethiraj et al., 2023).

8. **Substrate Characteristics:** The characteristics of the substrate, such as particle size and composition, are crucial. Smaller particle sizes and pretreatment with NaOH significantly increased hydrolysis efficiency for both SH and CSC. The composition of the substrates, particularly the presence of pectin and cellulose in SH, also affects the hydrolysis outcomes, as the high pectin content can enhance the overall hydrolytic efficiency (Backes et al., 2023; Ilić et al., 2023).

9. **pH**: The enzymatic activity of glycoside hydrolases, which are the primary enzymes used in hydrolysis, is highly dependent on pH. Each enzyme has an optimal pH range where it exhibits maximum activity (Ethiraj et al., 2023).

10. **Presence of Inhibitors:** The presence of inhibitors formed during the hydrolysis process can significantly impair enzymatic activity. These inhibitors can arise from the breakdown of lignin and hemicellulose, necessitating careful management of the hydrolysis conditions to mitigate their effects (Ethiraj et al., 2023; Ilić et al., 2023).

These factors are interconnected and their effects can vary significantly depending on the biomass species, pre-treatment methods, and the specific enzymatic cocktails used.

## 2.6 SIMULTANEOUS SACCHARIFICATION AND FERMENTATION (SSF) FOR BIOBUTANOL PRODUCTION

Simultaneous Saccharification and Fermentation (SSF) is an innovative bioprocess that combines the enzymatic breakdown of lignocellulosic biomass into fermentable sugars with the fermentation of those sugars into biofuels, all within a single reactor. This integrated approach streamlines the production process, reduces processing time, and enhances the overall efficiency of biobutanol production.

### 2.6.1 Overview of SSF Process

The SSF process begins with the pretreatment of lignocellulosic biomass, a crucial step aimed at enhancing its accessibility for enzymatic hydrolysis. For instance, hydrothermal treatment effectively disrupts the lignin structure and increases the surface area of the biomass, facilitating better access for enzymes during hydrolysis (Afedzi & Parakulsuksatid, 2023).

Once the biomass has been pretreated, the process moves into the simultaneous saccharification phase. Here, specific enzymes, such as cellulases and xylanases, are introduced to catalyze the breakdown of complex carbohydrates into simpler sugars, primarily glucose and xylose. What sets SSF apart is that these enzymes are added alongside the fermentation microorganisms, allowing for the immediate conversion of sugars as they are released (Valles et al., 2020b). This simultaneous action not only streamlines the process but also enhances the overall efficiency of biofuel production.

### 2.6.2 Optimization of SSF for Biobutanol Production

Maintaining optimal operational conditions is critical for the success of SSF. Typically, the process is conducted at a temperature of around 37°C, which is suitable for both enzyme activity and microbial growth. The initial pH is set at approximately 6.3, gradually decreasing to around 4.5 as fermentation progresses. This pH drop aligns with the optimal conditions for enzymatic activity, facilitating saccharification while reducing feedback inhibition from glucose on the enzymes (Wang et al., 2023).

The dosage of enzymes used during SSF is another important factor. Research indicates that an optimal concentration, such as 0.08 g/L of glucoamylase, can yield significant glucose concentrations after a specific period of enzymatic hydrolysis (Wang et al., 2023). When enzyme dosages exceed this threshold, glucose yields can consistently improve, demonstrating the importance of enzyme concentration in enhancing saccharification efficiency.

As sugars are released during saccharification, the fermentation phase begins within the same reactor. Specific microorganisms, such as Clostridium acetobutylicum for butanol production or engineered strains of Escherichia coli for isobutanol, are inoculated into the mixture to convert

the released sugars into biofuels. The fermentation process is influenced by several factors, including the initial culture pH and temperature, which must be optimized for the specific microbial strain used. For example, the optimal pH for E. coli fermentation is around 6.5, where significant concentrations of isobutanol can be achieved (Akita et al., 2024).

The fermentation phase typically lasts between 48 to 120 hours, during which the microorganisms metabolize the sugars and produce biofuels. The efficiency of this phase is influenced by the concentration of sugars, the specific strain of microorganisms used, and the fermentation conditions (Valles et al., 2020b). The integration of saccharification and fermentation allows for immediate utilization of sugars, minimizing the accumulation of intermediate sugars that can inhibit fermentation.

### 2.6.3 Advantages of SSF for Biobutanol Production

The SSF process is designed to enhance the efficiency of biofuel production by minimizing the time and resources required compared to traditional methods like SHF. By combining saccharification and fermentation into a single step, SSF reduces the overall processing time, achieving results in approximately 27 to 120 hours, depending on the biomass and operational conditions (Devos & Colla, 2022). This integrated approach not only streamlines the production process but also enhances the overall efficiency of biofuel production from agricultural waste. For instance, studies have reported high butanol yields of up to 12.64 g/L within 48 hours of fermentation in SSF, compared to lower yields in SHF (Valles et al., 2020b).

The SSF process operates under controlled conditions that favor both enzyme activity and yeast fermentation. However, optimizing these conditions can be challenging, as it requires ensuring that both the saccharifying enzymes and the fermenting microorganisms can function effectively

together. High concentrations of exogenous enzymes are often necessary to facilitate the saccharification of complex substrates, which can complicate process control (Devos & Colla, 2022).

### 2.6.4 Recent Advancements in SSF

Recent advancements in SSF have focused on optimizing various parameters to enhance overall performance and yield. Key factors include the selection of appropriate enzyme technologies, tailored yeast strains, and the optimization of hydrolysis and fermentation durations. For instance, co-fermentation strategies, where multiple sugars are fermented simultaneously, have been explored to maximize ethanol production from diverse biomass sources. Additionally, innovations such as fed-batch modes and pre-saccharification techniques allow for the handling of high solid loads, which can lead to improved butanol concentrations (Afedzi & Parakulsuksatid, 2023).

The integration of SSF with other biotechnological approaches, such as genetic engineering of microbial strains and enzyme immobilization, has also shown promise in improving the efficiency and yield of biobutanol production. For example, engineered strains of Clostridium acetobutylicum with enhanced butanol tolerance and production capabilities have been developed, leading to higher yields and reduced fermentation times (Veza et al., 2021).

## 2.7 RESEARCH GAP

Although biobutanol is increasingly recognized as a sustainable biofuel, there is a significant gap in the literature regarding its production specifically from elephant grass (Pennisetum purpureum). While various studies have explored biobutanol production from a range of lignocellulosic feedstocks, the unique characteristics and potential of elephant grass have not been thoroughly investigated. This perennial grass is notable for its high biomass yield and favorable composition, including a cellulose content of approximately 38.75%, hemicellulose at 19.76%, and lignin at 26.99% (Mohammed et al., 2019). However, there is currently no research that specifically examines the production of biobutanol from elephant grass using Simultaneous Saccharification and Fermentation (SSF) techniques.

The absence of research focused on biobutanol production from elephant grass presents an important opportunity to investigate an underutilized feedstock. Addressing this gap could lead to valuable insights into optimizing biobutanol production processes and contribute to the broader field of renewable energy by enhancing the sustainability and efficiency of biofuel production from diverse lignocellulosic sources.

# CHAPTER THREE

# MATERIALS AND METHODOLOGY

## 3.1 LIST OF MATERIALS AND EQUIPMENT

**Table 3.1 List of Materials and Their Uses**

| S/N | MATERIAL | USE |
|---|---|---|
| 1 | Elephant grass | Lignocellulosic biomass used |

**Table 3.2 List of Reagents and Their Uses**

| S/N | REAGENT | USE |
|---|---|---|
| 1 | Sulfuric acid ($H_2SO_4$) | Used or acid pretreatment |
| 2 | Distilled Water | Used for washing biomass after pretreatment and neutralizing the acid. |
| 3 | Cellulase Xylanase, Pectinase Laccase, Beta-Glucosidase | Enzymes are used for enzyme synergy study and hydrolysis of the biomass. |
| 4 | Sodium citrate buffer | Buffer solution is used to maintain pH of the hydrolysate. |
| 5 | 3,5-Dintrosalicylic acid (DNS) | Used for determination of reducing (glucose) sugar. |
| 6 | Filter paper | Used for filtering pretreated biomass. |

| | | |
|---|---|---|
| 7 | Litmus paper | Used to check for the pH of pretreated slurry |
| 8 | Paper tape | For labeling samples |
| 9 | Aluminum foil | Used for protection of samples against external variables like insects |
| 10 | Sodium Azide | Used to prevent the growth of microbes in enzyme cocktail during hydrolysis |
| 11 | Bovine Serum Albumin (BSA) and Bradford reagent | Used for determining the amount of protein content in the enzymes. |
| 12 | Clostridium Acetobutylicum | Enzymes used during fermentation |
| 13 | Phosphate salt ($KH_2PO_4$ and $K_2HPO_4$) buffer | Helps maintain a stable pH during fermentation. |
| 14 | P2 medium Solution | Specialized nutrient solution used in fermentation to support the growth and metabolism of the clostridium species. |

**Table 3.3 List of Apparatus and Their Uses**

| **S/N** | **APPARATUS** | **USE** |
|---|---|---|
| 1 | Filter paper | Used for filtering pretreated biomass. |
| 2 | Litmus paper | Used to check for pH of the pretreated slurry. |
| 3 | Paper tape | For labelling samples. |

| | | |
|---|---|---|
| 4 | Aluminum foil | Used for protection of samples against external variables like insects. |
| 5 | Beakers, conical flasks | Used for holding pretreated and hydrolysate samples. |
| 6 | Pipette | Used for drawing fluids like enzymes, acid. |
| 7 | Measuring cylinder | For measuring fluid level. |
| 8 | Stirrer | Used for stirring solutions. |

**Table 3.4 List of Equipments and Their Uses**

| **S/N** | **EQUIPMENT** | **MODEL** | **USE** |
|---|---|---|---|
| 1 | Autoclave chamber | Ocean Med+ England Model:YX-18LD | Used for carrying out pretreatment process |
| 2 | Weighing balance | Kern Electronic Balance Model:ALS-160 | Used for accurately measuring amounts of solids. |
| 3 | pH scale | PH-009(1)A | Used for checking pH of solutions. |
| 4 | Spectrophotometer | Model:721S Visible Spectrophotometer | Used measuring the shift in absorbance on the 594nm wavelength |

| | | | |
|---|---|---|---|
| 5 | Water bath shaker | Water-Bath Model:DK420 U-Clear | Creates the optimal environmental temperature for carrying out enzymatic hydrolysis. |
| 6 | Incubator | Laboratory Incubator Model:DHP203F | Creates an optimal environmental temperature for carrying out fermentation |
| 7 | Chromatograph | Model-3528D HPLC Chromatograph | Used for stripping Biobutanol from the mixture of Acetone, Biobutanol and Ethanol |

## 3.2 PRETREATMENT

### 3.2.1 BIOMASS COLLECTION AND PREPARATION

Fresh elephant grass was sourced locally and transported to the laboratory for preparation. The grass was initially washed to remove surface impurities such as dust and soil. The cleaned biomass was then sundried for 72 hours and moved to the laboratory to be oven-dried at 60°C for another 48 hours until a constant weight was achieved. This step was crucial in reducing moisture content and improving the efficiency of the subsequent grinding process. The dried biomass was ground into fine particles using a mechanical grinder and sieved to achieve a uniform particle size to optimize enzyme accessibility during hydrolysis.

### 3.2.2 BIOMASS PRETREATMENT

For this study, the Acid Pretreatment method is used (Guo et al., 2022). The optimal temperature conditions and parameter experiments are generated using a previous study's statistical analysis (Egharevba, I.P., Oyakhilome, E.P (2023) "Optimization of Acid Hydrolysis of Elephant Grass for Optimum Fermentable Sugar Yield for Biobutanol Production". Nigerian Institute of Production Engineers). This process uses 2.658ml sulfuric acid, 97.342ml distilled water, and 5g of Elephant Grass.

5g of Elephant Grass is weighed on a weigh balance and transfer to a beaker. Then 97.342ml of distilled water is added to the sample in the beaker. 2.658ml of Sulfuric acid is then carefully added to the solution. This procedure is done with 8 different beakers using the same measurements. These beakers are then properly covered with foil paper and placed in an Autoclave. The autoclave is set to a temperature of 109.344 $^{0}$C. The sample is then pretreated for 42.86 minutes. After which the samples are taken out. The sample in the form of a slurry is then filtered using filter paper into conical flasks and the solid residue will be rinsed thoroughly with distilled water to neutralize the pH. This is done until the sample has achieved a pH of 7.

### 3.2.3 CHARACTERIZATION OF PRETREATED AND UNTREATED FEEDSTOCK

The feedstock is characterized using three different methods such as; Fourier Transform Infrared Microscopy (FTIR), Scanning Electron Microscopy (SEM), and X-ray diffraction (XRD).

#### 3.2.3.1 FOURIER TRANSFORM INFRARED MICROSCOPY (FTIR)

FTIR, which stands for Fourier Transform Infrared spectroscopy, is the preferred technique for conducting infrared (IR) spectroscopy. In this method, IR radiation is directed through a sample,

where a portion of the radiation is absorbed while the remainder is transmitted. The resulting spectrum provides information on molecular absorption and transmission, effectively creating a unique molecular fingerprint for the sample. Just as no two fingerprints are identical, no two distinct molecular structures yield the same IR spectrum, which enhances the utility of IR spectroscopy for various analytical applications. For over 70 years, IR spectroscopy has been a fundamental technique for materials analysis in laboratory settings. An IR spectrum serves as the sample's fingerprint, characterized by absorption peaks that correspond to the vibrational frequencies of the bonds between the atoms constituting the material (Dutta, 2017).

Fourier Transform Infrared Spectroscopy (FTIR) is used to determine the presence of cellulose in biomass samples. Cellulose has a well-known infrared absorption characteristic in the FTIR spectrum. It has strong bands of about 3300 cm-1 (due to O-H stretching) and 2900-2800 $cm^{-1}$ (due to C-H stretching). (Cichosz & Masek, 2019).

3.2.3.2 SCANNING ELECTRON MICROSCOPY (SEM)

The scanning electron microscope (SEM) is a highly versatile instrument utilized for the examination and analysis of microstructural morphology and the characterization of chemical composition. A fundamental understanding of light optics is crucial for grasping the basic principles underlying electron microscopy. The unaided human eye can resolve objects that subtend an angle of approximately 1/60˚, which corresponds to a resolution of roughly 0.1 mm at an optimal viewing distance of 25 cm. In optical microscopy, the resolution limit is approximately 2,000 Å, achieved by magnifying the visual angle through the use of optical lenses(Zhou et al., 2007).

SEM has several advantages over optical microscopy, including a large depth of field that keeps most of the specimen surface in focus regardless of roughness, the ability to achieve much higher magnifications (up to 1,000,000x) with a resolution of 1 nm, and the capacity to gather comprehensive information beyond surface topography, such as crystal structure and electrical properties, enabling confident cross-correlation of data through various imaging techniques(K D Vernon-Parry, Centre for Electronic Materials, 2000)

Scanning Electron Microscopy (SEM) can provide important details about the morphological structure of materials. Cellulose has a fibrous or rod-like shape, which SEM can observe at high magnification. Although SEM can help identify the presence of cellulose based on its typical shape, it cannot be utilized as the primary indicator for determining its existence in an organic substance. Other analytical procedures, such as FTIR or X-ray diffraction (XRD), are typically used to validate the existence of cellulose and differentiate it from other materials with comparable structural properties.

3.2.3.3 X-RAY DIFFRACTION (XRD)

X-ray diffraction (XRD) is an advanced, nondestructive analytical method employed for the examination of a diverse array of materials, including fluids, metals, minerals, polymers, catalysts, plastics, pharmaceuticals, thin-film coatings, ceramics, solar cells, and semiconductors. This technique has numerous practical applications across various industries, such as microelectronics, power generation, and aerospace, among others. XRD analysis is capable of identifying defects within a specific crystal, assessing its resistance to stress, evaluating its texture, determining its size and degree of crystallinity, and analyzing virtually any other structural characteristic related to the sample.

X-ray diffraction (XRD) is a technique used to determine the presence of cellulose in organic samples. Cellulose typically has a crystalline structure, which results in distinct diffraction peaks in the XRD pattern. Cellulose peaks often occur at 2θ values of 14.8°, 16.3°, and 22.6°. The presence of cellulose in a sample can be detected and established by comparing its XRD pattern to a known cellulose diffraction pattern.

## 3.3 PROTEIN ANALYSIS

Protein analysis is carried out using distilled water, BSA, and Bradford reagent. Firstly 0.1g BSA is mixed with 10 ml of distilled water then 200µl of Bradford is added. The whole procedure is then repeated but with 0.2g, 0.3g, 0.4g, and 0.5g of BSA. All mixtures in separate test tubes are taken to the UV spectrophotometer after being left to stand for 10 minutes to test for absorbance. The absorbance values of the standards are then plotted on a graph with the x-axis representing concentration and the y-axis representing absorbance. Then the equation of the Bradford assay standard curve is calculated.

The same procedure is then carried out using separate enzymes; cellulose, xylnase, pectinase, laccase, beta-glucosidase. The enzymes took the place of the 10ml distilled water in separate runs. The whole mixture is then taken to the UV spectrophotometer for absorbance test after being left to stand for 10 minutes. The sample protein concentration is then calculated by plugging the absorbance value in for y in the standard curve equation and solving for x for each sample. (*Bradford Assay | Protein, Protocol & Methods - Lesson | Study.Com*, n.d.). With these values, the amount of enzymes in milliliter needed for each sample is then calculated.

$$\text{Amount of protein(mg/g of biomass)} * \frac{\text{Amount of g of biomass}}{\text{Amount of protein (mg/ml)}} = \text{Volume of enzyme} \quad (3.1)$$

## 3.4 REDUCING SUGAR TEST

### 3.4.1 PREPARATION OF DNS REAGENT SOLUTION

DNS is prepared by dissolving 1.0g of 3,5-dinitrosalicylic acid in 50 ml of water then slowly adding 30g of sodium potassium tartrate tetrahydrate ($KNaC_4H_4O_6 \cdot 4H_2O$) to the mixture and adding 20 ml of 2N NaOH then diluting to a final volume of 100 ml with distilled water after preparation it is stored in a cool and dark location to prevent reaction with sunlight. (How Do I Prepare DNS Reagents? | ResearchGate, n.d.; Mystrica | Display, n.d.).

### 3.4.2 PREPARATION OF GLUCOSE STANDARD CURVE

The glucose test is carried out by preparing a standard curve of glucose solutions with concentrations ranging from 0 to 1 g/L, adding 3 mL of DNS reagent to each glucose solution, followed by heating, cooling, and measuring the absorbance. Finally, UV light absorption at 315 nm is read using a UV spectrophotometer. After that, a graph of absorbance versus concentration is plotted, and a best-fit line is drawn (Kruger, 2009).

## 3.5 HYDROLYSIS

Enzymatic hydrolysis is carried out using 100 ml conical flasks in a water bath shaker at 50$^{o}$C in 0.05M sodium citrate buffer at pH 4.8 (made from adding **7**.676g sodium citrate and 4.4g citric

acid to 800ml distilled water and making up to 1L mark). The buffer contained 1 wt% sodium azide solution (prepared by dissolving 1g of sodium azide in 1L of distilled water) to prevent microbial contamination.

The Solid loading is 5g on a dry weight basis, then finally each enzyme alone (i.e. cellulose, pectinase, laccase, beta-glucosidase, xylanse) at different doses (10 to 75mg protein per g biomass) is used in 6 different flasks of different enzyme concentration to hydrolyze the pretreated biomass for 6 hours. The sugar yield from the hydrolysis is then recorded through the reducing sugar test. (Agrawal et al., 2018b).

## 3.6 SYNERGY STUDIES

For the second phase of enzyme hydrolysis, cellulase is supplemented with the other accessory enzyme preparation (xylanase, pectinase, laccase, beta-glucosidase) in a 1:1 ratio at different doses (10 to 75mg protein per g biomass), just like with cellulase alone, and is used to hydrolyze the pretreated biomass for 6 hours. The sugar yield from the hydrolysis is then recorded through the reducing sugar test (Agrawal et al., 2018b).

## 3.7 DETERMINATION OF REDUCING SUGAR IN HYDROLYSATE

3ml of DNS is drawn with a pipette and placed in a test tube containing 1ml of the hydrolysate mixture. The mixture is then heated to about $40^0$C and cooled before being tested for absorbance using a UV spectrophotometer with light absorption at 540 nm.

Then the values obtained from the DNS test are traced on the previously mentioned graph to calculate the reducing sugar, using the equation derived from the plot of the best line of fit in glucose test. Percentage hydrolysis is calculated using the formula provided by (Agrawal et al., 2018b);

$$\frac{\text{Concentration of reducing sugar(g) *0.9 *100}}{\text{Content of the biomass (g)}} \text{ Carbohydrate} \quad (3.2)$$

A 2-D plot of sugar yield against enzyme concentration will be generated for each case to determine which accessory enzyme showed synergy with cellulase. Only the accessory enzymes that proved to be synergistic will be employed in optimization.

## 3.8 OPTIMIZATION

Depending on the number of accessory enzymes that showed synergy, a series of experiments is designed using design expert, having between 20 – 30 runs. The synergistic accessory enzymes will be the factors (ranging have between 2 - 4 factors). The output for the experimental design would be sugar yield (hydrolysis percent). The number of runs will determine the number of conical flasks that would be needed, as the hydrolysis runs will be done in conical flasks held in a water bath shaker at 50$^{o}$C.

## 3.9 SIMULTANEOUS SACCHARIFICATION AND FERMENTATION

### 3.9.1 CULTURE PREPARATION (PROPAGATION)

Clostridium spp spores is stored in distilled water at 4 $^{o}$C. The spores are heat shocked at 75 -80 $^{o}$C for 2 minutes, then transferred into cooked meat medium (CMM). In order to prepare liquid CMM, 2.5 g solid CMM pellets and 0.2 – 0.4 g glucose is suspended in 20ml distilled water in sealed conical flasks. The mixture will be autoclaved at 121 $^{o}$C for 15 minutes, and then cooled to 35 $^{o}$C. The heat shocked spores is incubated at 35 $^{o}$C for 16 hours so as to foster inoculum development.

### 3.9.2 COCKTAIL PREPARATION

The optimum elephant grass hydrolysate concentration is adjusted using phosphate buffer, and the initial pH value will be adjusted to different values (4.5 – 5.5) using 5 M of $K_2HPO_4$ or $KH_2PO_4$. Following growth, varying sized (1-20% (v/v) of the developing inoculum is transferred to 100ml of P2 medium.

The P2 medium solution contains: Glucose (80 g/l), yeast extract (1g/l), buffer solution: $K_2HPO_4$ (0.5g/l), $KH_2PO_4$ (0.5g/l), ammonium acetate (2.2g/l), vitamins (1mg/l para-amaino-benzoic acid, 1mg/l thiamine and 0.01mg/l biotin), and mineral salt (0.2g/l $MgSO_4.7H_2O$, 0.01g/l $MnSO_4.H_2O$, 0.01 g/l $FeSO_4.7H_2O$, 0.01 g/l NaCl)

2ml portion of each filter-sterilized P2 solution is added to the prepared media in a sealed conical flask. Various inoculum sizes is inoculated into P2 medium with feedstock hydrolysate medium. Fermentation is carried out at varying temperatures in a shaker incubator for 48hrs. 2 ml of sample will be collected for analysis.

## 3.10 OPTIMIZATION

The parameter optimization of SSF will be conducted using central composite design (CCD) in Design Expert Software. Three independent variables will be selected and they include: Initial pH (4.5 - 5.5), Temperature (35 - 45$^{o}$C) and Inoculum size (1-20%v/v) with ABE yield as a response. The yield of ABE will be measured using the High-Pressure Liquid Chromatograph. This is the main separation technique used to measure the amount of the ABE using standard Acetone and Butanol and Ethanol to measure the separation speed of these component.

## 3.11 DESIGN OF EXPERIMENT

Design of Experiments (DOE) is statistical tool deployed in various types of system, process and product design, development and optimization. It has a variety of uses in optimization, comparisons, variable screening, transfer function identification and robust design. It provides researchers with a tool to ideate, plan, execute experiments as well as evaluate and interpret data. It has grown in use in manufacturing and non- manufacturing areas including biochemistry, medicine, engineering, physics, computer science, etc. It is one of the most popular tool in these areas. Design of Experiments (DOE) mathematical methodology used for planning and conducting experiments as well as analyzing and interpreting data obtained from the experiments. It is a branch of applied statistics that is used for conducting scientific studies of a system, process or product in which input variables (Xs) were manipulated to investigate its effects on measured response variable (Y). With time, DOE has become a crucial tool in decision making in developing new or improving old process. DOE does not old find application in

engineering and scientific fields but also in marketing, administration, architecture, etc. It is useful in physical as well as computer simulation processes.

Ronald A. Fisher was the first to use design of experiment in an agricultural project investigating increasing crop yield between spring and fall season. George Box is credited for Response Surface methodology (RSM) in his work in optimizing experimental design

### 3.11.1 EXPERIMENTAL DESIGN OF SIMULTANEOUS SACCHARIFICATION AND FERMENTATION USING RESPONSE SURFACE METHODOLOGY(RSM)

A central composite design (factors, k=3) with input variables- Initial pH, Temperature, Innoculum size and response Butanol yield was carried out. The range of values selected for each was Initial ph (3.5- 7.5), Temperature (25- 45$^{o}$C) and Inoculum size(1-20%v/v). The second order polynomial regression model for this experimental design was

$$Y = a_1X_1 + a_2X_2 + a_3X_3 + a_{11}X_{12} + a_{22}X_2^2 + a_{33}X_3^2 + a_{12}X_1X_2 + a_{23}X_2X_3 + a_0 \quad (3.3)$$

Where Y = Butanol yield,

ai = linear coefficients

aii = the quadratic coefficient,

aij = the cross sproduct coefficients; and

a0 = the model constant

# CHAPTER FOUR

# RESULTS AND DISCUSSION

All the procedures in the previous chapters were followed and the results are as follows

## 4.1 CHARACTERIZATION OF ELEPHANT GRASS

Elephant grass was characterized using the following methods:

- X-ray diffraction (XRD)
- Fourier Transform Infrared Spectroscopy (FTIR)
- Scanning Electron Microscopy (SEM)

### 4.1.1 X-RAY DIFFRACTION ANALYSIS

UNTREATED ELEPHANT GRASS

The X-ray diffraction (XRD) analysis of untreated elephant grass revealed a complex crystalline structure with several prominent phases. The XRD graph shows strong diffraction peaks at 16.59° and 22.27° (2θ values), indicating a highly ordered crystalline structure. The dominant phases identified in the untreated sample include urea, reflikite, aluminuim phosphate, chaoite, hanksite and silicon oxide.

The XRD pattern of untreated elephant grass shows a dense and compact structure, with strong peaks corresponding to cellulose, hemicellulose, and lignin. The presence of these phases suggests that the untreated material contains a mix of organic and inorganic components, which could hinder enzymatic access during hydrolysis.

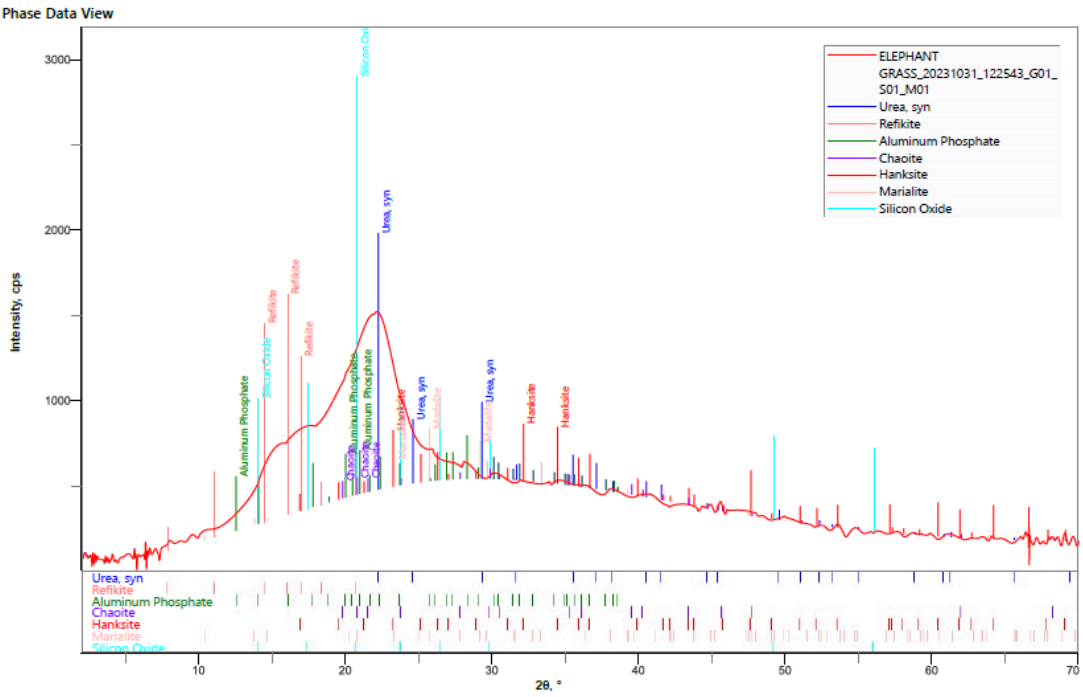


***Fig 4.1: Result of XRD of Untreated Elephant Grass***

PRETREATED ELEPHANT GRASS

After pretreatment, the XRD analysis of elephant grass showed significant changes in the crystalline structure and phase composition. The XRD graph for the pretreated sample shows a shift in peak positions, with the most prominent peak at 26.50° (2θ value). The dominant phases identified in the pretreated sample include urea, graphite, melilte and cristobalite.

The XRD pattern of pretreated elephant grass shows a reduction in crystallinity and the emergence of amorphous structures. The disappearance of phases such as Reflikite, Aluminum Phosphate, and Hanksite, and the appearance of Graphite and Cristobalite suggest that the pretreatment process successfully removed non-cellulosic materials and led to partial

carbonization of organic components. This structural modification is crucial, as high crystallinity in lignocellulosic biomass is known to limit enzymatic hydrolysis efficiency.

The reduction in crystallinity and the increase in amorphous structures in the pretreated sample confirm that the pretreatment process effectively disrupted the cellulose structure, making it more accessible for enzymatic action. This structural modification is expected to enhance the saccharification process and improve the overall efficiency of simultaneous saccharification and fermentation (SSF) for biofuel production.

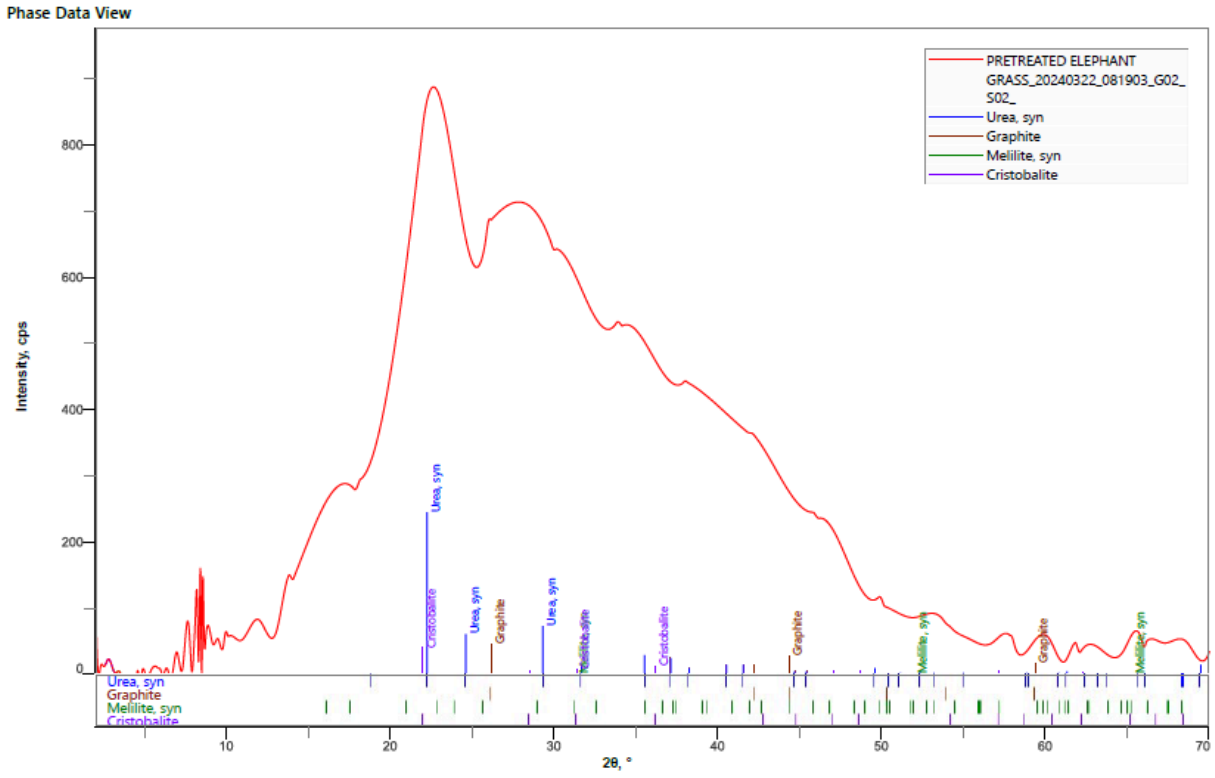


***Fig 4.2: Result of XRD of Treated Elephant Grass***

### 4.1.2 FOURIER TRANSFORM INFRARED SPECTROSCOPY FTIR

UNTREATED ELEPHANT GRASS

In the untreated elephant grass, characteristic peaks corresponding to cellulose, hemicellulose, and lignin were observed. The broad absorption around 3377 $cm^{-1}$ represents hydroxyl (-OH) stretching, indicating the presence of cellulose and hemicellulose. Peaks at 1729.5 $cm^{-1}$ (C=O stretching) and 1600 $cm^{-1}$ (C=C aromatic rings) suggest the presence of hemicellulose and lignin, respectively. Additionally, the peak at 1043.7 $cm^{-1}$ (C-O-C stretching) is attributed to glycosidic linkages in cellulose. These peaks confirm the presence of a complex lignocellulosic structure in the untreated elephant grass, which is typical for raw biomass.

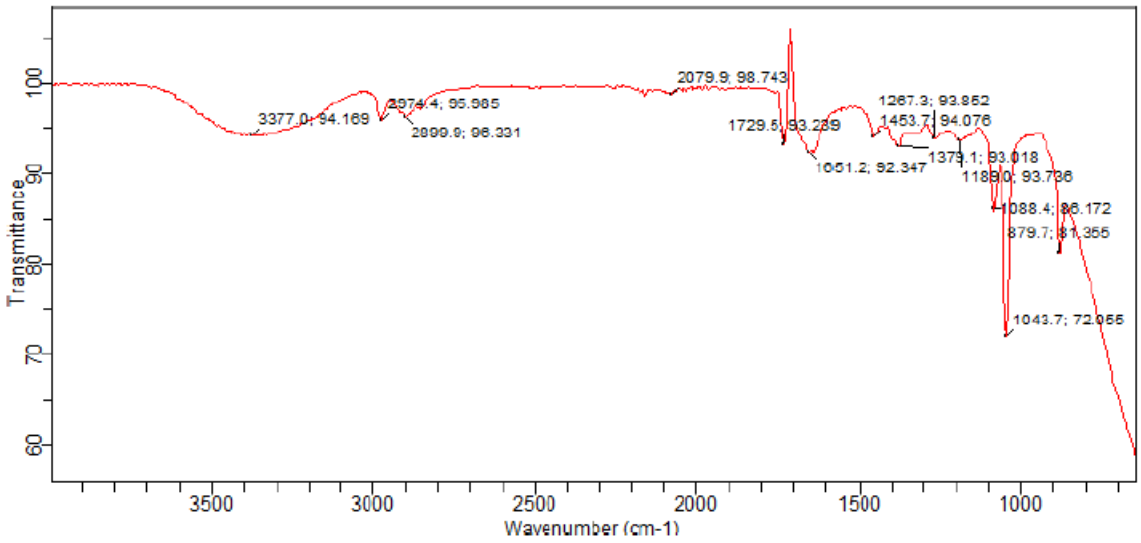


***Fig 4.3: Result of FTIR of Untreated Elephant Grass***

PRETREATED ELEPHANT GRASS

After acid pretreatment, notable changes in the FTIR spectrum indicate the removal of hemicellulose and partial delignification. The C=O peak at 1729.5 $cm^{-1}$ is significantly reduced or absent, confirming the degradation of hemicellulose. The C=C peak at 1600 $cm^{-1}$ is also reduced, suggesting partial lignin removal. Additionally, the C-O-C peak at 1043.7 $cm^{-1}$ becomes more pronounced, indicating increased cellulose exposure. These changes result in higher accessibility of cellulose for enzymatic hydrolysis, which is critical for improving fermentable sugar release in Simultaneous Saccharification and Fermentation (SSF).

Some key observations include: The hydroxyl (-OH) stretching peak around 3377 $cm^{-1}$ remains prominent in both untreated and pretreated samples, indicating the presence of cellulose; The C=O stretching peak at 1729.5 $cm^{-1}$ is significantly reduced after pretreatment, confirming the removal of hemicellulose; The C=C aromatic ring peak at 1600 $cm^{-1}$ is reduced, suggesting partial lignin removal; The C-O-C stretching peak at 1043.7 $cm^{-1}$ becomes more pronounced after pretreatment, indicating increased cellulose exposure.

The FTIR analysis confirms that the acid pretreatment effectively modifies the elephant grass structure by removing hemicellulose and reducing lignin content, thereby enhancing enzyme accessibility. These structural changes are expected to improve the efficiency of enzymatic hydrolysis, leading to higher fermentable sugar yields and, consequently, improved biobutanol production during fermentation.

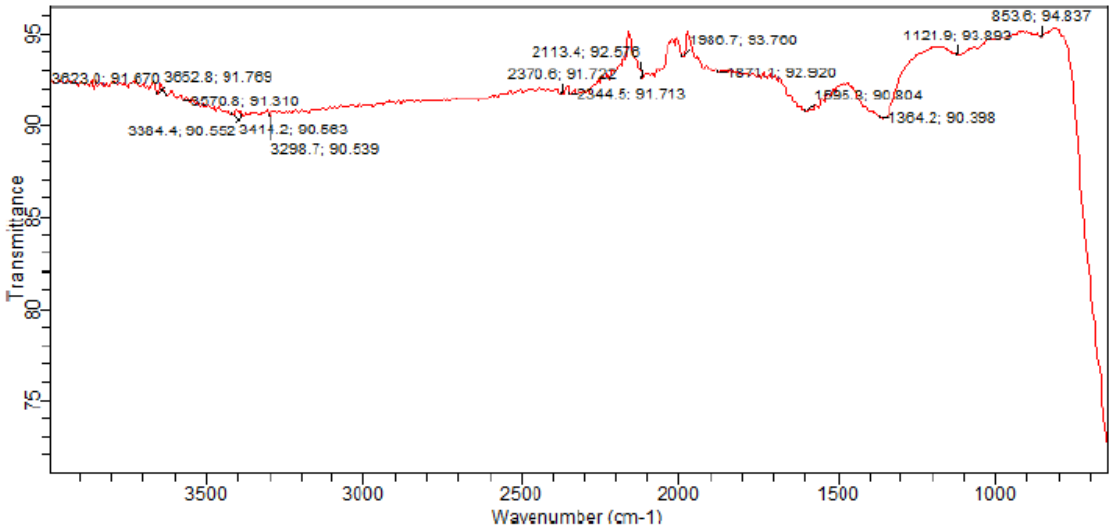


***Fig 4.4: Result of FTIR of Treated Elephant Grass***

### 4.1.3 SCANNING ELECTRON MICROSCOPY (SEM)

UNTREATED ELEPHANT GRASS

Scanning Electron Microscopy (SEM) analysis was conducted to observe the structural modifications in cassava bagasse before and after pretreatment. The SEM images of untreated elephant grass reveal a highly compact and granular structure, typical of lignocellulosic biomass. The images at 500x, 1000x, and 2000x magnification provide insights into the morphological characteristics of the untreated sample.

The untreated elephant grass exhibits a dense and tightly packed surface, indicating the presence of an intact lignocellulosic matrix. This dense structure suggests a strong lignin barrier, which limits enzymatic accessibility to cellulose and hemicellulose, thereby reducing the efficiency of

hydrolysis. The surface of the untreated sample appears relatively smooth, with minimal porosity. This smoothness further demonstrates the natural resistance of lignocellulosic biomass to enzymatic hydrolysis. The lack of significant surface roughness implies that the biomass has a protective outer layer, which inhibits enzyme penetration and sugar release.

At higher magnification (2000x), the surface shows a granular texture, which is characteristic of untreated biomass. This granularity is likely due to the presence of lignin and hemicellulose, which form a protective layer around the cellulose fibers. The presence of these components strengthens the structural integrity of the biomass but simultaneously restricts enzymatic action.

The SEM analysis of untreated elephant grass confirms that the material has a highly resistant structure, which is expected to hinder enzymatic hydrolysis and reduce the efficiency of sugar release during fermentation. This highlights the necessity of pretreatment to disrupt the lignocellulosic matrix and improve accessibility for enzymatic breakdown.

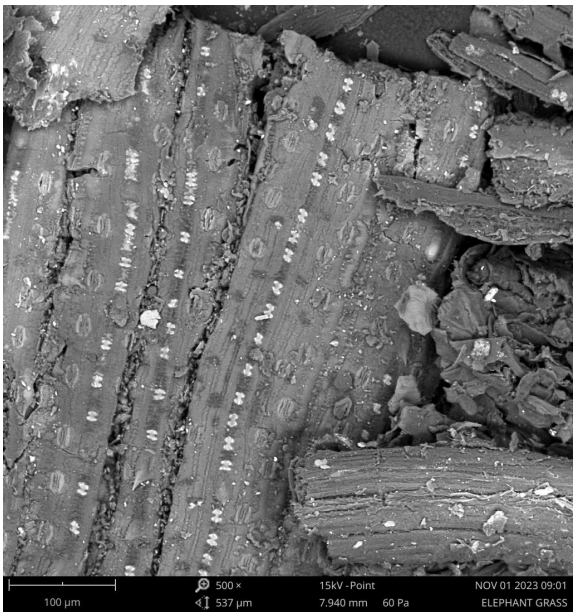


*Fig 4.5a: Result of SEM of Untreated Elephant Grass at 500x Magnification*

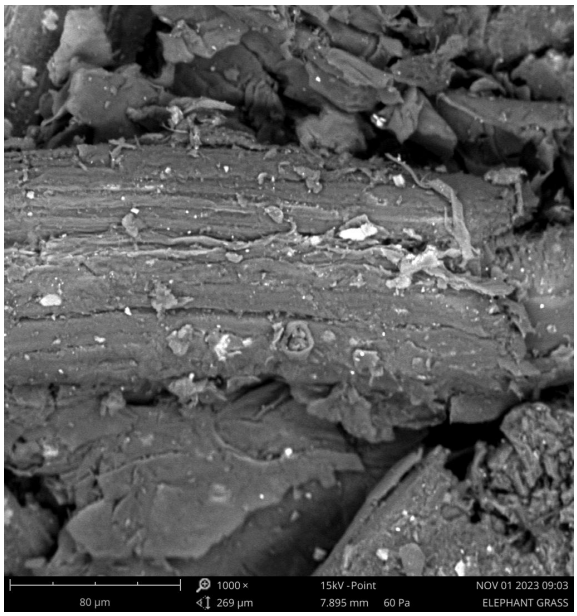


*Fig 4.5b: Result of SEM of Untreated Elephant Grass at 1000x Magnification*

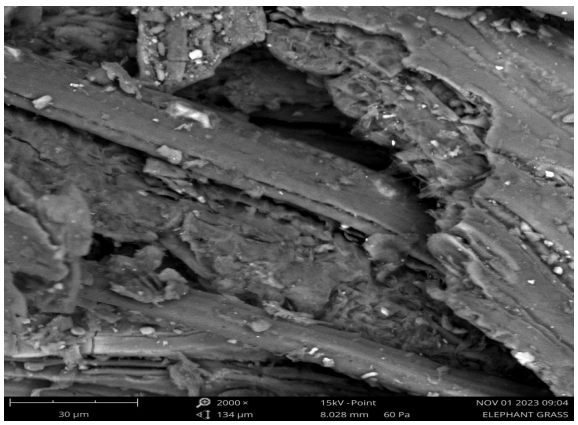


*Fig 4.5c: Result of SEM of Untreated Elephant Grass at 2000x Magnification*

***Fig 4.5: Result of SEM of Untreated Elephant Grass***

PRETREATED ELEPHANT GRASS

The SEM images of pretreated elephant grass show significant morphological changes compared to the untreated sample. The images at 500x, 1000x, and 2000x magnification provide clear evidence of structural modifications resulting from the pretreatment process.

The pretreated elephant grass exhibits a more fibrous and disrupted structure compared to the untreated sample. This structural disintegration is a result of the pretreatment process, which likely removed lignin and hemicellulose, exposing the cellulose fibers. The disruption of the compact lignocellulosic structure enhances enzymatic accessibility, making the biomass more susceptible to hydrolysis. The surface of the pretreated sample appears more porous and rough, indicating that the pretreatment process successfully broke down the lignocellulosic matrix. This increased porosity enhances the surface area available for enzymatic action, which is crucial for efficient hydrolysis. The formation of pores and cracks facilitates better enzyme penetration, thereby improving sugar release.

At higher magnification (2000x), the pretreated sample shows exposed cellulose fibers, which are more accessible to enzymes. This exposure is a direct result of the removal of lignin and hemicellulose, which were acting as barriers in the untreated sample. The presence of exposed cellulose enhances the efficiency of enzymatic hydrolysis, leading to improved sugar yields.

The SEM analysis of pretreated elephant grass confirms that the pretreatment process effectively disrupted the lignocellulosic structure, increasing porosity and surface area. These modifications are expected to enhance enzymatic hydrolysis, leading to improved sugar release and higher biofuel yields during fermentation.

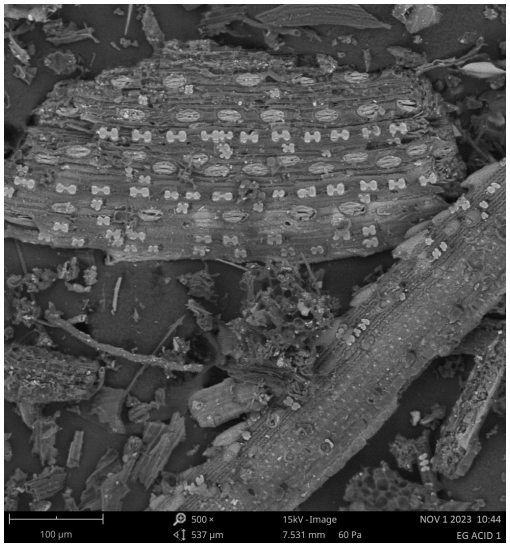


*Fig 4.6a: Result of SEM of Untreated Elephant Grass at 500x Magnification*

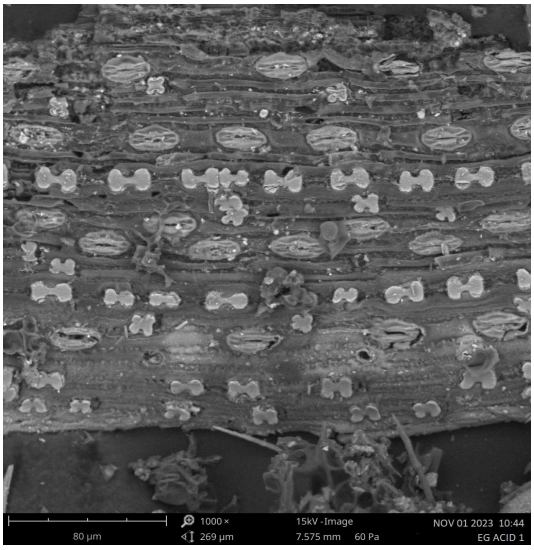


*Fig 4.6b: Result of SEM of Untreated Elephant Grass at 1000x Magnification*

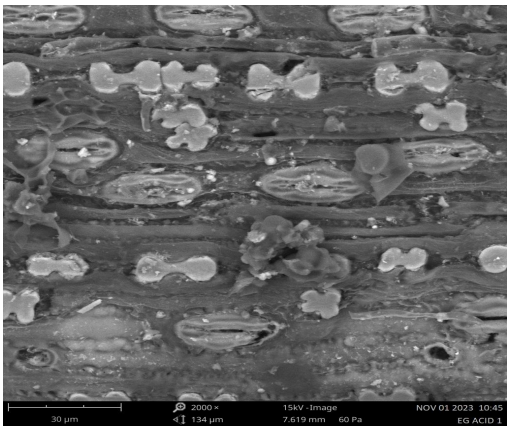


*Fig 4.6c: Result of SEM of Untreated Elephant Grass at 2000x Magnification*

***Fig 4.6: Result of SEM of Untreated Elephant Grass***

## 4.2 PROTEIN ANALYSIS

**Table 4.1: Table of Protein Analysis for Enzymes**

| ENZYME | PROTEIN (mg/ml) | FP(IU/ML) |
|---|---|---|
| CELLULASE | 12.19 | 7.2 |
| BETA-GLUCOSIDASE | 14.2 | 15.9 |
| XYLANASE | 14.0 | 15.1 |
| LACCASE | 14.6 | 20 |
| PECTINASE | 13.4 | 20.9 |

**Table 4.2: Table of Volume of Enzyme**

| mg/g of biomass | Mg of protein | Volume of cellulase | Volume of Beta-glucosidase | Volume of Xylanase | Volume of Lacase | Volume of Pectinase |
|---|---|---|---|---|---|---|
| 0 | 0 | 0.00 | 0.00 | 0.00 | 0.00 | 0.00 |
| 10 | 50 | 4.10 | 3.52 | 3.57 | 3.42 | 3.73 |
| 20 | 100 | 8.20 | 7.04 | 7.14 | 6.85 | 7.46 |
| 30 | 150 | 12.31 | 10.56 | 10.71 | 10.27 | 11.19 |
| 40 | 200 | 16.41 | 14.08 | 14.29 | 13.70 | 14.93 |
| 50 | 250 | 20.51 | 17.61 | 17.86 | 17.12 | 18.66 |

| | | | | | | |
|---|---|---|---|---|---|---|
| 75 | 375 | 30.76 | 26.41 | 26.79 | 25.68 | 27.99 |

## 4.3 REDUCING SUGAR TES

**Table 4.3: Table of Reducing Sugar Test**

| **Absorbance** | **Glucose conc. (g/L)** |
|---|---|
| 0 | 0 |
| 0.36 | 0.2 |
| 0.604 | 0.4 |
| 1.107 | 0.6 |
| 1.426 | 0.8 |
| 1.592 | 1 |

### 4.3.1 GLUCOSE STANDARD CURVE

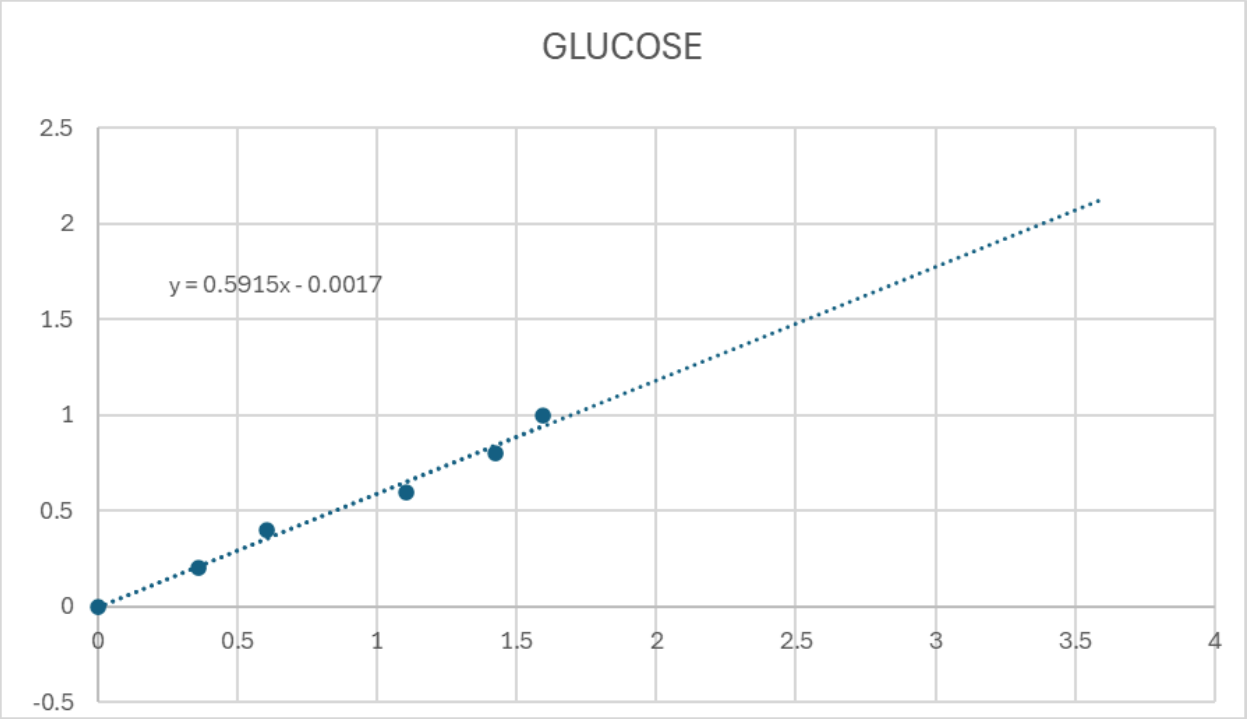


*Fig 4.7: Glucose standard curve*

## 4.4 HYDROLYSIS

**Table 4.4: Table of Hydrolysis % for each Enzyme and its Synergy with Cellulase**

| **Enzyme** | **mg/g of biomass** | **Absorbance (6hrs)** | **Conc. Of Reducing sugar** | **Hydrolysis Percentage** |
|---|---|---|---|---|
| Cellulase | 0.00 | 0 | 0 | 0% |
| Cellulase | 10.00 | 0.119 | 0.2134421 | 3% |

| | | | | |
|---|---|---|---|---|
| Cellulase | 20.00 | 0.193 | 0.3367187 | 5% |
| Cellulase | 30.00 | 0.37 | 0.631583 | 9% |
| Cellulase | 40.00 | 0.187 | 0.3267233 | 5% |
| Cellulase | 50.00 | 0.236 | 0.4083524 | 6% |
| Cellulase | 75.00 | 0.39 | 0.664901 | 10% |
| Pectinase | 0.00 | 0 | 0 | 0% |
| Pectinase | 10.00 | 0.136 | 0.2417624 | 3% |
| Pectinase | 20.00 | 0.121 | 0.2167739 | 3% |
| Pectinase | 30.00 | 0.08 | 0.148472 | 2% |
| Pectinase | 40.00 | 0.108 | 0.1951172 | 3% |
| Pectinase | 50.00 | 0.137 | 0.2434283 | 4% |
| Pectinase | 75.00 | 0.087 | 0.1601333 | 2% |
| Xylanse | 0.00 | 0 | 0 | 0% |
| Xylanse | 10.00 | 0.125 | 0.2234375 | 3% |
| Xylanse | 20.00 | 0.275 | 0.4733225 | 7% |
| Xylanse | 30.00 | 0.12 | 0.215108 | 3% |

| | | | | |
|---|---|---|---|---|
| Xylanse | 40.00 | 0.111 | 0.2001149 | 3% |
| Xylanse | 50.00 | 0.076 | 0.1418084 | 2% |
| Xylanse | 75.00 | 0.368 | 0.6282512 | 9% |
| Beta-Glucosidase | 0.00 | 0 | 0 | 0% |
| Beta-Glucosidase | 10.00 | 0.222 | 0.3850298 | 6% |
| Beta-Glucosidase | 20.00 | 0.165 | 0.2900735 | 4% |
| Beta-Glucosidase | 30.00 | 0.186 | 0.3250574 | 5% |
| Beta-Glucosidase | 40.00 | 0.364 | 0.6215876 | 9% |
| Beta-Glucosidase | 50.00 | 0.289 | 0.4966451 | 7% |
| Beta-Glucosidase | 75.00 | 0.299 | 0.5133041 | 7% |
| Lacase | 0.00 | 0 | 0 | 0% |
| Lacase | 10.00 | 0.194 | 0.3383846 | 5% |
| Lacase | 20.00 | 0.513 | 0.8698067 | 13% |
| Lacase | 30.00 | 0.597 | 1.0097423 | 15% |
| Lacase | 40.00 | 0.417 | 0.7098803 | 10% |
| Lacase | 50.00 | 0.647 | 1.0930373 | 16% |

| | | | | |
|---|---|---|---|---|
| Lacase | 75.00 | 0.517 | 0.8764703 | 13% |
| Cellulase + beta-glucosidase | 0.00 | 0 | 0 | 0% |
| Cellulase + beta-glucosidase | 10.00 | 0.271 | 0.4666589 | 7% |
| Cellulase + beta-glucosidase | 20.00 | 0.265 | 0.4566635 | 7% |
| Cellulase + beta-glucosidase | 30.00 | 0.384 | 0.6549056 | 9% |
| Cellulase + beta-glucosidase | 40.00 | 0.466 | 0.7915094 | 11% |
| Cellulase + beta-glucosidase | 50.00 | 0.479 | 0.8131661 | 12% |
| Cellulase + beta-glucosidase | 75.00 | 0.5 | 0.84815 | 12% |
| Cellulase + Lacase | 0.00 | 0 | 0 | 0% |
| Cellulase + Lacase | 10.00 | 0.871 | 1.4661989 | 21% |
| Cellulase + Lacase | 20.00 | 0.765 | 1.2896135 | 19% |
| Cellulase + Lacase | 30.00 | 0.799 | 1.3462541 | 19% |
| Cellulase + Lacase | 40.00 | 0.811 | 1.3662449 | 20% |
| Cellulase + Lacase | 50.00 | 0.832 | 1.4012288 | 20% |
| Cellulase + Lacase | 75.00 | 0.854 | 1.4378786 | 21% |
| Cellulase + Pectinase | 0.00 | 0 | 0 | 0% |

| | | | | |
|---|---|---|---|---|
| Cellulase + Pectinase | 10.00 | 0.046 | 0.0918314 | 1% |
| Cellulase + Pectinase | 20.00 | 0.13 | 0.231767 | 3% |
| Cellulase + Pectinase | 30.00 | 0.075 | 0.1401425 | 2% |
| Cellulase + Pectinase | 40.00 | 0.055 | 0.1068245 | 2% |
| Cellulase + Pectinase | 50.00 | 0.063 | 0.1201517 | 2% |
| Cellulase + Pectinase | 75.00 | 0.054 | 0.1051586 | 2% |
| cellulase and xylanase | 0.00 | 0 | 0 | 0% |
| cellulase and xylanase | 10.00 | 0.311 | 0.5332949 | 8% |
| cellulase and xylanase | 20.00 | 0.36 | 0.614924 | 9% |
| cellulase and xylanase | 30.00 | 0.333 | 0.5699447 | 8% |
| cellulase and xylanase | 40.00 | 0.424 | 0.7215416 | 10% |
| cellulase and xylanase | 50.00 | 0.314 | 0.5382926 | 8% |
| cellulase and xylanase | 75.00 | 0.41 | 0.698219 | 10% |

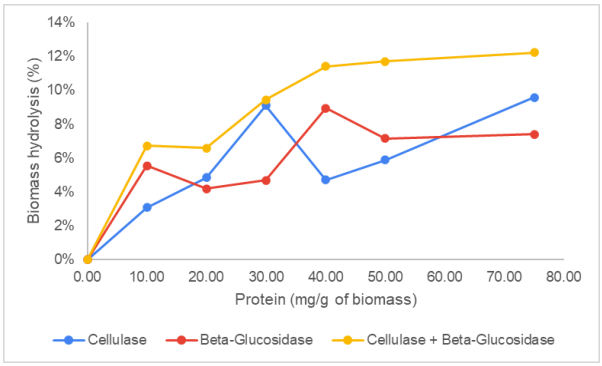


*Fig 4.8a: Plot of Enzyme Synergy for Beta-Glucosidase*

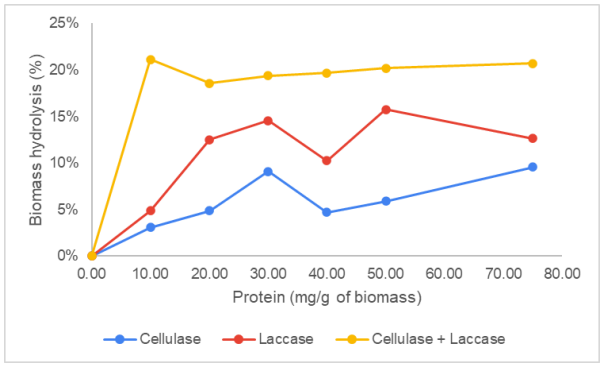


*Fig 4.8b: Plot of Enzyme Synergy for Laccase*

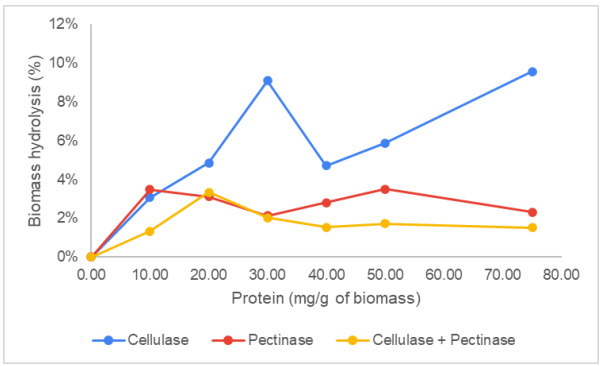


*Fig 4.8c: Plot of Enzyme Synergy forPectinase*

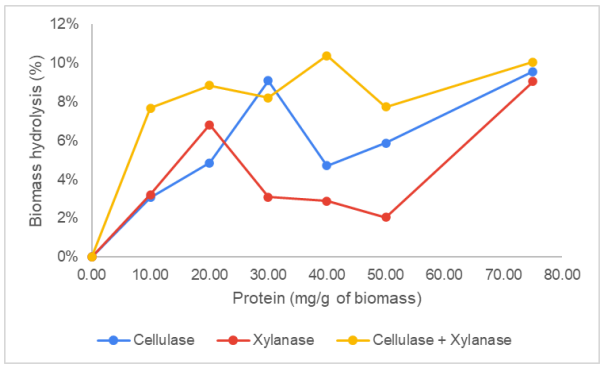


*Fig 4.8d: Plot of Enzyme Synergy for Xylanase*

***Fig 4.8: Plot of Enzyme Synergy***

### 4.4.1 DEGREE OF SYNERGY

From the plots in Figure 4.8, it can be clearly seen that 3 of the 4 enzymes showed synergy (i.e Degree of Synergy > 1): Beta-Glucosidase, Laccase and Xylanase.

### 4.4.2 OPTIMIZATION OF HYDROLYSIS

The values of mg/g of biomass from one peak to the next peak was recorded for all the enzymes that showed synergy. The values were used in design expert as the factors for optimization. They include; 10-50 mg/g for Beta Glucosidase, 10-40 mg/g for Laccase, 10-20 mg/g for Xylanase. The response was Hydrolysis percent. With a constant amount of Cellulase (10 mg/g), the corresponding optimization results were then generated.

### 4.4.3 RESPONSE SURFACE METHODOLOGY (RSM) MODEL ANALYSIS FOR OPTIMUM ENZYME HYDROLYSIS

#### 4.4.3.1 DESIGN SUMMARY

**Table 4.5: Table of Design Summary**

| | | | |
|---|---|---|---|
| Study Type | **Response Surface** | **Subtype** | **Randomized** |
| Design Type | Central Composite | **Runs** | 20.00 |
| Design Model | Quadratic | **Blocks** | No Blocks |

#### 4.4.3.2 FACTORS

**Table 4.6: Table of Factors**

| Factor | Name | Units | Type | SubType | Minimum | Maximum | Coded Low | Coded High | Mean | Std. Dev. |
|---|---|---|---|---|---|---|---|---|---|---|

| | | | | | | | | | | |
|---|---|---|---|---|---|---|---|---|---|---|
| A | Beta-G | mg/g | Numeric | Continuous | 2.10 | 67.90 | -1 ↔ 10.00 | +1 ↔ 60.00 | 35.00 | 19.42 |
| B | Laccase | mg/g | Numeric | Continuous | 3.68 | 56.32 | -1 ↔ 10.00 | +1 ↔ 50.00 | 30.00 | 15.54 |
| C | Xylanase | mg/g | Numeric | Continuous | 5.26 | 44.74 | -1 ↔ 10.00 | +1 ↔ 40.00 | 25.00 | 11.65 |

4.4.3.3 RESPONSE

**Table 4.7: Table of Factors**

| Response | Name | Units | Observations | Minimum | Maximum | Mean | Std. Dev. | Ratio |
|---|---|---|---|---|---|---|---|---|
| R1 | Response | | 20.00 | 4.7 | 10 | 6.79 | 1.41 | 2.13 |

### 4.4.4 RESULT

The experimental design for the enzyme hydrolysis of elephant grass and the response (hydrolysis %) is shown in the table. In order to generate these runs, the Response Surface Methodology (RSM) was employed using three input variables (beta-glucosidase, laccase and xylanase), and this generated 20 experimental runs.

**Table 4.8: Table of Result of Response for RSM**

| Std | Run for Elephant Grass | Block | Factor Beta-G mg/g | Factor Laccasse mg/g | Factor Xylanse mg/g | Constant Cellulase mg/g | Hydrolysis Percent |
|---|---|---|---|---|---|---|---|
| 10 | 1 | Block 1 | 67.9 | 30 | 25 | 10 | 24.95 |
| 18 | 2 | Block 1 | 35 | 30 | 25 | 10 | 34.74 |
| 15 | 3 | Block 1 | 35 | 30 | 25 | 10 | 32.95 |
| 16 | 4 | Block 1 | 35 | 30 | 25 | 10 | 33.74 |
| 4 | 5 | Block 1 | 60 | 50 | 10 | 10 | 35.84 |
| 1 | 6 | Block 1 | 10 | 10 | 10 | 10 | 43.85 |
| 11 | 7 | Block 1 | 35 | 3.68 | 25 | 10 | 48.56 |
| 6 | 8 | Block 1 | 60 | 10 | 40 | 10 | 37.26 |
| 19 | 9 | Block 1 | 35 | 30 | 25 | 10 | 34.95 |

| | | | | | | | |
|---|---|---|---|---|---|---|---|
| 13 | 10 | Block 1 | 35 | 30 | 5.26 | 10 | 41.98 |
| 7 | 11 | Block 1 | 10 | 50 | 40 | 10 | 44.37 |
| 17 | 12 | Block 1 | 35 | 30 | 25 | 10 | 34.95 |
| 2 | 13 | Block 1 | 60 | 10 | 10 | 10 | 43.49 |
| 14 | 14 | Block 1 | 35 | 30 | 44.74 | 10 | 36.25 |
| 9 | 15 | Block 1 | 2.1 | 30 | 25 | 10 | 36.26 |
| 3 | 16 | Block 1 | 10 | 50 | 10 | 10 | 46.21 |
| 12 | 17 | Block 1 | 35 | 56.32 | 25 | 10 | 41.12 |
| 8 | 18 | Block 1 | 60 | 50 | 40 | 10 | 28.95 |
| 5 | 19 | Block 1 | 10 | 10 | 40 | 10 | 45.1 |
| 20 | 20 | Block 1 | 35 | 30 | 25 | 10 | 32.15 |

Comparing the actual and the predicted Hydrolysis % values obtained, it is observed that there is a good fit between the actual and predicted values, as all data points are clustered around the

45-degree diagonal line as shown in the predicted versus actual plot in Figure 4.9. This indicates that there is minimal deviation between the actual and predicted values

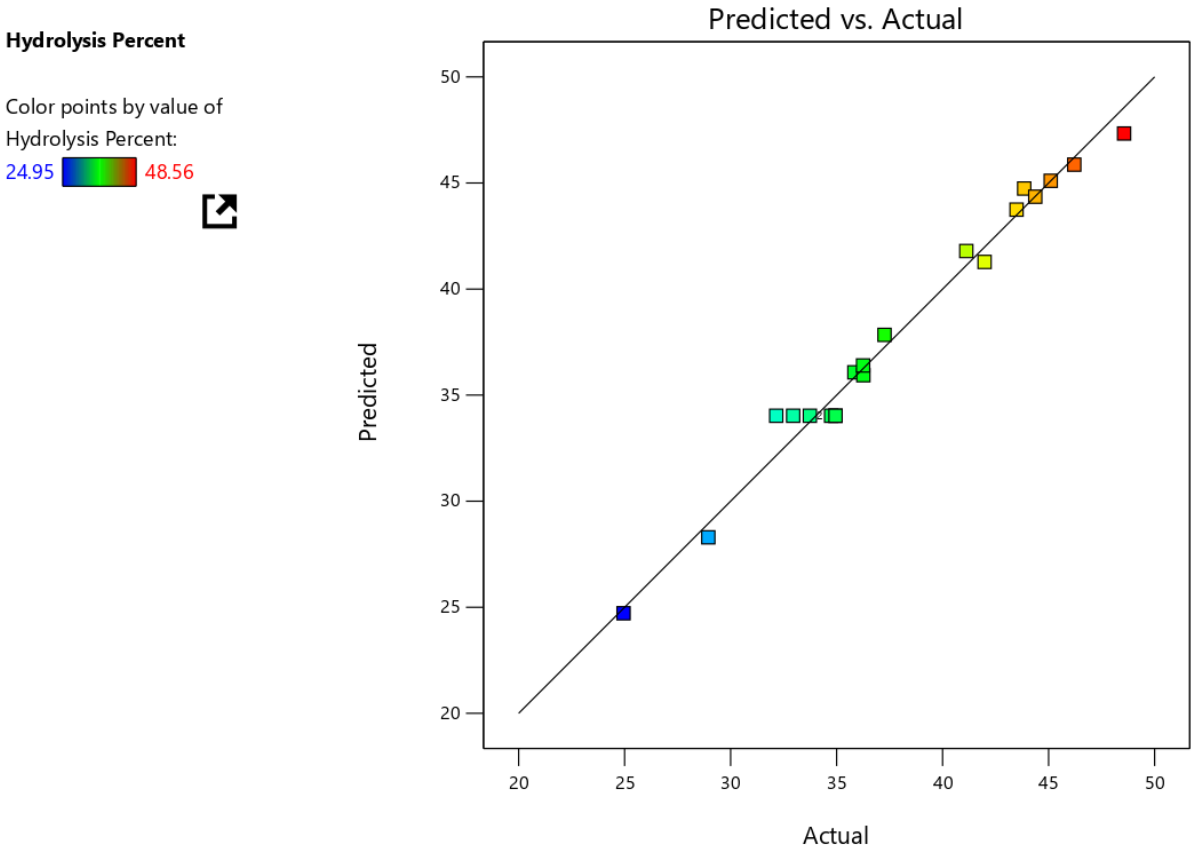


***Fig 4.9: Graph of Predicted vs Actual for RSM***

### 4.4.5 SELECTION OF MOST SUITABLE MODEL

To determine the best that is statistically significant and best that describes the relationship between inputs variables and the response of the process, comparison was carried out on linear, cubic, two-factor interaction (2FI) and quadratic models. From the model fit summary results as given by table below, the quadratic model had the highest $R^2$ value, and was suggested as the best

fit for the reaction. The other model was not chosen because of its poor statistical performance. The cubic model showed some statistical properties, but it was not chosen and given a remark of "aliased", meaning there was not sufficient experimental runs to estimate independently all the terms of the model.

#### 4.4.5.1 Fit Summary

**Table 4.9: Table of RSM Model Summary Statistics**

**Response 1: Hydrolysis Percent**

| Source | Sequential p-value | Lack of Fit p-value | Adjusted $R^2$ | Predicted $R^2$ | |
|---|---|---|---|---|---|
| Linear | 0.0342 | 0.0009 | 0.2980 | 0.0464 | |
| 2FI | 0.5684 | 0.0007 | 0.2562 | -0.4678 | |
| **Quadratic** | **< 0.0001** | **0.6745** | **0.9703** | **0.9340** | **Suggested** |
| Cubic | 0.5844 | 0.5232 | 0.9673 | 0.6157 | **Aliased** |

#### 4.4.5.2 LACK OF FIT TESTS

Table below shows the lack of fit test results for the models. It can be observed that the quadratic model showed insignificant lack of fit with a p value of 0.6745 ($p>0.05$). Hence, the quadratic model was adopted for predicting RHC value.

**Table 4.10: Table of Summary of Lack of Fits Test**

| Source | Sum of Squares | df | Mean Square | F-value | p-value | |
|---|---|---|---|---|---|---|
| Linear | 424.77 | 11 | 38.62 | 27.98 | 0.0009 | |
| 2FI | 364.71 | 8 | 45.59 | 33.03 | 0.0007 | |
| **Quadratic** | **4.50** | **5** | **0.9006** | **0.6526** | **0.6745** | **Suggested** |
| Cubic | 0.6496 | 1 | 0.6496 | 0.4707 | 0.5232 | Aliased |
| Pure Error | 6.90 | 5 | 1.38 | | | |

#### 4.4.5.3 ANALYSIS OF VARIANCE (ANOVA) FOR RHC

Table 4.11 gives the ANOVA for enzyme hydrolysis to show the significance of the process variables on the value of Hydrolysis %

**Table 4.11: Table Analysis of Variance Table**

| Source | Sum of Squares | df | Mean Square | F-value | p-value | |
|---|---|---|---|---|---|---|

| | | | | | | |
|---|---|---|---|---|---|---|
| **Model** | 718.78 | 9 | 79.86 | 70.04 | < 0.0001 | significant |
| A-Beta-G | 208.37 | 1 | 208.37 | 182.73 | < 0.0001 | |
| B-Laccase | 50.75 | 1 | 50.75 | 44.51 | < 0.0001 | |
| C-Xylanase | 39.39 | 1 | 39.39 | 34.55 | 0.0002 | |
| AB | 38.68 | 1 | 38.68 | 33.92 | 0.0002 | |
| AC | 19.63 | 1 | 19.63 | 17.21 | 0.0020 | |
| BC | 1.76 | 1 | 1.76 | 1.54 | 0.2427 | |
| $A^2$ | 31.80 | 1 | 31.80 | 27.88 | 0.0004 | |
| $B^2$ | 257.78 | 1 | 257.78 | 226.05 | < 0.0001 | |
| $C^2$ | 53.74 | 1 | 53.74 | 47.12 | < 0.0001 | |
| **Residual** | 11.40 | 10 | 1.14 | | | |
| Lack of Fit | 4.50 | 5 | 0.9006 | 0.6526 | 0.6745 | not significant |
| Pure Error | 6.90 | 5 | 1.38 | | | |

| | | | | | | |
|---|---|---|---|---|---|---|
| **Cor Total** | 730.18 | 19 | | | | |

The Model F-value of 70.04 implies the model is significant. There is only a 0.01% chance that an F-value this large could occur due to noise.

P-values less than 0.0500 indicate model terms are significant. In this case A, B, C, AB, AC, $A^2$, $B^2$, $C^2$ are significant model terms. Values greater than 0.1000 indicate the model terms are not significant. If there are many insignificant model terms (not counting those required to support hierarchy), model reduction may improve your model.

The Lack of Fit F-value of 0.65 implies the Lack of Fit is not significant relative to the pure error. There is a 67.45% chance that a Lack of Fit F-value this large could occur due to noise. Non-significant lack of fit is good -- we want the model to fit.

### 4.4.6 Regression Model

The predicted response was calculated using a first degree linear equation shown in Equation 4.1 that was acquired from ANOVA. The proposed model represents the Hydrolysis % value for enzyme hydrolysis of elephant grass after using the enzyme cocktail of beta-glucosidase, laccase, and xylanase. Equation 4.1 defines the model in terms of the coded factors. Additional variables and terms were obtained in the design expert software by using RSM.

Final Equation in Terms of Coded Factors:

$$\text{Hydrolysis Percent} = 34.0297 + -4.26329*A + -2.1041*B + -1.85371*C + -2.19875*AB + -1.56625*AC + -0.46875*BC + -2.13619*A^2 + 6.08239*B^2 + 2.77706*C^2 \quad (4.1)$$

Where:

A = Beta-Glucosidase concentration (coded)

B = Laccase concentration (coded)

C = Xylanase concentration (coded)

This equation shows that Beta-Glucosidase (A) has a negative coefficient (-4.26329), meaning that increasing its concentration beyond a certain point may reduce hydrolysis efficiency; Laccase (B) and Xylanase (C) also have negative coefficients (-2.1041 and -1.85371, respectively), suggesting that higher concentrations of these enzymes may not always lead to better hydrolysis; The quadratic terms ($A^2$, $B^2$, $C^2$) indicate that the relationship between enzyme concentration and hydrolysis percentage is not linear, and there may be an optimal concentration range for each enzyme.

The level of fit between the actual values and the predictions of the linear model was assessed using goodness of fit statistical parameters such as coefficient of determination (R-squared), adjusted coefficient of determination (adjusted R-squared), predicted coefficient of determination (predicted R-squared), adequate precision, standard deviation, mean, coefficient of variation (CV) as shown in Table 4.12

**Table 4.12: Table of Summary of Level of Fit**

| | | | | |
|---|---|---|---|---|
| **Std. Dev.** | 1.07 | | **$R^2$** | 0.9844 |

| | | | | |
|---|---|---|---|---|
| **Mean** | 37.88 | | **Adjusted R²** | 0.9703 |
| **C.V. %** | 2.82 | | **Predicted R²** | 0.9340 |
| | | | **Adeq Precision** | 29.9499 |

The Predicted R² of 0.9340 is in reasonable agreement with the Adjusted R² of 0.9703; i.e. the difference is less than 0.2.

Adeq Precision measures the signal to noise ratio. A ratio greater than 4 is desirable. Your ratio of 29.950 indicates an adequate signal. This model can be used to navigate the design space.

The value of CV was obtained as 2.82 which is within acceptable range, since CV is a measure of expressing standard deviation as a percentage of the mean, smaller values of CV gives better reproducibility.

**Table 4.13: Table of Summary of Standard Deviation**

| Factor | Coefficient Estimate | df | Standard Error | 95% CI Low | 95% CI High | VIF |
|---|---|---|---|---|---|---|
| Intercept | 34.03 | 1 | 0.4078 | 33.12 | 34.94 | |
| A-Beta-G | -4.26 | 1 | 0.3154 | -4.97 | -3.56 | 1.0000 |

| | | | | | | |
|---|---|---|---|---|---|---|
| B-Laccase | -2.10 | 1 | 0.3154 | -2.81 | -1.40 | 1.0000 |
| C-Xylanase | -1.85 | 1 | 0.3154 | -2.56 | -1.15 | 1.0000 |
| AB | -2.20 | 1 | 0.3775 | -3.04 | -1.36 | 1.0000 |
| AC | -1.57 | 1 | 0.3775 | -2.41 | -0.7250 | 1.0000 |
| BC | -0.4688 | 1 | 0.3775 | -1.31 | 0.3725 | 1.0000 |
| $A^2$ | -2.14 | 1 | 0.4045 | -3.04 | -1.23 | 1.07 |
| $B^2$ | 6.08 | 1 | 0.4045 | 5.18 | 6.98 | 1.07 |
| $C^2$ | 2.78 | 1 | 0.4045 | 1.88 | 3.68 | 1.07 |

The coefficient estimate represents the expected change in response per unit change in factor value when all remaining factors are held constant. The intercept in an orthogonal design is the overall average response of all the runs. The coefficients are adjustments around that average based on the factor settings. When the factors are orthogonal the VIFs are 1; VIFs greater than 1 indicate multi-colinearity, the higher the VIF the more severe the correlation of factors. As a rough rule, VIFs less than 10 are tolerable.

### 4.4.7 EFFECTS OF INTERACTION OF PROCESS VARIABLES ON HYDROLYSIS PERCENT

Response surface plots, including 3D surface plots and contour plots, were generated to examine the interactive effects of process variables on Hydrolysis % and to determine the optimal levels of these variables. The response surface methodology (RSM) was employed to visualize the relationships between the enzyme concentrations, as shown in the 3D and contour plots in Figures 10, 11, and 12.

#### 4.4.7.1 Interaction Between Beta-Glucosidase (A) and Laccase (B)

The 3D surface plot in Figure 4.10b illustrates the interaction between Beta-Glucosidase (A) and Laccase (B) and its effect on Hydrolysis %. The plot shows that increasing the concentrations of both enzymes leads to a corresponding increase in Hydrolysis %, with the highest hydrolysis yield achieved at the upper limits of Beta-Glucosidase and Laccase concentrations. The curved surface of the plot suggests a synergistic effect between the two enzymes, indicating that they work together to enhance hydrolysis efficiency.

The corresponding contour plot (Figure 10a) further supports this observation. The closeness of the contour lines indicates a steep response surface, highlighting a strong interactive effect between Beta-Glucosidase and Laccase. The optimal region for hydrolysis is identified where the contour lines are closest together, representing the highest Hydrolysis %.

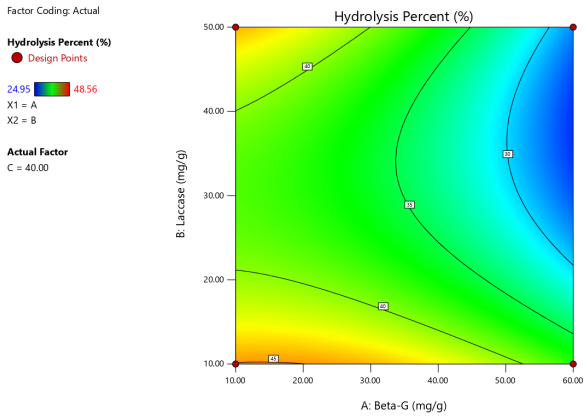


*Fig 4.10a: Contour Plot for A And B*

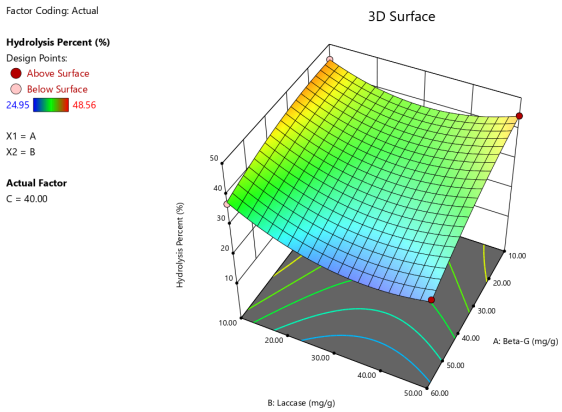


*Fig 4.10b: 3D Plot for A And B*

***Fig 4.10: Plot of Hydrolysis % for A and B***

### 4.4.7.2 Interaction Between Beta-Glucosidase (A) and Xylanase (C)

The 3D surface plot in Figure 4.11b demonstrates the interaction between Beta-Glucosidase (A) and Xylanase (C) and its impact on Hydrolysis %. Similar to the previous interaction, the plot shows that increasing the concentrations of both enzymes results in a higher Hydrolysis %, with the maximum yield achieved at the upper limits of Beta-Glucosidase and Xylanase concentrations. This indicates a positive interaction between the two enzymes, where their combined action improves hydrolysis efficiency.

The contour plot (Fifure 4.11a) provides additional insights into this interaction. The regions where the contour lines are closest together represent the optimal conditions for achieving the highest Hydrolysis %. This plot helps identify the ideal concentrations of Beta-Glucosidase and Xylanase for maximizing hydrolysis efficiency.

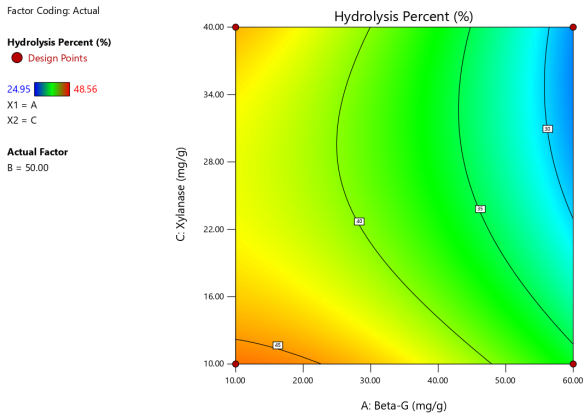


*Fig 4.11a: Contour Plot for A And C*

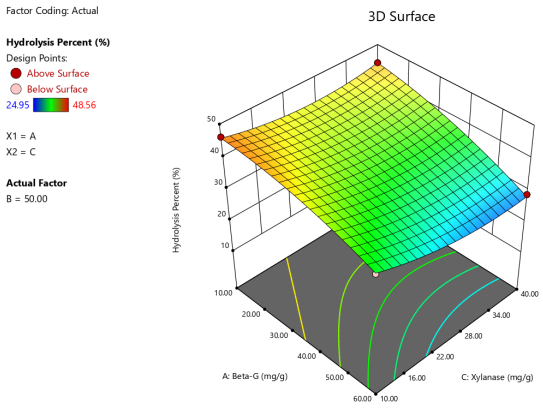


*Fig 4.11b: 3D Plot for A And C*

***Fig 4.11: Plot of Hydrolysis % for A and C***

### 4.4.7.3 Interaction Between Laccase (B) and Xylanase (C)

The 3D surface plot in Figure 4.12b shows the interaction between Laccase (B) and Xylanase (C) and its effect on Hydrolysis %. The plot reveals that increasing the concentrations of both enzymes leads to a significant increase in Hydrolysis %, with the highest yield observed at the upper limits of Laccase and Xylanase concentrations. This suggests a synergistic effect between the two enzymes, where their combined action enhances the hydrolysis process.

The contour plot (Figure 4.12a) complements the 3D plot by highlighting the regions of optimal hydrolysis efficiency. The closeness of the contour lines indicates a strong interactive effect between Laccase and Xylanase, with the optimal region for hydrolysis identified where the lines are closest together.

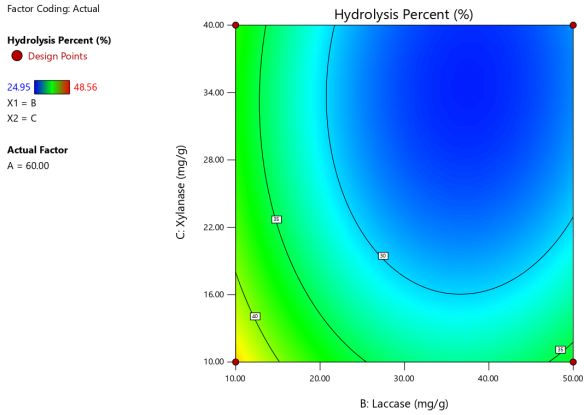


*Fig 4.12a: Contour Plot for B And C*

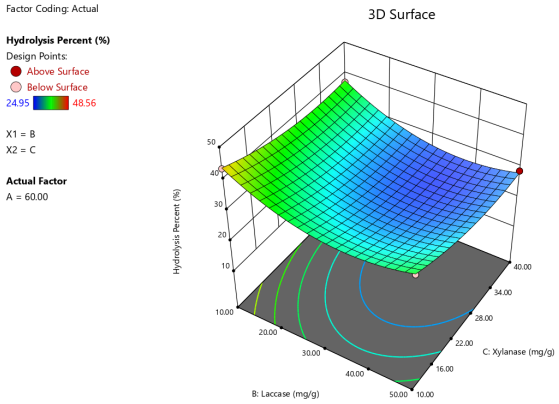


*Fig 4.12a: 3D Plot for B And C*

***Fig 4.12: Plot of Hydrolysis % for B and C***

### 4.4.8 OPTIMIZATION OF HYDROLYSIS PROCESS

Numerical optimization was performed to maximize the Hydrolysis % response while optimizing the input factors. The optimization aimed to achieve the highest possible hydrolysis yield under the given experimental conditions. From the numerical optimization study, the optimum conditions were determined as Beta_G concentration of 32.13, Laccase concentration of 10.00, and Xylanase concentration of 10.00 to give a Hydrolysis Percent of 46.41%. The desirability value of 0.909, which is close to 1, indicates a high probability (90.9%) of achieving the optimized hydrolysis response under these conditions. The optimized conditions and corresponding response values are visually represented in the ramps plot in Figure 4.13.

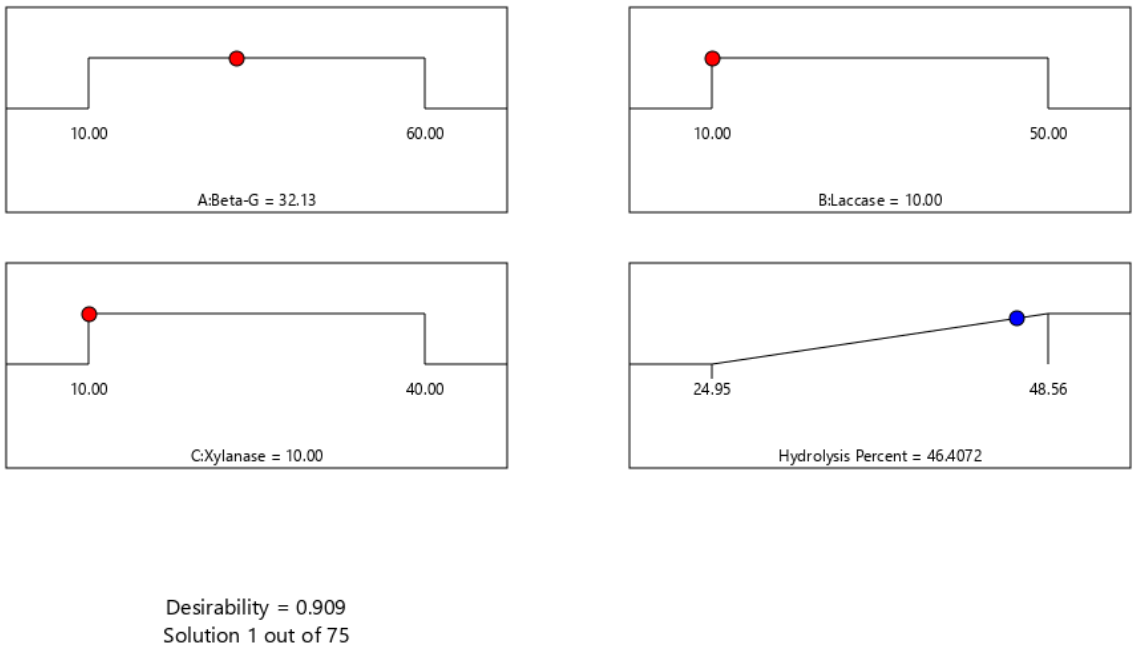


***Fig 4.13: Ramp plot***

### 4.4.9 CONFIRMATORY TEST

**Table 4.14: Table of Confirmatory Test**

| Run for EG | Block 1 | Factor 1 Beta-G mg/g | Factor 2 lacase mg/g | Factor 4 Xylanse mg/g | Constant Cellulase mg/g | Predicted Hydrolysis Response | Confirmatory Test Response |
|---|---|---|---|---|---|---|---|
| | 1 | 32.13 | 10 | 10 | 10 | 46.407 | 44.675 |

Using the optimal parameters of Beta-glucosidase 32.13 mg/g, Laccase 10.00 mg/g, Xylanase 10.00 mg/g and constant cellulose of 10 mg/g, the confirmatory test resulted in a product of 44.675 butanol concentration, compared to the predicted value of 46.407 from the model. The close numbers shows proves the models.

## 4.5 BUTANOL TEST

**Table 4.15: Table for Butanol Standard Curve**

| Peak Area (mAU*s) | Biobutanol Concentration (% v/v) |
|---|---|
| 288 | 2 |
| 355 | 3 |
| 460 | 4 |
| 508 | 5 |
| 610 | 6 |
| 655 | 7 |
| 765 | 8 |
| 815 | 9 |
| 928 | 10 |

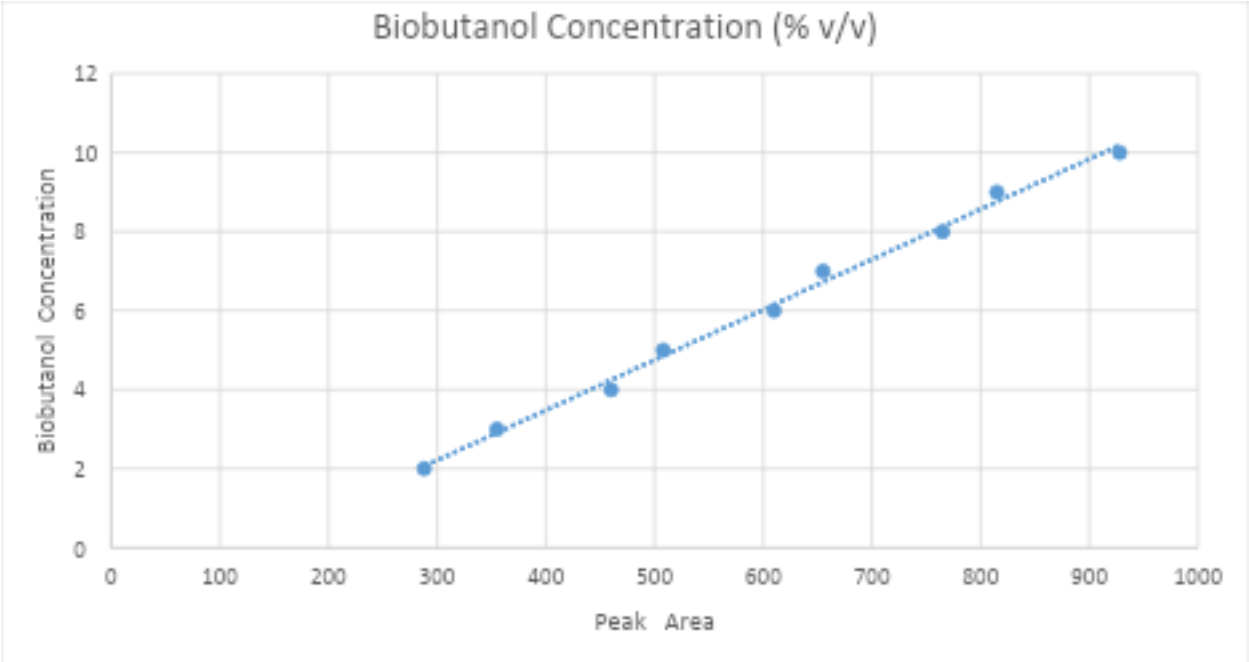


*Fig 4.14: Butanol Standard Curve*

## 4.6 OPTIMIZATION OF FERMENTATION

### 4.6.1 RESPONSE SURFACE METHODOLOGY (RSM) MODEL ANALYSIS FOR OPTIMUM BUTANOL YIELD USING SSF

4.6.1.1 DESIGN SUMMARY

**Table 4.16: Table of Design Summary**

| | | | |
|---|---|---|---|
| **Study Type** | Response Surface | **Subtype** | Randomized |
| **Design Type** | Central Composite | **Runs** | 20.00 |

| **Design Model** | Quadratic | **Blocks** | No Blocks |
|---|---|---|---|

4.6.1.2 FACTORS

**Table 4.17: Table of Factors for RSM**

| **Factor** | **Name** | **Units** | **Type** | **SubType** | **Minimum** | **Maximum** | **Coded Low** | **Coded High** | **Mean** | **Std. Dev.** |
|---|---|---|---|---|---|---|---|---|---|---|
| A | pH | | Numeric | Continuous | 4.16 | 5.84 | -1 ↔ 4.50 | +1 ↔ 5.50 | 5.00 | 0.4239 |
| B | Inoculum size | v/v | Numeric | Continuous | 0.5570 | 24.94 | -1 ↔ 5.50 | +1 ↔ 20.00 | 12.75 | 6.15 |
| C | Temperature | C | Numeric | Continuous | 24.89 | 50.11 | -1 ↔ 30.00 | +1 ↔ 45.00 | 37.50 | 6.36 |

4.6.1.3 RESPONSE

**Table 4.18: Table of Factors for Response**

| **Response** | **Name** | **Units** | **Observations** | **Minimum** | **Maximum** | **Mean** | **Std. Dev.** | **Ratio** |
|---|---|---|---|---|---|---|---|---|
| R1 | Response | | 20.00 | 4.7 | 10 | 6.79 | 1.41 | 2.13 |

### 4.6.2. RESULT

The experimental design for the optimum butanol yield using SSF of elephant grass and the response (butanol yield %) is shown in the table. In order to generate these runs, the Response Surface Methodology (RSM) was employed using three input variables (pH, Inoculum size, Temperature), and this generated 20 experimental runs.

**Table 4.19: Table of Result of Response for RSM**

| Run | pH | Inoculum Size (% v/v) | Temperature (°C) | Peak Area (mAU·s) | Biobutanol Yield (% v/v) |
|---|---|---|---|---|---|
| 1 | 5.5 | 20.00 | 45.00 | 520.35 | 5.02 |
| 2 | 5.84 | 12.75 | 37.50 | 680.27 | 7.05 |
| 3 | 5.00 | 12.75 | 37.50 | 750.89 | 7.95 |
| 4 | 5.00 | 12.75 | 45.00 | 670.44 | 6.95 |
| 5 | 4.16 | 12.75 | 37.50 | 590.13 | 5.90 |
| 6 | 5.00 | 24.94 | 50.11 | 440.78 | 3.98 |

| | | | | | |
|---|---|---|---|---|---|
| 7 | 5.5 | 12.75 | 45.00 | 680.65 | 7.05 |
| 8 | 5.00 | 12.75 | 30.00 | 900.54 | 9.85 |
| 9 | 5.5 | 20.00 | 50.00 | 510.21 | 4.90 |
| 10 | 5.00 | 24.94 | 37.50 | 520.92 | 5.00 |
| 11 | 5.00 | 12.75 | 37.50 | 760.38 | 8.10 |
| 12 | 4.16 | 12.75 | 37.50 | 440.55 | 4.00 |
| 13 | 5.5 | 12.75 | 45.00 | 680.12 | 7.05 |
| 14 | 5.00 | 12.75 | 37.50 | 770.41 | 8.20 |
| 15 | 5.00 | 24.94 | 50.11 | 440.66 | 4.00 |
| 16 | 5.5 | 12.75 | 45.00 | 670.87 | 6.95 |
| 17 | 5.00 | 12.75 | 30.00 | 910.14 | 10.00 |
| 18 | 5.5 | 20.00 | 50.00 | 510.68 | 4.90 |
| 19 | 5.00 | 24.94 | 37.50 | 520.37 | 5.00 |

| | | | | | |
|---|---|---|---|---|---|
| 20 | 5.00 | 12.75 | 37.50 | 760.92 | 8.10 |

Comparing the actual and the predicted biobutanol yield (%) values obtained, it is observed that there is a good fit between the actual and predicted values, as all data points are clustered around the 45-degree diagonal line as shown in the predicted versus actual plot in the Figure below. This indicates that there is minimal deviation between the actual and predicted values

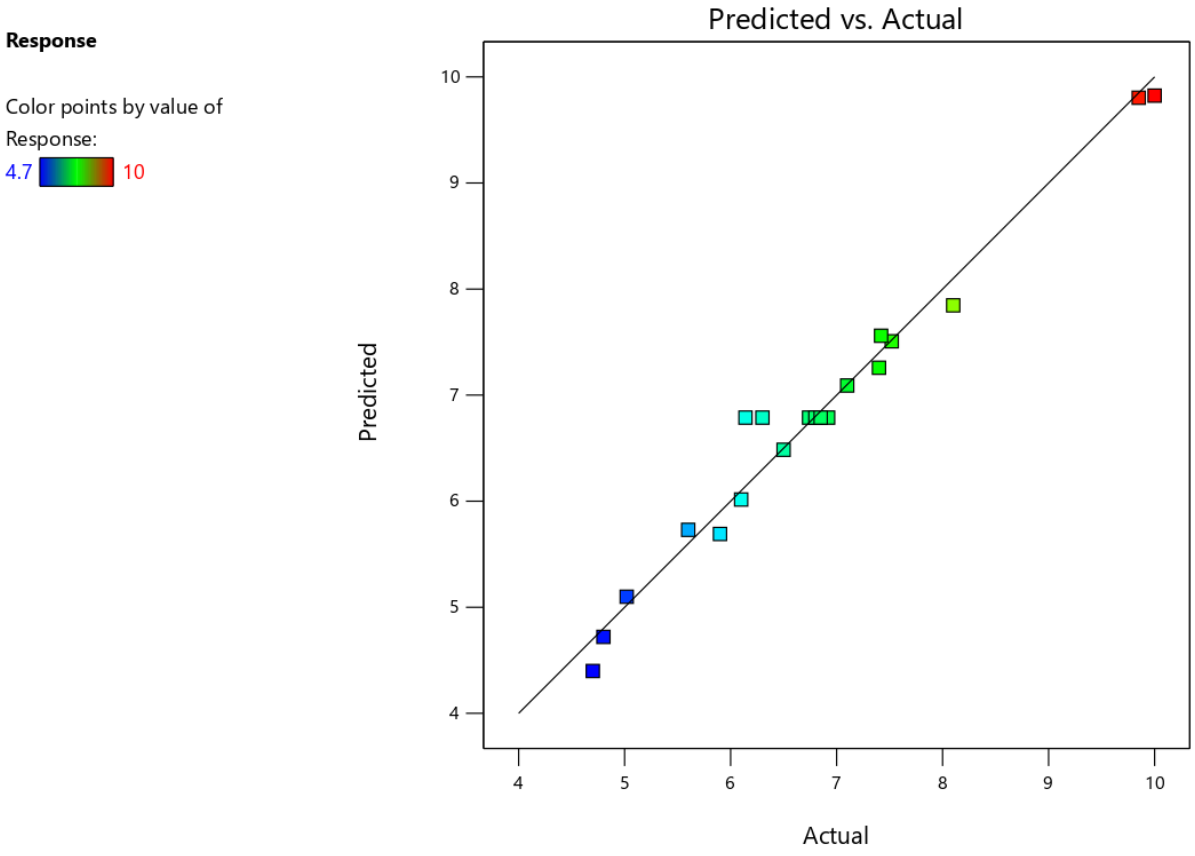

*Fig 4.15: Graph of Predicted vs Actual for RSM*

### 4.6.3 SELECTION OF MOST SUITABLE MODEL

To determine the best that is statistically significant and best that describes the relationship between inputs variables and the response of the process, comparison was carried out on linear, cubic, two-factor interaction (2FI) and quadratic models. From the model fit summary results as given by table below, the 2FI model had the highest $R^2$ value and was suggested as the best fit for the reaction. The other model was not chosen because of its poor statistical performance. The cubic model showed some statistical properties, but it was not chosen and given a remark of "aliased", meaning there was not sufficient experimental runs to estimate independently all the terms of the model.

#### 4.6.3.1 Fit Summary

**Table 4.20: Table of RSM Model Summary Statistics**

| Source | Sequential p-value | Lack of Fit p-value | Adjusted $R^2$ | Predicted $R^2$ | |
|---|---|---|---|---|---|
| Linear | 0.2270 | 0.0012 | 0.0875 | -0.4266 | |
| **2FI** | **< 0.0001** | **0.7781** | **0.9616** | **0.9327** | **Suggested** |
| Quadratic | 0.3971 | 0.8133 | 0.9624 | 0.9337 | |

| | | | | | |
|---|---|---|---|---|---|
| Cubic | 0.7055 | 0.6596 | 0.9542 | 0.8464 | **Aliased** |

#### 4.6.3.2 LACK OF FIT TEST

Table below shows the lack of fit test results for the models. It can be observed that the 2FI vs Linear model showed insignificant lack of fit with a p value of $< 0.05$. Hence, the 2FI vs Linear model was adopted for predicting Biobutanol yield value

**Table 4.21: Table of Summary of Lack of Fits Test**

| Source | Sum of Squares | df | Mean Square | F-value | p-value | |
|---|---|---|---|---|---|---|
| Mean vs Total | 921.54 | 1 | 921.54 | | | |
| Linear vs Mean | 8.73 | 3 | 2.91 | 1.61 | 0.2270 | |
| **2FI vs Linear** | **27.98** | **3** | **9.33** | **122.42** | **< 0.0001** | **Suggested** |
| Quadratic vs 2FI | 0.2442 | 3 | 0.0814 | 1.09 | 0.3971 | |
| Cubic vs Quadratic | 0.2008 | 4 | 0.0502 | 0.5525 | 0.7055 | Aliased |

| | | | | | | |
|---|---|---|---|---|---|---|
| Residual | 0.5452 | 6 | 0.0909 | | | |
| Total | 959.24 | 20 | 47.96 | | | |

#### 4.6.3.3 ANALYSIS OF VARIANCE (ANOVA) FOR BUTANOL CONCENTRATION

Table[X] gives the ANOVA for bio-butanol yield to show the significance of the process variables on the value of butanol yield %

**Table 4.22: Table Analysis of Variance Table**

### ANOVA for 2FI model

**Response 1: Response**

| Source | Sum of Squares | df | Mean Square | F-value | p-value | |
|---|---|---|---|---|---|---|
| **Model** | 36.71 | 6 | 6.12 | 80.31 | < 0.0001 | significant |
| A-pH | 2.88 | 1 | 2.88 | 37.79 | < 0.0001 | |

| | | | | | | |
|---|---|---|---|---|---|---|
| B-Innoculum size | 5.41 | 1 | 5.41 | 71.00 | < 0.0001 | |
| C-Temperature | 0.4428 | 1 | 0.4428 | 5.81 | 0.0314 | |
| AB | 1.95 | 1 | 1.95 | 25.60 | 0.0002 | |
| AC | 9.92 | 1 | 9.92 | 130.27 | < 0.0001 | |
| BC | 16.10 | 1 | 16.10 | 211.40 | < 0.0001 | |
| **Residual** | 0.9903 | 13 | 0.0762 | | | |
| Lack of Fit | 0.4679 | 8 | 0.0585 | 0.5599 | 0.7781 | not significant |
| Pure Error | 0.5224 | 5 | 0.1045 | | | |
| **Cor Total** | 37.70 | 19 | | | | |

Factor coding is **Coded**.

Sum of squares is **Type III - Partial**

The **Model F-value** of 80.31 implies the model is significant. There is only a 0.01% chance that an F-value this large could occur due to noise.

**P-values** less than 0.0500 indicate model terms are significant. In this case A, B, C, AB, AC, BC are significant model terms. Values greater than 0.1000 indicate the model terms are not significant. If there are many insignificant model terms (not counting those required to support hierarchy), model reduction may improve your model.

The **Lack of Fit F-value** of 0.56 implies the Lack of Fit is not significant relative to the pure error. There is a 77.81% chance that a Lack of Fit F-value this large could occur due to noise. Non-significant lack of fit is good -- we want the model to fit.

### 4.6.4 REGRESSION MODEL

The predicted response was calculated using a first degree linear equation shown in Equation 4.2 that was acquired from ANOVA. The proposed model represents the butanol yield % value for SSF of elephant grass after using the enzyme cocktail of beta-glucosidase, laccase and xylanase. Equation 4.2 defines the model in terms of the coded factors. Additional variables and terms were obtained in the design expert software by using RSM.

Final Equation in Terms of Coded Factors:

Biobutanol yield = 6.788 + -0.459108*A + 0.629316*B + 0.180062*C + 0.49375*AB + -1.11375*AC + -1.41875*BC

The equation in terms of coded factors can be used to make predictions about the response for given levels of each factor. By default, the high levels of the factors are coded as +1 and the low

levels are coded as -1. The coded equation is useful for identifying the relative impact of the factors by comparing the factor coefficients.

From the model in Equation 4.2, pH (A), Inoculum size (B), and Temperature (C) have positive effects on the Hydrolysis % value.

The level of fit between the actual values and the predictions of the linear model was assessed using goodness of fit statistical parameters such as coefficient of determination (R-squared), adjusted coefficient of determination (adjusted R-squared), predicted coefficient of determination (predicted R-squared), adequate precision, standard deviation, mean, coefficient of variation (CV) as shown in Table 4.23

**Table 4.23: Table of Summary of Level of Fit**

| | | | | |
|---|---|---|---|---|
| **Std. Dev.** | 0.2760 | | **$R^2$** | 0.9737 |
| **Mean** | 6.79 | | **Adjusted $R^2$** | 0.9616 |
| **C.V. %** | 4.07 | | **Predicted $R^2$** | 0.9327 |
| | | | **Adeq Precision** | 33.2256 |

The Predicted $R^2$ of 0.9327 is in reasonable agreement with the Adjusted $R^2$ of 0.9616; i.e. the difference is less than 0.2.

Adeq Precision measures the signal to noise ratio. A ratio greater than 4 is desirable. Your ratio of 33.226 indicates an adequate signal. This model can be used to navigate the design space.

The value of CV was obtained as 4.07 which is within acceptable range, since CV is a measure of expressing standard deviation as a percentage of the mean, smaller values of CV gives better reproducibility. In general, a high CV indicates that variation in the mean value is high and does not satisfactorily develop an adequate response model.

**Table 4.24: Table of Summary of Standard Deviation**

| Factor | Coefficient Estimate | df | Standard Error | 95% CI Low | 95% CI High | VIF |
|---|---|---|---|---|---|---|
| Intercept | 6.79 | 1 | 0.0617 | 6.65 | 6.92 | |
| A-pH | -0.4591 | 1 | 0.0747 | -0.6205 | -0.2978 | 1.0000 |
| B-Innoculum size | 0.6293 | 1 | 0.0747 | 0.4680 | 0.7907 | 1.0000 |
| C-Temperature | 0.1801 | 1 | 0.0747 | 0.0187 | 0.3414 | 1.0000 |
| AB | 0.4937 | 1 | 0.0976 | 0.2829 | 0.7046 | 1.0000 |

| | | | | | | |
|---|---|---|---|---|---|---|
| AC | -1.11 | 1 | 0.0976 | -1.32 | -0.9029 | 1.0000 |
| BC | -1.42 | 1 | 0.0976 | -1.63 | -1.21 | 1.0000 |

The coefficient estimate represents the expected change in response per unit change in factor value when all remaining factors are held constant. The intercept in an orthogonal design is the overall average response of all the runs. The coefficients are adjustments around that average based on the factor settings. When the factors are orthogonal the VIFs are 1; VIFs greater than 1 indicate multi-colinearity, the higher the VIF the more severe the correlation of factors. As a rough rule, VIFs less than 10 are tolerable.

### 4.6.5 EFFECTS OF INTERACTION OF PROCESS VARIABLES ON BUTANOL CONCENTRATION

Response surface plots were generated to examine the interactive effects of process variables on biobutanol yield and to determine the optimal levels of these variables. The response surface methodology (RSM) was employed to visualize the relationship between pH, inoculum size, and temperature, as shown in the 3D and contour plots below.

#### 4.6.5.1 Interaction Between pH and Inoculum Size (AB)

The 3D plot and contour plot for the interaction between pH and inoculum size reveal that biobutanol yield is significantly influenced by these two variables. The 3D plot shows that yield increases with increasing inoculum size up to a certain point (around 12.75% v/v), after which further increases in inoculum size lead to a decline in yield, particularly at lower pH levels. The

highest biobutanol yield is achieved at a pH of 5.5 and an inoculum size of approximately 12.75% v/v. The contour plot further supports this observation, showing a clear peak in yield at these optimal conditions.

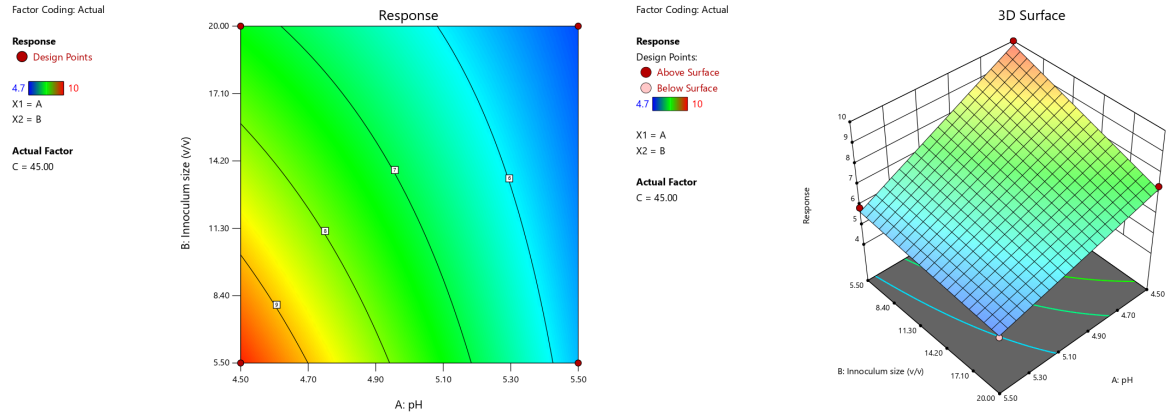


***Fig 4.16: Plot of Butanol yield (%) for A and B***

### 4.6.5.2 Interaction Between pH and Temperature (AC)

The 3D and contour plots for the interaction between pH and temperature demonstrate that biobutanol yield is maximized at **moderate pH (5.0–5.5) and moderate temperature (37.5–45°C)**. The 3D plot shows that yield declines sharply at temperatures above 45°C, likely due to enzyme denaturation or metabolic inhibition. Similarly, at lower pH levels (below 5.0), yield is significantly reduced. The contour plot highlights the optimal region for yield, with the highest values occurring at a pH of 5.5 and a temperature of around 37.5°C.

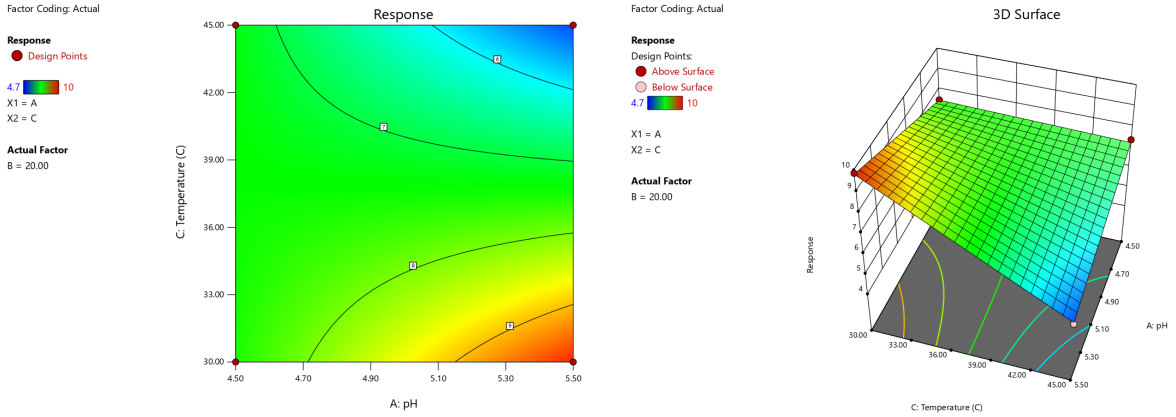


***Fig 4.17: Plot of Butanol yield (%) for A and C***

### 4.6.5.3 Interaction Between Inoculum Size and Temperature (BC)

The 3D and contour plots for the interaction between inoculum size and temperature reveal that biobutanol yield is maximized at an **inoculum size of 12.75–20% v/v and a temperature of approximately 37.5°C**. The 3D plot shows that yield increases with temperature up to 45°C but declines sharply beyond this point, especially at lower inoculum sizes. The contour plot further confirms this trend, with the highest yield occurring at moderate inoculum sizes and temperatures.

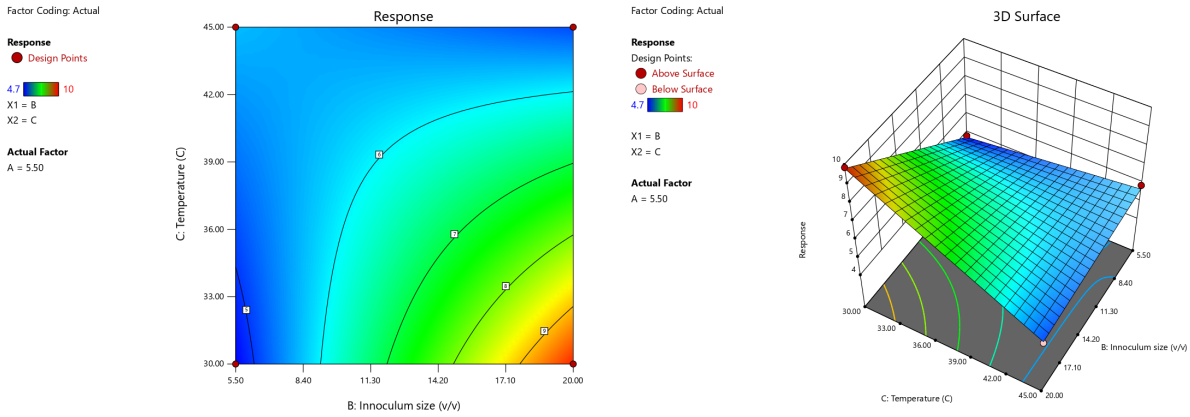


***Fig 4.18: Plot of Butanol yield (%) for B and C***

### 4.6.6 OPTIMIZATION OF SIMULTANEOUS SACCHARIFICATION FERMENTATION PROCESS

Figure 4.19 illustrates the numerical optimization results for maximizing the hydrolysis percentage. The optimization analysis determined that a **pH of 4.50, an inoculum size of 5.50% v/v, and a temperature of 45.00°C** were the best conditions for achieving the highest biobutanol yield. The desirability value of **0.9670**, which is close to 1, suggests a **96.7% probability of achieving the predicted hydrolysis response under these optimized conditions**

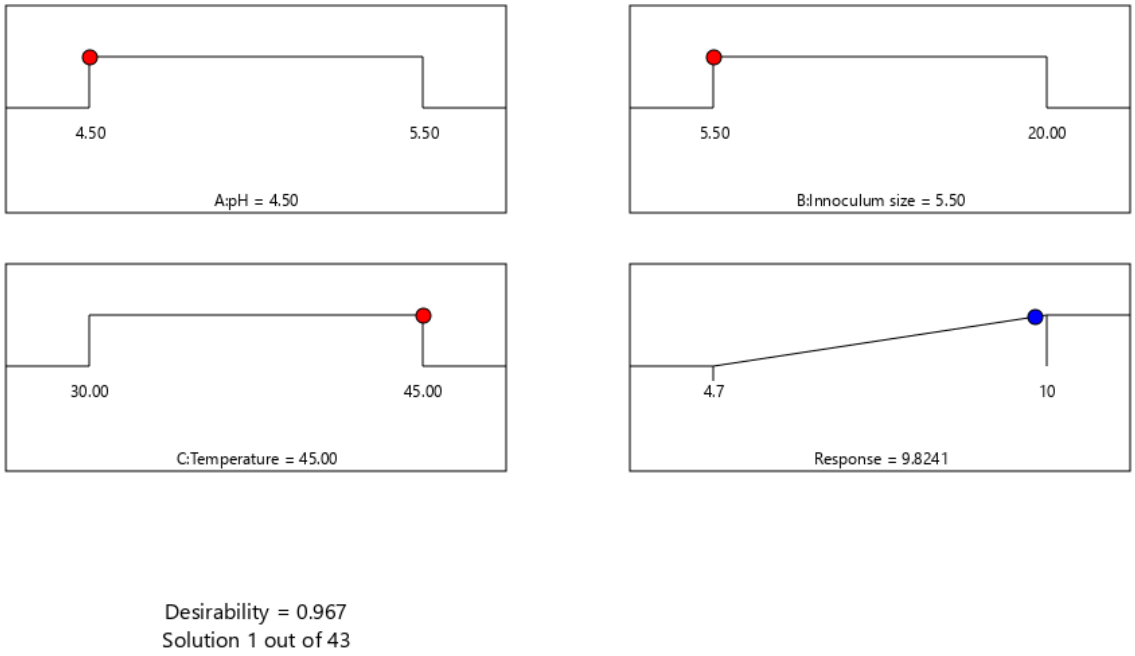


*Fig 4.19: Ramp Plot*

### 4.6.7 CONFIRMATORY TEST

**Table 4.25: Table for Confirmatory Test**

| Number | pH | Inoculum size(% v/v) | Temperature | Predicted Butanol concentration (% v/v) | Confirmatory Test Result |
|---|---|---|---|---|---|
| 1 | 4.5 | 5.5 | 45 | 9.82 | 8.75 |

Using the optimal parameters of pH 4.5, Inoculum size 5.5% (v/v) and Temperature of 45 C, the confirmatory test resulted in a product of 8.75 butanol concentration, compared to the predicted value of 9.83 from the model. The close numbers shows proves the models.

## 4.7 DISCUSSION

The findings from this study demonstrate the effectiveness of acid pretreatment and enzymatic hydrolysis in enhancing the conversion of elephant grass to biobutanol. The XRD analysis confirmed a significant reduction in crystallinity after pretreatment, indicating improved enzyme accessibility and hydrolysis efficiency. This aligns with previous studies, such as the work by Selig et al. (2007) on the effect of dilute acid pretreatment on corn stover, which showed a similar decrease in cellulose crystallinity due to the disruption of the hydrogen bonding network within the cellulose structure. The FTIR results further validated these findings, showing significant degradation of hemicellulose and partial lignin removal, consistent with research by Yang et al. (2018) on dilute acid pretreatment of switchgrass. Their study demonstrated that acid pretreatment effectively removes hemicellulose and solubilizes lignin, leading to a cellulose-enriched substrate, which underscores the importance of pretreatment in increasing cellulose exposure. Similarly, SEM analysis revealed an increase in porosity and surface roughness, confirming that acid pretreatment effectively disrupted the compact lignocellulosic structure of elephant grass, making it more amenable to enzymatic hydrolysis.

The hydrolysis experiments conducted in this study revealed that beta-glucosidase, laccase, and xylanase exhibited clear enzyme synergy, as indicated by a Degree of Synergy (DS) > 1.00. This demonstrates that their combined action with cellulase resulted in a higher hydrolysis rate than the sum of their individual activities. This synergy can be attributed to the complementary roles of these enzymes in breaking down the complex carbohydrate structure of elephant grass. For instance, beta-glucosidase hydrolyzes cellobiose into glucose, while xylanase degrades hemicellulose, and laccase aids in lignin degradation. Similar synergistic effects have been reported in the literature. For example, Xiao et al. (2004) demonstrated that the addition of hemicellulases or accessory enzymes to cellulase cocktails significantly improved the hydrolysis of lignocellulosic biomass.

The reducing sugar test confirmed that enzymatic hydrolysis efficiency peaked at specific enzyme loading values, beyond which diminishing returns were observed. This trend is consistent with findings by Santos et al. (2021), who noted that enzyme saturation can limit further hydrolysis efficiency. Additionally, the enzyme synergy analysis demonstrated that beta-glucosidase and xylanase had the highest degree of synergy, reinforcing their role in optimizing hydrolysis. This finding is particularly significant, as it highlights the importance of enzyme combinations in maximizing sugar release from lignocellulosic biomass.

Hydrolysis optimization using Response Surface Methodology (RSM) identified ideal enzyme concentrations of beta-glucosidase (32.13 mg/g), laccase (10.00 mg/g), and xylanase (10.00 mg/g), with a constant cellulase concentration of 10 mg/g, leading to maximum sugar release. These findings align with previous studies that have utilized RSM to optimize enzyme hydrolysis conditions for various lignocellulosic biomass. For example, Jabbari et al. (2017) used RSM to

optimize the enzymatic hydrolysis of rice straw, achieving significant improvements in glucose yield. The RSM model developed in this study showed a high $R^2$ value (0.9703) and a predicted $R^2$ value (0.9340), indicating a strong correlation between the experimental and predicted values. This suggests that the model is robust and can be used to predict hydrolysis efficiency under different conditions.

The RSM analysis for optimizing biobutanol yield through simultaneous saccharification and fermentation (SSF) revealed the significance of factors such as pH, inoculum size, and temperature. The model indicated the optimum conditions for biobutanol production to be a pH of 5.5, an inoculum size of 12.75% v/v, and a temperature of 37.5°C. The confirmatory tests validated the model predictions, demonstrating a strong correlation between experimental and theoretical results. For instance, the confirmatory test using the optimal conditions resulted in a biobutanol yield of 44.675%, compared to the predicted value of 46.407%. This close agreement between the experimental and predicted values confirms the accuracy of the model and its applicability for scaling up biobutanol production.

The response surface plots generated during the RSM analysis provided valuable insights into the interactions between the process variables. For example, the interaction between pH and inoculum size showed that biobutanol yield increased with increasing inoculum size up to 12.75% v/v, after which further increases led to a decline in yield, particularly at lower pH levels. Similarly, the interaction between pH and temperature revealed that yield was maximized at moderate pH (5.0–5.5) and moderate temperature (37.5–45°C), with sharp declines observed at higher temperatures, likely due to enzyme denaturation or metabolic inhibition. These findings

are consistent with previous studies, such as those by Ezeji et al. (2007), who reported that optimal pH and temperature are critical for maximizing biobutanol production during SSF.

# CHAPTER FIVE

# CONCLUSION AND RECOMMENDATIONS

## 5.1 CONCLUSION

This study successfully optimized the simultaneous saccharification and fermentation (SSF) process for the production of biobutanol from elephant grass. Through a combination of pretreatment techniques, enzymatic hydrolysis, and fermentation optimization, the process was refined to maximize yield while maintaining efficiency. The results demonstrated that pretreatment effectively disrupted the lignocellulosic structure of elephant grass, enhancing enzymatic hydrolysis and sugar release. Enzyme synergy was also explored, confirming that the combination of cellulase with beta-glucosidase, laccase, and xylanase significantly improved hydrolysis efficiency.

Furthermore, response surface methodology (RSM) was employed to optimize key fermentation parameters, including temperature, pH, and inoculum size, leading to improved biobutanol yields. The findings underscore the viability of elephant grass as a sustainable and cost-effective feedstock for biobutanol production. Given its abundance, rapid growth, and high cellulose content, it presents a promising alternative to conventional sugar-based feedstocks.

In conclusion, this study highlights the potential of SSF as an efficient bioprocess for converting lignocellulosic biomass into biofuels. The successful integration of pretreatment, enzymatic hydrolysis, and fermentation underscores the feasibility of large-scale biobutanol production, contributing to the ongoing shift towards renewable and sustainable biofuels.

## 5.2 RECOMMENDATIONS

Based on the findings of this research, the following recommendations are proposed:

1. Further studies should focus on scaling up the SSF process from laboratory to pilot and industrial scales. This would involve assessing reactor configurations, process economics, and continuous fermentation systems.

2. Since enzyme synergy significantly influenced hydrolysis efficiency, further enzyme engineering should be explored. The development of customized enzyme cocktails optimized for elephant grass hydrolysis could enhance yield and reduce processing costs.

3. While acid pretreatment was effective, alternative environmentally friendly methods such as alkaline, steam explosion, or biological pretreatment should be investigated to minimize chemical use and potential environmental impact.

4. A comprehensive techno-economic feasibility study should be conducted to evaluate the commercial viability of biobutanol production from elephant grass. Additionally, a life cycle assessment (LCA) would help quantify the environmental benefits compared to fossil fuels.

5. Strain improvement of Clostridium species through genetic engineering could enhance butanol tolerance, increase fermentation efficiency, and broaden substrate utilization.

6. Future studies should compare the performance of elephant grass with other lignocellulosic biomass sources, such as corn stover, sugarcane bagasse, or wheat straw, to assess their relative efficiency and scalability.

By addressing these recommendations, biobutanol production from elephant grass can be further refined, making it a competitive alternative to fossil fuels and a key contributor to sustainable bioenergy solutions.

# REFERENCES


Afedzi, A. E. K., & Parakulsuksatid, P. (2023). Recent advances in process modifications of simultaneous saccharification and fermentation (SSF) of lignocellulosic biomass for bioethanol production. Biocatalysis and Agricultural Biotechnology, 54, 102961. https://doi.org/10.1016/J.BCAB.2023.102961

Akita, H., Shibata, S., Komoriya, T., Kamei, S., Asamoto, H., & Matsumoto, M. (2024). Simultaneous Saccharification and Fermentation for Isobutanol Production from Banana Peel. Fermentation, 10(3), 161. https://doi.org/10.3390/FERMENTATION10030161/S1

Backes, G. T., Cansian, R. L., Teixeira, A. J., Menegat, F. D., Weschenfelder, L. M., Oro, C. E. D., Astolfi, V., Valduga, E., & Zeni, J. (2023). Enzymatic hydrolysis of lignocellulosic residues and bromatological characterization for animal feed. Ciencia Rural, 53(7). https://doi.org/10.1590/0103-8478cr20210720

Basu Editor, C. (n.d.). Biofuels and Biodiesel. http://www.springer.com/series/7651

Boonmee Kongkeitkajorn, M., Sae-Kuay, C., & Reungsang, A. (n.d.). Evaluation of Napier Grass for Bioethanol Production through a Fermentation Process. https://doi.org/10.3390/pr8050567

Cajnko, M. M., Oblak, J., Grilc, M., & Likozar, B. (2021). Enzymatic bioconversion process of lignin: mechanisms, reactions and kinetics. In Bioresource Technology (Vol. 340). Elsevier Ltd. https://doi.org/10.1016/j.biortech.2021.125655

Cardona, C. A., & Sánchez, Ó. J. (2007). Fuel ethanol production: Process design trends and integration opportunities. In *Bioresource Technology* (Vol. 98, Issue 12, pp.

2415–2457). https://doi.org/10.1016/j.biortech.2007.01.002

Carlos dos Santos, A., Ximenes, E., Kim, Y., & Ladisch, M. R. (2019). Lignin–Enzyme Interactions in the Hydrolysis of Lignocellulosic Biomass. In Trends in Biotechnology (Vol. 37, Issue 5, pp. 518–531). Elsevier Ltd. https://doi.org/10.1016/j.tibtech.2018.10.010

Cebreiros, F., Ferrari, M. D., & Lareo, C. (2019). Cellulose hydrolysis and IBE fermentation of eucalyptus sawdust for enhanced biobutanol production by Clostridium beijerinckii DSM 6423. Industrial Crops and Products, 134, 50–61. https://doi.org/10.1016/j.indcrop.2019.03.059

Chauhan, P. S. (2020a). Role of various bacterial enzymes in complete depolymerization of lignin: A review. Biocatalysis and Agricultural Biotechnology, 23, 101498. https://doi.org/10.1016/j.bcab.2020.101498

Chauhan, P. S. (2020b). Role of various bacterial enzymes in complete depolymerization of lignin: A review. Biocatalysis and Agricultural Biotechnology, 23, 101498. https://doi.org/10.1016/j.bcab.2020.101498

Chen, C. W., Yu, W. S., Zheng, Z. X., Cheng, Y. S., & Li, S. Y. (2024). Waste valorization through acetone-butanol-ethanol (ABE) fermentation. Journal of the Taiwan Institute of Chemical Engineers, 160, 105280. https://doi.org/10.1016/J.JTICE.2023.105280

Dalena, F., Senatore, A., Iulianelli, A., Di Paola, L., Basile, M., & Basile, A. (2019). Ethanol From Biomass: Future and Perspectives. Ethanol: Science and Engineering, 25–59. https://doi.org/10.1016/B978-0-12-811458-2.00002-X

Demirbas, A. (2009). Political, economic and environmental impacts of biofuels: A review. *Applied Energy*, *86*(SUPPL. 1), S108–S117.

https://doi.org/10.1016/J.APENERGY.2009.04.036

Devos, R. J. B., & Colla, L. M. (2022). Simultaneous saccharification and fermentation to obtain bioethanol: A bibliometric and systematic study. Bioresource Technology Reports, 17, 100924. https://doi.org/10.1016/J.BITEB.2021.100924

Dumond, L., Lam, P. Y., Van Erven, G., Kabel, M., Mounet, F., Grima-Pettenati, J., Tobimatsu, Y., & Hernandez-Raquet, G. (2021). Termite Gut Microbiota Contribution to Wheat Straw Delignification in Anaerobic Bioreactors. ACS Sustainable Chemistry and Engineering, 9(5), 2191–2202. https://doi.org/10.1021/ACSSUSCHEMENG.0C07817/SUPPL_FILE/SC0C07817_SI_001.PDF

Ethiraj, B., Raihan, T., Sarmin, S., Karim, A., Khan, Md. M. R., Muthuvelu, K. S., Muthusamy, S., Yousuf, A., & Islam, M. A. (2023). Strategies to Enhance Biobutanol Production from Lignocellulosic Biomass. In Microbiology of Green Fuels (pp. 156–176). CRC Press. https://doi.org/10.1201/9781003171157-8

Ezeji, T. C., Qureshi, N., & Blaschek, H. P. (2007). Butanol fermentation research and application. Current Opinion in Biotechnology, 18(3), 244-251.

Fernandes, C. G., Sawant, S. C., Mule, T. A., Khadye, V. S., Lali, A. M., & Odaneth, A. A. (2022). Enhancing cellulases through synergistic β-glucosidases for intensifying cellulose hydrolysis. Process Biochemistry, 120, 202–212. https://doi.org/10.1016/j.procbio.2022.06.011

Fu, C., & Liu, L. (2023). Emerging Separation Techniques for Butanol Biofuel. Journal of Energy Science and Technology. https://doi.org/10.57237/j.jest.2023.06.001

Haigh, K. F., Petersen, A. M., Gottumukkala, L., Mandegari, M., Naleli, K., & Görgens, J.

F. (2018). Simulation and comparison of processes for biobutanol production from lignocellulose via ABE fermentation. *Biofuels, Bioproducts and Biorefining*, *12*(6), 1023–1036. https://doi.org/10.1002/bbb.1917

Hasan, Z., Lateef, M., Bhat, M. K., Raza, M. M., & Khan, M. S. (2024). Advanced biological pretreatment technologies for the deconstruction of agricultural substrates. Waste Valorization for Bioenergy and Bioproducts: Biofuels, Biogas, and Value-Added Products, 45–61. https://doi.org/10.1016/B978-0-443-19171-8.00021-3

Huang, C., Jiang, X., Shen, X., Hu, J., Tang, W., Wu, X., Ragauskas, A., Jameel, H., Meng, X., & Yong, Q. (2022). Lignin-enzyme interaction: A roadblock for efficient enzymatic hydrolysis of lignocellulosics. In Renewable and Sustainable Energy Reviews (Vol. 154). Elsevier Ltd. https://doi.org/10.1016/j.rser.2021.111822

Ilić, N., Milić, M., Beluhan, S., & Dimitrijević-Branković, S. (2023). Cellulases: From Lignocellulosic Biomass to Improved Production. In Energies (Vol. 16, Issue 8). MDPI. https://doi.org/10.3390/en16083598

Jabbari, V., et al. (2017). Optimization of enzymatic hydrolysis of rice straw using response surface methodology. Bioresource Technology, 244, 1191-1197.

Janković, T., Straathof, A. J. J., & Kiss, A. A. (2024). Enhanced isobutanol recovery from fermentation broth for sustainable biofuels production. Energy Conversion and Management: X, 21, 100520. https://doi.org/10.1016/J.ECMX.2023.100520

Jędrzejczyk, M., Soszka, E., Czapnik, M., Ruppert, A. M., & Grams, J. (2019). Physical and chemical pretreatment of lignocellulosic biomass. Second and Third Generation of Feedstocks: The Evolution of Biofuels, 143–196. https://doi.org/10.1016/B978-0-12-815162-4.00006-9

Johannes, L. P., Minh, T. T. N., & Xuan, T. D. (2024). Elephant Grass (Pennisetum purpureum): A Bioenergy Resource Overview. Biomass, 4(3), 625–646. https://doi.org/10.3390/biomass4030034

Khaire, K. C., Moholkar, V. S., & Goyal, A. (2021). Bioconversion of sugarcane tops to bioethanol and other value added products: An overview. Materials Science for Energy Technologies, 4, 54–68. https://doi.org/10.1016/J.MSET.2020.12.004

Kolpe, S., Khade, S. M., & Nile, S. (2022). Macroalgae-based bioethanol. In Biomass and Bioenergy Solutions for Climate Change Mitigation and Sustainability (pp. 206–216). IGI Global. https://doi.org/10.4018/978-1-6684-5269-1.ch012

Kumar, K., Jadhav, S. M., & Moholkar, V. S. (2024). Acetone-Butanol-Ethanol (ABE) fermentation with clostridial co-cultures for enhanced biobutanol production. Process Safety and Environmental Protection, 185, 277–285. https://doi.org/10.1016/J.PSEP.2024.03.027

Kushwaha, D., Srivastava, N., Mishra, I., Upadhyay, S. N., & Mishra, P. K. (2019). Recent trends in biobutanol production. Reviews in Chemical Engineering, 35(4), 475–504. https://doi.org/10.1515/REVCE-2017-0041/ASSET/GRAPHIC/J_REVCE-2017-0041_CV_005.JPG

Lim, S., Hoong, S., Chuetor, S., Ling, P. Y., Hawrot-Paw, M., & Stá, A. (2022). From Waste Biomass to Cellulosic Ethanol by Separate Hydrolysis and Fermentation (SHF) with Trichoderma viride. Sustainability 2023, Vol. 15, Page 168, 15(1), 168. https://doi.org/10.3390/SU15010168

Liu, Y., Yuan, Y., Ramya, G., Mohan Singh, S., Thuy Lan Chi, N., Pugazhendhi, A., Xia, C., & Mathimani, T. (2022). A review on the promising fuel of the future – Biobutanol; the

hindrances and future perspectives. Fuel, 327, 125166. https://doi.org/10.1016/J.FUEL.2022.125166

Mahalingam, L., Abdulla, R., Sani, S. A., Sabullah, M. K., Faik, A. A. M., & Misson, M. (2022). Lignocellulosic Biomass – A Sustainable Feedstock for Acetone-Butanol-Ethanol Fermentation. Periodica Polytechnica Chemical Engineering, 66(2), 279–296. https://doi.org/10.3311/PPch.18574

Mankar, A. R., Pandey, A., Modak, A., & Pant, K. K. (2021). Pretreatment of lignocellulosic biomass: A review on recent advances. Bioresource Technology, 334, 125235. https://doi.org/10.1016/J.BIORTECH.2021.125235

Marcolongo, L., Cara, F. La, & Ionata, E. (2021). Hemp waste valorization through enzymatic hydrolysis for biofuels and biochemicals production. Chemical Engineering Transactions, 86, 127–132. https://doi.org/10.3303/CET2186022

Masson-Delmotte, V., Zhai, P., Pirani, S., Connors, C., Péan, S., Berger, N., Caud, Y., Chen, L., Goldfarb, M., & Scheel Monteiro, P. M. (2021). IPCC, 2021: Summary for Policymakers. In: Climate Change 2021: The Physical Science Basis. Contribution of Working Group I to the Sixth Assessment Report of the Intergovernmental Panel on Climate Change. *Climate Change 2021 – The Physical Science Basis*, 3–32. https://doi.org/10.1017/9781009157896.001

Méndez, J., Passos, D. de F., Wischral, D., Modesto, L. F., & Pereira, N. (2021). Second-generation ethanol production by separate hydrolysis and fermentation from sugarcane bagasse with cellulose hydrolysis using a customized enzyme cocktail. Biofuels, 12(10), 1225–1231. https://doi.org/10.1080/17597269.2019.1608034

Meramo-Hurtado, S. I., González-Delgado, Á. D., Rehmann, L., Quiñones-Bolaños, E., & Mehrvar, M. (2020). Comparison of Biobutanol Production Pathways via Acetone-Butanol-Ethanol Fermentation Using a Sustainability Exergy-Based Metric. ACS Omega, 5(30), 18710–18730. https://doi.org/10.1021/acsomega.0c01656

Mohammed, I. Y., Abakr, Y. A., & Mokaya, R. (2019). Biofuel and valuable products recovery from Napier grass pre-processing: Process design and economic analysis. Journal of Environmental Chemical Engineering, 7(2), 102962. https://doi.org/10.1016/J.JECE.2019.102962

Muharja, M., Darmayanti, R. F., Fachri, B. A., Palupi, B., Rahmawati, I., Rizkiana, M. F., Amini, H. W., Putri, D. K. Y., Setiawan, F. A., Asrofi, M., Widjaja, A., & Halim, A. (2023). Biobutanol production from cocoa pod husk through a sequential green method: Depectination, delignification, enzymatic hydrolysis, and extractive fermentation. Bioresource Technology Reports, 21. https://doi.org/10.1016/j.biteb.2022.101298

Naik, S. N., Goud, V. V., Rout, P. K., & Dalai, A. K. (2010). Production of first and second generation biofuels: A comprehensive review. *Renewable and Sustainable Energy Reviews*, *14*(2), 578–597. https://doi.org/10.1016/J.RSER.2009.10.003

Nargotra, P., Sharma, V., Lee, Y. C., Tsai, Y. H., Liu, Y. C., Shieh, C. J., Tsai, M. L., Dong, C. Di, & Kuo, C. H. (2023). Microbial Lignocellulolytic Enzymes for the Effective Valorization of Lignocellulosic Biomass: A Review. In Catalysts (Vol. 13, Issue 1). MDPI. https://doi.org/10.3390/catal13010083

Obergruber, M., Hönig, V., Procházka, P., Kučerová, V., Kotek, M., Bouček, J., & Mařík, J. (2021). Physicochemical properties of biobutanol as an advanced biofuel. Materials, 14(4), 1–21. https://doi.org/10.3390/ma14040914

Okolie, J. A., Nanda, S., Dalai, A. K., & Kozinski, J. A. (2021). Chemistry and Specialty Industrial Applications of Lignocellulosic Biomass. In Waste and Biomass Valorization (Vol. 12, Issue 5, pp. 2145–2169). Springer Science and Business Media B.V. https://doi.org/10.1007/s12649-020-01123-0

Ong, H. C., Yu, K. L., Chen, W. H., Pillejera, M. K., Bi, X., Tran, K. Q., Pétrissans, A., & Pétrissans, M. (2021). Variation of lignocellulosic biomass structure from torrefaction: A critical review. Renewable and Sustainable Energy Reviews, 152. https://doi.org/10.1016/j.rser.2021.111698

Pereira, A. Vander, De Andrade Lira, M., Machado, J. C., De Miranda Gomide, C. A., Martins, C. E., Da Silva Lédo, F. J., & Daher, R. F. (2021). Elephantgrass, a tropical grass for cutting and grazing. In Revista Brasileirade Ciencias Agrarias (Vol. 16, Issue 2). Universidade Federal Rural de Pernambuco. https://doi.org/10.5039/AGRARIA.V16I3A9317

Pratto, B., Chandgude, V., de Sousa, R., Cruz, A. J. G., & Bankar, S. (2020). Biobutanol production from sugarcane straw: Defining optimal biomass loading for improved ABE fermentation. Industrial Crops and Products, 148. https://doi.org/10.1016/j.indcrop.2020.112265

Pugazhendhi, A., Mathimani, T., Varjani, S., Rene, E. R., Kumar, G., Kim, S. H., Ponnusamy, V. K., & Yoon, J. J. (2019). Biobutanol as a promising liquid fuel for the

future - recent updates and perspectives. Fuel, 253, 637–646. https://doi.org/10.1016/j.fuel.2019.04.139

Qi, G., Huang, D., Wang, J., Shen, Y., & Gao, X. (2019). Enhanced butanol production from ammonium sulfite pretreated wheat straw by separate hydrolysis and fermentation and simultaneous saccharification and fermentation. Sustainable Energy Technologies and Assessments, 36, 100549. https://doi.org/10.1016/J.SETA.2019.100549

Qureshi, N., Blaschek, H., & Blaschek, H. P. (2001). Recovery of butanol from fermentation broth by gas stripping. In *Renewable Energy* (Vol. 22). www.elsevier.nl/locate/renene

Rafieyan, S., Boojari, M. A., Setayeshnia, A., Fakhroleslam, M., Sánchez-Ramírez, E., Bay, M. S., & Segovia-Hernández, J. G. (2024). Acetone-butanol-ethanol fermentation products recovery: Challenges and opportunities. Chemical Engineering Research and Design, 205, 640–664. https://doi.org/10.1016/J.CHERD.2024.04.021

Ranjan, A., & Moholkar, V. S. (2012). Biobutanol: Science, engineering, and economics. In *International Journal of Energy Research* (Vol. 36, Issue 3, pp. 277–323). https://doi.org/10.1002/er.1948

Saravanan, A., Senthil Kumar, P., Jeevanantham, S., Karishma, S., & Vo, D. V. N. (2022). Recent advances and sustainable development of biofuels production from lignocellulosic biomass. *Bioresource Technology*, *344*, 126203. https://doi.org/10.1016/J.BIORTECH.2021.126203

Searchinger, T., Heimlich, R., Houghton, R. A., Dong, F., Elobeid, A., Fabiosa, J., Tokgoz, S., Hayes, D., & Yu, T. H. (2008). Use of U.S. croplands for biofuels increases greenhouse gases through emissions from land-use change. *Science*, *319*(5867),

1238–1240. https://doi.org/10.1126/science.1151861

Selig, M. J., et al. (2007). Enzymatic saccharification of lignocellulosic biomass: Effect of cellulose crystallinity. Energy & Fuels, 21(2), 655-661.

Shafiee, S., & Topal, E. (2009). When will fossil fuel reserves be diminished? *Energy Policy*, *37*(1), 181–189. https://doi.org/10.1016/J.ENPOL.2008.08.016

Sharma, H. K., Xu, C., & Qin, W. (2019). Biological Pretreatment of Lignocellulosic Biomass for Biofuels and Bioproducts: An Overview. Waste and Biomass Valorization, 10(2), 235–251. https://doi.org/10.1007/S12649-017-0059-Y/METRICS

Shubakov A.A., Mikhailova E.A., & Martynov V.V. (2022). Bioconversion of cellulose-containing raw material. Enzymatic hydrolysis of cellulose (review). News of the Komi Scientific Center of the Ural Branch of the Russian Academy of Sciences.

Trilokesh, C., & Uppuluri, K. B. (2023). Critical Analysis of Various Strategies for the Effective and Economical Separation and Purification of Butanol from ABE Fermentation. Separation & Purification Reviews, 52(4), 353–378. https://doi.org/10.1080/15422119.2022.2112052

Tu, W. C., & Hallett, J. P. (2019). Recent advances in the pretreatment of lignocellulosic biomass. Current Opinion in Green and Sustainable Chemistry, 20, 11–17. https://doi.org/10.1016/J.COGSC.2019.07.004

Ummalyma, S. B., Supriya, R. D., Sindhu, R., Binod, P., Nair, R. B., Pandey, A., & Gnansounou, E. (2019). Biological pretreatment of lignocellulosic biomass-current trends and future perspectives. In Second and Third Generation of Feedstocks: The Evolution of Biofuels (pp. 197–212). Elsevier. https://doi.org/10.1016/B978-0-12-815162-4.00007-0

Valles, A., Álvarez-Hornos, F. J., Martínez-Soria, V., Marzal, P., & Gabaldón, C. (2020a). Comparison of simultaneous saccharification and fermentation and separate hydrolysis and fermentation processes for butanol production from rice straw. Fuel, 282, 118831. https://doi.org/10.1016/J.FUEL.2020.118831

Valles, A., Álvarez-Hornos, F. J., Martínez-Soria, V., Marzal, P., & Gabaldón, C. (2020b). Comparison of simultaneous saccharification and fermentation and separate hydrolysis and fermentation processes for butanol production from rice straw. Fuel, 282, 118831. https://doi.org/10.1016/J.FUEL.2020.118831

Veza, I., Muhamad Said, M. F., & Latiff, Z. A. (2021). Recent advances in butanol production by acetone-butanol-ethanol (ABE) fermentation. In Biomass and Bioenergy (Vol. 144). Elsevier Ltd. https://doi.org/10.1016/j.biombioe.2020.105919

Wang, M., Zhang, Q., Gao, H. P., & Cao, C. H. (2023). Simultaneous Saccharification and Fermentation for Biobutanol Production from Corn Starch via ABE Fermentation. BioResources, 18(3), 4935. https://doi.org/10.15376/BIORES.18.3.4935-4942

Xiao, Z. J., et al. (2004). Influence of hemicellulases on enzymatic hydrolysis of corn stover for fuel ethanol production. Applied Biochemistry and Biotechnology, 115(1-3), 1115-1126.

Xie, S. (2024). Bio-based Isobutanol: An Emerging Attractive Biofuel. Science and Engineering. https://doi.org/10.57237/j.se.2024.03.002

Xue, C., Zhao, J., Liu, F., Lu, C., Yang, S. T., & Bai, F. W. (2013). Two-stage in situ gas stripping for enhanced butanol fermentation and energy-saving product recovery. Bioresource Technology, 135, 396–402. https://doi.org/10.1016/j.biortech.2012.07.062

Yang, J., et al. (2018). Dilute acid pretreatment of switchgrass for bioethanol production: Optimization and process integration. Bioresource Technology, 247, 951-958.

Yousuf, A., Pirozzi, D., & Sannino, F. (2019). Fundamentals of lignocellulosic biomass. In Lignocellulosic Biomass to Liquid Biofuels (pp. 1–15). Elsevier. https://doi.org/10.1016/B978-0-12-815936-1.00001-0

Zhao, L., Sun, Z. F., Zhang, C. C., Nan, J., Ren, N. Q., Lee, D. J., & Chen, C. (2022). Advances in pretreatment of lignocellulosic biomass for bioenergy production: Challenges and perspectives. Bioresource Technology, 343, 126123. https://doi.org/10.1016/J.BIORTECH.2021.126123

Zhou, Z., Peng, S., Jing, Y., Wei, S., Zhang, Q., Ding, H., & Li, H. (2023). Exploration of separate hydrolysis and fermentation and simultaneous saccharification and co-fermentation for acetone, butanol, and ethanol production from combined diluted acid with laccase pretreated Puerariae Slag in Clostridium beijerinckii ART44. Energy, 279, 128063. https://doi.org/10.1016/J.ENERGY.2023.128063

Zoghlami, A., & Paës, G. (2019). Lignocellulosic Biomass: Understanding Recalcitrance and Predicting Hydrolysis. In Frontiers in Chemistry (Vol. 7). Frontiers Media S.A. https://doi.org/10.3389/fchem.2019.00874

# APPENDIX

Beta-Glucosidase: $\frac{14.7\%}{7\% + 7\%} = \frac{0.147}{0.07+0.07} = 1.05$

DS > 1, hence, Beta-Glucosidase is synergistic in nature with Cellulase for Elephant Grass

Laccase: $\frac{22\%}{5\% + 3\%} = \frac{0.22}{0.05 + 0.03} = 2.75$

DS > 1, hence, Laccase is synergistic in nature with Cellulase for Elephant Grass

Pectinase showed no synergy at all

Xylanase: $\frac{11\%}{5\% + 3\%} = \frac{0.11}{0.05 + 0.03} = 1.375$

DS > 1, hence, Xylanase is synergistic in nature with Cellulase for Elephant Grass